CALIFORNIA INSTITUTE OF TECHNOLOGY

ELECTRON TUBE AND MICROWAVE LABORATORY

THEORY OF PARAMETRICALLY-PUMPED LONGITUDINAL-FIELD ELECTRON BEAMS

by

Donald C. Forster

Technical Report No. 14

June 1960

A REPORT ON RESEARCH CONDUCTED UNDER

CONTRACT WITH THE OFFICE OF NAVAL RESEARCH

THEORY OF
PARAMETRICALLY-PUMPED LONGITUDINAL-FIELD ELECTRON BEAMS

by

Donald C. Forster

Technical Report 14

CALIFORNIA INSTITUTE OF TECHNOLOGY
Pasadena, California

A Technical Report to the Office of Naval Research

Contract Nonr 220(13)

June 1960

ABSTRACT

The general equations describing electron beams which have been excited by both a moderately strong pump source (or local oscillator) and a weak signal source are formulated in terms of coupled modes, including coupling to slow-wave circuits, and solved numerically for four problems of interest:

a) space-charge pumped longitudinal parametric amplifiers

b) circuit-pumped longitudinal parametric amplifiers

c) parametric cooling of slow space-charge waves, and

d) traveling-wave tubes with pump space-charge waves excited on the electron stream.

Emphasis is placed on the parametric amplifier solutions, and realization of noise temperatures as low as $55^{\circ}K$ are indicated. Amplifiers with this noise temperature and with gain of about 20 db per plasma wavelength should be realized by increasing the phase velocity of the pump wave through the use of circuit pumping. Reasons for the poor performance of the space-charge-pumped parametric amplifier are established. A discussion of the form of the general equations leads to new concepts about the coupling of positive and negative energy carriers through the action of parametric pumping.

Experimental results are presented which tend to verify qualitatively some of the theoretical predictions for the behavior of the parametric amplifiers.

TABLE OF CONTENTS

CHAPTER I

INTRODUCTION

The motivation for this investigation was based upon the need for a more complete understanding of the principles of operation of the longitudinal-field electron-beam type of parametric amplifier. The predictions of the existing approximate theories (1,2) did not adequately describe the performance of the experimental amplifiers (3,4) that had been built. In addition, the theories could not predict many of the important features of the amplifiers. The most glaring inadequacy was the inability to include the noise performance, which is of ultimate importance since the potential achievement of very low-noise amplification is the sole justification for resorting to this relatively complex method of operation. In the course of the work on this particular problem, it was recognized that the theoretical formulation could be generalized to account for the general multiple-frequency electron-beam problem by appropriate choice of models and parameters. As a result, in addition to the parametric amplifier, the performance of electron-beam mixers, up-converters, and other beam-type devices involving multiple frequencies can be predicted from the equations developed here.

1.0 Origin of the Parametric Amplifier

The basic principles of parametric amplification have been known and recorded for many years. The operations of several analogous mechanical systems, particularly pendulums, have been discussed in efforts to provide physical insight into these principles. Certain properties have been found to be common to all types of parametric amplifiers. For example, they all depend for their operation on the periodic variation of some

reactive or energy-storage element. In the case of the pendulum, the oscillation amplitude can be enhanced by periodic variation of the moment of inertia accomplished by periodically changing the length of the suspending cord. From this simple model the basic conditions that the frequency of the variation, or pumping frequency, must be twice the natural frequency of the pendulum for monotonic increase in amplitude, and that the choice of the pumping phase relative to that of the oscillations is critical. In addition, it is noted that some small initial vibration or displacement of the pendulum is necessary before the buildup occurs.

The mere existence of this novel amplification process does not justify the effort that has been expended on it in the last few years. It is relatively complex; the need for a periodic pumping source of energy is in itself a tremendous disadvantage. The recent realization (5) that this amplification process was potentially one which would introduce relatively small amounts of internal noise, and thus be very sensitive, and that electrical amplifiers working down to wavelengths in the centimeter range were readily envisioned, provided the stimulus for the interest. There still exists a need for low-noise amplifiers at microwave frequencies to fill the gap between the very sensitive maser and the more conventional microwave amplifiers. The complexity and inflexibility of the maser preclude its use in some applications. The more conventional amplifiers have yet to realize the degree of low-noise performance that can be effectively utilized, even though much has been accomplished in this area in recent years (6).

1.1 Regenerative or Negative-Resistance Amplifiers

Much of the work to date in the parametric amplifier field has been concentrated in the areas which utilize the variable capacitance effect in semiconductor diodes. The capacitance effect at the diode junction is due to the depletion of carriers in this region and the width of the depletion layer, which determines the capacity, is a function of the applied bias voltage. The magnitude of the capacity is varied periodically through the impression of a driving voltage at the pump frequency. The diode is mounted in a cavity structure which resonates at both pump and signal frequency. Manley and Rowe (7) have derived some basic general energy relations for systems employing nonlinear elements which are very useful for determining more of the properties of parametric amplifiers. The most important of these is the necessity for the provision of some means to support an "idler" signal (8), whose frequency is given by the difference between the pump and signal frequencies. Thus the cavity must also be resonant at the "idler" frequency. The amplifier is a single port device in which a negative admittance is presented at the input terminals. A typical arrangement is shown in Fig. 1.1, in which the cavity and diode are represented by an equivalent circuit. In order to provide some means of separating input and output signals, suitable filters and a circulator must be used. The amplifier's frequency response is not limited by transit time of the carriers in the width variation of the depletion layer, but by the resistance of the bulk material on each side of the junction, which is represented by R_s. It is readily seen that this resistance will drop more of the applied voltage across the diode as frequency increases.

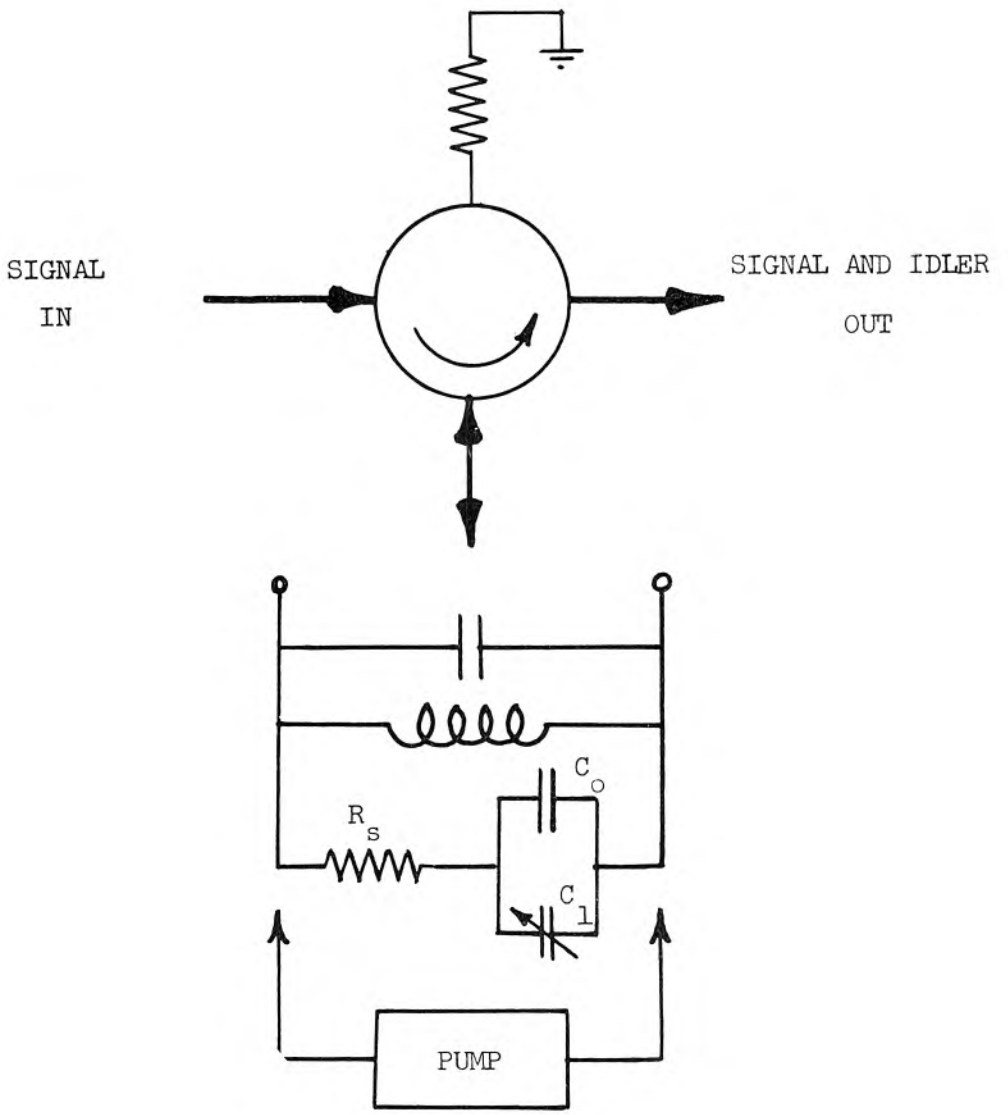

Fig. 1.1 Schematic representation of a semiconductor diode parametric amplifier of the regenerative type. The diode is represented by the series-parallel combination of R_s, C_o, and C_1.

The early success of these amplifiers stimulated interest in the application of other materials with analogous properties. Ferrites in biasing magnetic fields have been used as variable inductances (9,10) in parametric amplifiers. So far the pump power needed in ferrite amplifiers has been very large, but continued efforts are yielding some encouraging results in this area. Bridges (11) has demonstrated that an electron beam modulated at the pump frequency can be used in reentrant cavity gaps to achieve negative resistance.

Unfortunately, this general type of parametric amplifier has the disadvantage of all regenerative amplifiers in that it operates near the oscillation threshold and tends to be unstable and have a narrow bandwidth. The need for the use of a circulator is also a decided disadvantage. To circumvent these difficulties, much effort is being directed toward the understanding of traveling-wave parametric amplifiers, a large variety of which have been proposed.

1.2 Traveling-Wave Parametric Amplifiers

Early work in traveling-wave amplifiers has been performed on broadband, iterated propagating structures with lumped nonlinear reactive elements included. It is hoped that the knowledge gained from these investigations may lead eventually to a continuous distributed amplifier with continuous reactive elements. As in the regenerative amplifier, most of the traveling-wave amplifiers have used semiconductor diodes as the lumped reactive elements. Pumping of these diodes has been achieved by causing a pump wave to propagate down the structure and thus periodically vary the potential across the diodes. Tien and Suhl (12) have

shown that certain relations between the frequencies of the pump, signal and idler waves, and their respective propagation constants must be maintained in order to achieve gain. Ferromagnetic materials have also been considered for use as reactive elements in traveling-wave amplifiers.

This type of amplifier suffers from certain stability problems due to the fact that the circuit is capable of propagation of energy in the reverse direction. Calculations by Currie and Gould (13) have shown that it may be very difficult to get large gains because of oscillations occurring near the band edges. The effects of the inclusion of non-reciprocal elements in the structures are presently under investigation.

The stability difficulties of the amplifiers discussed thus far do not occur in the traveling-wave electron-beam types of parametric amplifiers. They are unconditionally stable due to the unidirectional power flow on the electron beam and the lack of coupling from the output to the input terminals. In the longitudinal-interaction amplifiers, the electron beam is the nonlinear element and the stored energy in this system is in the fields due to the space-charge bunches induced by the pumping signal. The concepts involved in the detailed operation of the beam type of parametric amplifier are considerably different from those encountered in the lumped reactance amplifiers, and will bear considerably more detailed examination. A knowledge of the kinetic power flow on electron beams (14) and of the consequences of the random current and velocity fluctuations in the beam is essential to the understanding of the mechanisms which are exploited in these amplifiers.

1.3 Space-Charge Waves and Kinetic Power Flow on Electron Beams

The conventional electron beam type of amplifier depends for its

source of energy upon the kinetic energy carried by the beam. The process of the extraction of a portion of this energy is discussed either from a purely kinematic point of view or in terms of the mutual coupling of waves or modes which propagate on the stream and on the circuits which may be coupled to the stream. The wave picture will be used here since it is by far the most popular and seems to have yielded far more insight into the energy exchange process. It is particularly adaptable to the problems which lend themselves to treatment involving small-signal approximations.

The two orthogonal modes which can propagate on a moving electron stream are known as slow and fast space-charge waves (15,16). They can be considered to be the waves resulting from the Doppler shifting of the two oppositely-directed traveling waves which are used to describe sinusoidal plasma oscillations in a stationary electron plasma. They are obtained as solutions of the set of linearized one-dimensional homogeneous equations which relate the a.c. current, velocity, charge density and electric fields which are set up by some sinusoidal perturbing quantity of frequency $f = \omega/2\pi$. The solutions show that the normal modes possess wave properties which are described as a function of time and distance by

$$f^i(z,t) = C^i e^{j(\omega t - \beta^i z)} \tag{1.1}$$

where the propagation constant is given by

$$\beta^{\pm} = \frac{\omega \mp \omega_p}{u_o} \tag{1.2}$$

The upper sign is used to denote the fast space-charge wave and the lower

the slow wave. The notation conventions are obvious upon examination of the phase velocities of these waves, which are written

$$v^{\pm} = \frac{\omega}{\beta^{\pm}} = \frac{u_o}{1 \mp \frac{\omega_p}{\omega}} \approx u_o\left(1 \pm \frac{\omega_p}{\omega}\right) \tag{1.3}$$

The approximation is valid since $\omega_p/\omega \ll 1$ in the practical cases where microwave frequencies are involved.

Since the modes are orthogonal, they can be separately excited. Chu (14) has shown that the slow space-charge wave has the interesting property that as its mode amplitude is increased, the a.c. power flow on the wave in the group velocity direction is decreased in an algebraic sense. This can be explained in terms of the kinetic energy density of the electrons involved in the wave motion at a given instant in time. The a.c. power flow on the fast space-charge wave behaves in the more conventional manner in which power flow and mode amplitude are positively related, as they are for modes propagating on circuits. Whenever a slow space-charge wave is coupled to a wave which carries positive a.c. energy through simple mutual interaction of their associated fields, an unstable condition arises and the amplitude of each wave will grow, but energy will be conserved because the positive energy-carrying wave can extract energy from the slow space-charge wave. It is this property of the slow space-charge wave that is exploited in the traveling-wave tube and other conventional microwave amplifiers. Haus and Robinson (17) have shown that there is a lower limit to the noise behavior of these amplifiers which is somewhat above that which can be advantageously utilized in various practical applications. This limit is imposed by the very property of the slow

space-charge wave that is being exploited to achieve gain; this wave is excited in the cathode region by current and velocity fluctuations which generate noise in the interaction region, and any efforts to dissipate these fluctuations by passive field coupling result in the absorption of energy from the beam with the attendant increase in the fluctuations. At present, many studies are being conducted to find the optimum noise excitation conditions in the region of the potential minimum (18), and noise figures as low as 3 db. are being obtained (6) experimentally.

The concept of a minimum noise excitation does not occur for the fast space-charge wave since passive energy absorption of noise power from this wave results in decreased mode amplitude. It seems evident, therefore, that an amplifier which depends only upon coupling to the fast space-charge wave could conceptually be made ideal, i.e., could be made so that it contributed no noise in the course of the amplification process. A new source of energy must be found in such an amplifier since one is no longer free to draw upon the d.c. beam energy. The beam type of parametric amplifier has been proposed as one which fulfills both these requirements. Certain limitations of both a practical and theoretical nature to be explored in the course of this work preclude the achievement of ideal amplification; however, these limitations are far less stringent than those encountered to date in conventional amplifiers, and improved performance by an order of magnitude may be achieved.

1.4 Electron-Beam Parametric Amplifiers

Two basic types of electron-beam parametric amplifiers have been proposed; they are commonly known as the transverse-field-interaction or cyclotron-wave type (19) and the longitudinal-field-interaction or space-

charge-wave type (1,2). In the former, waves known as cyclotron waves interact with transverse components of the fields which couple the circuit to the beam, while in the latter type, the space-charge waves interact with the longitudinal components of the circuit fields. The cyclotron-wave amplifier has been by far the more successful to date; noise temperatures as low as $35^{\circ}K$ have been reported (20). As has been mentioned, a satisfactory analysis of the space-charge-wave type has not been achieved and the experimental results have been disappointing.

These amplifiers are analogous to the extent that the qualitative arguments which have been presented for the noise behavior and a.c. power flow on fast and slow space-charge waves are also valid for fast and slow cyclotron waves. The basic difference in the complexity of the analytical approaches to the two problems can be attributed to the difference in the velocity dispersion of the two types of waves. The phase velocities of the cyclotron waves are given by

$$v_{cyc.}^{\pm} = \frac{u_o}{1 \mp \frac{\Omega_c}{\omega}} \tag{1.4}$$

where the cyclotron frequency Ω_c is related to the axial magnetic field B by

$$\Omega_c = \frac{eB}{m} \tag{1.5}$$

Since parametric amplifiers involve multiple frequencies and beams are nonlinear, it becomes important to know what the effects of the frequencies generated as mixing products are on the performance of the amplifier. These effects can be shown to result from the coupling of the waves excited on the beam at the various frequencies, and the amount

of the coupling in turn can be shown to depend on the relative phase velocities of the waves in question. If harmonics of the pump frequency are neglected, the frequencies generated in the amplifier are given by

$$\omega_m = \omega + m\omega_c \qquad m = \cdots -2, -1, 0, 1, 2 \cdots \qquad (1.6)$$

where ω_c is the pump frequency and is higher than the signal frequency (usually $\approx 2\omega$) . Keeping in mind the fact that $\omega_p \ll \omega$, and that Ω_c can be arbitrary, it is seen that the velocities of all the waves in the space-charge-wave amplifiers are close to u_o, while the fast cyclotron wave velocity at the signal frequency can be made infinite if $\Omega_c = \omega$, as is normally the case. This large dispersion in the phase velocities of the cyclotron waves allows one to ignore the effects of any wave for which $m \neq 0$ or -1, and excellent analyses of the performance of these amplifiers have been made. The principal effort of the work to follow is directed toward finding adequate solutions for the space-charge-wave amplifier pumping problem which include the effects of the higher order mixing products.

1.5 Functional Description of Electron-Beam Parametric Amplifiers

The four basic operations that must be performed in these amplifiers are: a) removal of the noise from the fast signal wave, b) exciting the fast signal wave with the incoming signal, c) amplifying (or pumping) this wave, and d) removing the amplified signal energy from the beam wave. These operations are usually performed as illustrated in Fig. 1.2 .

Gould (21) and Ashkin (22), et al, have shown that couplers can be built which will perform the dual function of simultaneous noise removal

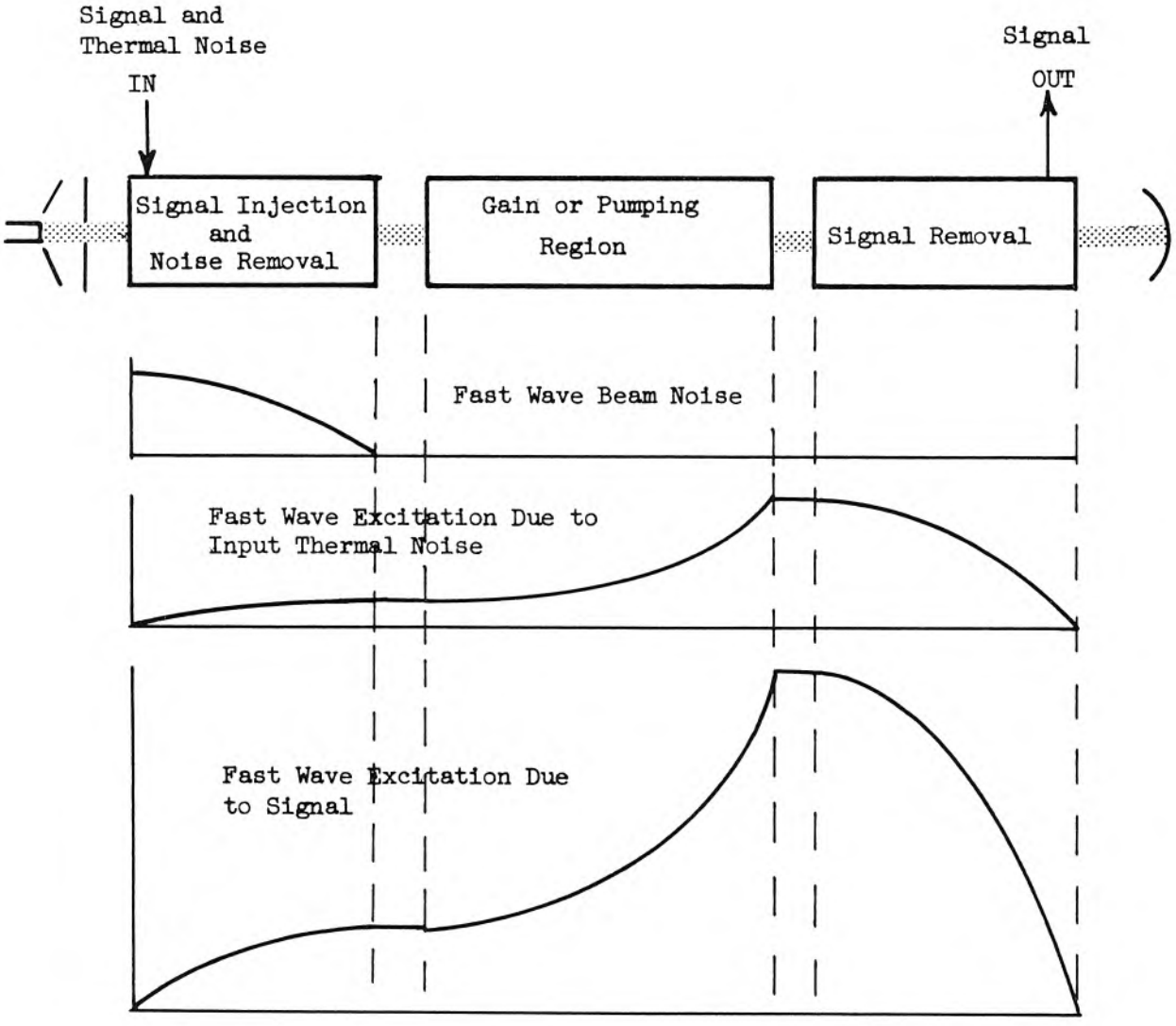

Fig. 1.2 A functional diagram of the electron-beam type of traveling-wave parametric amplifier.

and signal injection for space-charge-wave amplifiers. Two-gap cavity couplers can also be used for this purpose. The conditions for optimum coupling to space-charge waves with these cavity couplers are derived in Appendix I. Couplers with analogous properties exist for cyclotron waves. As can be seen in Fig. 1.2, if the noise removal operation is perfect, the signal-to-noise ratio at the entrance to the gain region is apparently the same as that at the input signal port. Unfortunately, all parametric amplifiers convert signal or noise input at the difference or idler frequency to signal output with a conversion gain almost equal to that of the signal gain. Thus, even though the beam noise at the idler frequency is removed in the input coupler, the idler frequency noise input at the input signal terminals causes the signal-to-noise ratio to be halved at the entrance to the pumping region. This will not be true for signals with a noise-type spectrum, however, since signal will then be injected at both the signal and idler frequencies. Special techniques can be used to reduce the effects of the idler frequency noise in certain applications. This extra noise contribution, together with any contributions from higher order idler waves, precludes the possibility of ideal amplification.

It is evident that the basis for the expectation of low noise amplification in the beam type of amplifier is completely different from that in the diode amplifier. There the nonlinear element is a "cold" device in which no current flow (with attendant noise fluctuations) takes place across the junction. The periodic variation in the width of the depletion layer is minute and is not expected to contribute noise. In the beam-type amplifier, however, the "hot" electron stream is initially very noisy and only the ability to "cool" it in a specified manner provides the key to low noise amplification.

Pumping of cyclotron waves is achieved by the use of quadrupole fields as described by Adler, et al (23). Several related methods for pumping space-charge waves have been proposed by Louisell and Quate (1) and Wade and Adler (24) and, as mentioned, these will be discussed in detail. Suffice it to say here that exponential growth takes place in the pump region. The signal removal function is performed by using the reciprocal properties of the type of coupler which was used at the input.

The cyclotron-wave amplifier has been very successful to date at the lower frequencies. However, the extension of operation to higher frequencies poses some problems of fundamental nature (25). The magnetic field and pump power requirements would seem to limit its operation to frequencies below 10 kmc. Diode amplifiers have also been confined to this same frequency range due to the state of the diode fabrication art. Higher diode cutoff frequencies (or higher Q's) must be obtained to extend the frequency range of these amplifiers.

The two factors which determine the high frequency limit for the space-charge wave amplifier are: a) the availability of a pumping source, and b) the conventional problems encountered in extending all microwave tubes into the near-millimeter wavelength range. These problems are due to practical difficulties encountered in fabricating very small parts and in realizing circuits which have electric fields of sufficient strength in regions where an electron stream can be positioned. An estimate of this limit within the present state of the art might be about 30 kmc with the possibility of extension as better high-frequency pump sources become available.

It is interesting to note that the limiting factors for higher

frequency operation of diode and cyclotron-wave amplifiers do not apply to space-charge wave amplifiers. The "Q values" of electron beams are many orders of magnitude higher than those of modern diodes since the only losses in the beam are due to collisions, which are rare. The magnetic field required by space-charge-wave amplifiers is simply that required to confine the electron stream. The principal gain parameter for the space-charge-wave amplifier is the degree of saturation of the electron beam by the pump power. The power necessary to saturate the stream is given by

$$P_s = 2P_o \frac{\omega_p}{\omega} \tag{1.7}$$

where P_o is the d.c. power in the stream. Thus, for a given beam, the pump power decreases with frequency. The implication of this result is that the amplifier will saturate at lower power levels, but this is of little interest since these amplifiers operate far below saturation in practice. On the basis of these arguments, it seems that the space-charge-wave amplifier is the most promising for operation at high microwave frequencies.

1.6 Parametric Pumping of Space-Charge Waves

The first proposal for parametric pumping of space-charge waves by Louisell and Quate (1) described a system in which fast space-charge waves at both the signal and pump frequencies were excited on a stream which was then allowed to drift. This "drifting-beam, space-charge-pumped" amplifier depends upon coupling between the strong pump-space-charge wave and the weakly excited signal space-charge wave. A physical description of the gain mechanism in this amplifier can be obtained from a consideration of the excess charge density or bunching produced on an electron beam which

has been modulated by two space-charge waves. The gain depends upon the proper disposition of the dense electron bunches produced by the pump signal about the weak signal bunches. If the signal space-charge wave propagates as

$$e^{j(\omega t - \beta z)}$$

then the pump space-charge wave whose time dependence is 2ω must propagate as

$$e^{j(2\omega t - 2\beta z)}$$

in order to achieve velocity synchronism between the waves. Under these conditions, when one views the bunching on the beam in a moving frame of reference traveling at the phase velocity of the waves, the charge density distribution might appear as in Fig. 1.3. When the proper periodicity, phase, and velocity conditions are fulfilled as shown, the forces due to the electric fields of the pump bunches will enhance the signal space-charge wave. Note that a shift of 180° in the phase of the pump wave causes suppression of the signal bunches, and attenuation instead of gain results. It should be noted also that individual electrons move through this bunching pattern, since the phase velocity of the space-charge waves is different from that of the average electron velocity. These conditions can be approached in practice by use of very thin beams. If these optimum conditions are not met exactly, a more complex picture of one wave moving through the other results, and the signal bunches will tend to be alternately enhanced and suppressed.

Since the beam is nonlinear, its behavior must be represented by the inclusion of idler waves whose time dependence is given by equation 1.6 .

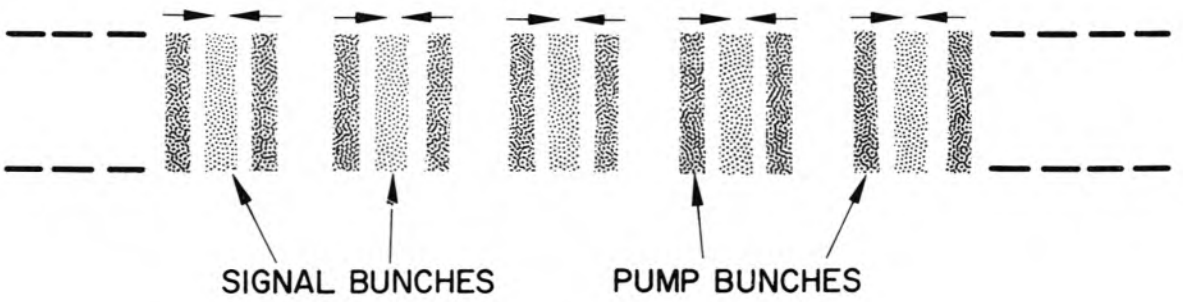

Fig. 1.3 A pictorial representation of the bunches on the electron beam for a space-charge-pumped amplifier as viewed in a reference frame moving at the phase velocity common to both pump and signal space-charge-waves. Pump frequency is twice the signal frequency. The arrows represent the forces on the signal bunches due to the more dense pump bunching.

The expression "idler" is usually associated with the wave for which m = -1, and the other waves are referred to as higher order idlers or mixing products. These frequencies are also present in the output spectrum of the amplifier unless selective output coupling is employed.

In addition to these idler waves, the apparent necessity for pumping the beam into the nonlinear or near-saturation operating region to achieve reasonable gains results in the generation of harmonics of the pump frequency (26). Each of these harmonics then has its own set of idler waves. The time dependence for all of the waves present on the beam is then written

$$\sum_{m=-\infty}^{\infty} \sum_{n=-\infty}^{\infty} e^{j(n\omega_s + m\omega_p)t}$$

No quantitative estimates of the amount of noise introduced by these waves has been made. However, this noise contribution is not expected to be large and the effects of pump harmonics will be ignored in this work.

Wade and Adler (24) have proposed a different type of longitudinal-interaction beam-type parametric amplifier. It consists of an electron beam, which has been premodulated at the signal frequency, traveling through a slow-wave propagating circuit. The circuit propagates a strong pump wave at the same velocity as that of the signal space-charge wave which is propagating on the beam. A physical representation of the behavior in a frame of reference moving at the phase velocity of the waves is shown in Fig. 1.4. Comparison with Fig. 1.3 reveals that this amplifier utilizes the longitudinal component of the

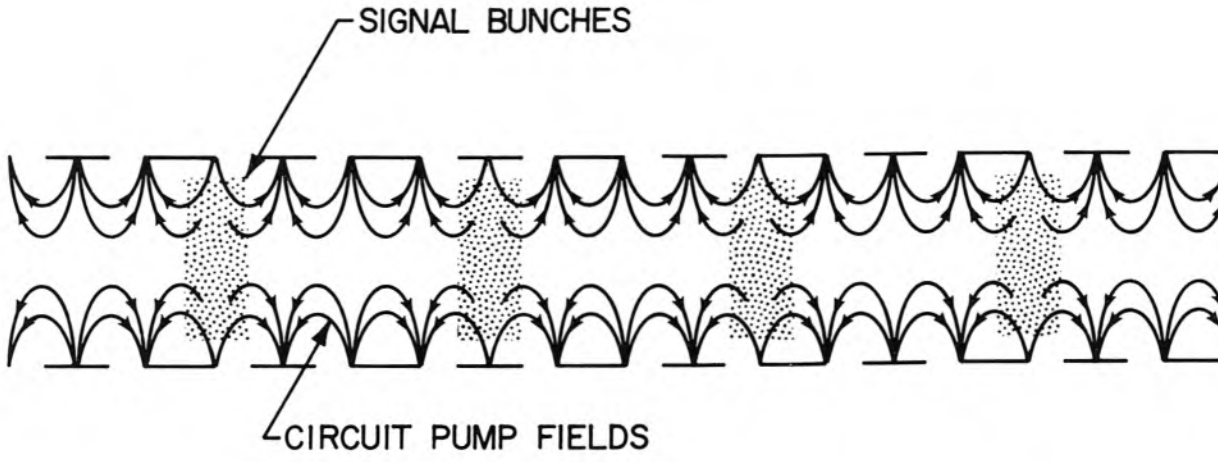

Fig. 1.4 A pictorial representation of the interaction of the circuit fields with the signal bunches in a circuit-pumped amplifier as viewed in a reference frame moving at the phase velocity of the waves. The signal bunching is enhanced by the action of the longitudinal component of the pump fields.

electric field of the circuit wave to enhance the signal bunches in the same manner as the fields due to the dense pump bunches are used in the space-charge-pumped amplifier. This new type of amplifier will be referred to as the "circuit-pumped" amplifier.

For the special case in which the pump frequency is exactly twice the signal frequency and the waves have synchronous velocities and proper phase, Wade and Adler have derived a gain expression from an analogy to a harmonic oscillator in a time-varying perturbation field. In Chapter II, a more general analysis to establish quantitatively the possible advantages to be gained with this type of amplifier is presented. The analysis allows for arbitrary pump-wave phase velocity and arbitrary pump frequency. It is a "three-frequency" (pump, signal and idler frequencies) analysis in that the effects of higher order idler waves are ignored. In the process of the analysis, it is seen that the space-charge-pumped amplifier can be treated as a special case of the circuit-pumped amplifier, since the gain in the latter amplifier results from coupling to a wave on the beam which is induced by the circuit pump wave and whose phase velocity is related to the circuit phase velocity. Allowing this wave to assume the properties of a pump space-charge wave yields the results of Louisell and Quate.

In Chapter III, the equations describing the system are put into a coupled-mode formulation so that the effects of the higher order idlers can be readily determined. Pumping is still achieved by a beam wave of arbitrary phase velocity, and provision is made for coupling to a circuit at the signal and all idler frequencies. The coupled mode equations which result are three infinite sets of simultaneous, linear

first-order differential equations with constant coefficients. However, only a few of the equations are needed for the solution of most problems. Cook and Louisell (38) have published a similar set of equations which differ by a constant phase factor in the definitions of the mode amplitudes.

In Chapter IV a more exact coupled-mode formulation is obtained which allows for the inclusion of all three of the pumping waves which are induced on the beam by a circuit pump wave. The equations are complicated to the extent that the coefficients become z dependent and more adequate computer facilities are required for solution. Solutions to these equations have not been obtained.

Solutions to the equations derived in Chapter III are presented in Chapter V. They clearly indicate the reasons for the failure of the experimental amplifiers and demonstrate that new areas of operation may yield excellent results. Cook, et al (39), have obtained results very similar to those presented in Fig. 5.15.

In Chapter VI the flexibility of the general equations derived in Chapter III is demonstrated by applying them to other devices which involve multiple-frequency electron beams, such as the parametric cooling principle proposed very recently by Sturrock (34).

Some interesting experimental results obtained from an amplifier which was designed to operate on the space-charge-pumped principle are presented in Chapter VII. Although the amplifier was quite noisy, interpretation of the results show that this behavior could have resulted from shortcomings in the experimental tube and is probably not due to fundamental limitations of the parametric amplification process. Verification of several other predictions of the theory was obtained and courses of action for further experimental work are indicated.

CHAPTER II

A GENERALIZED THREE-FREQUENCY ANALYSIS OF THE CIRCUIT-PUMPED SPACE-CHARGE-WAVE AMPLIFIER

2.1 Introduction

The analysis of Wade and Adler (24) deals with the special case in which the circuit pumping wave and the signal space-charge wave have the same phase velocity, and in which the pump frequency is twice the signal frequency. In this chapter, a wave analysis is performed which includes the effects of varying the relative frequency and phase velocity of the pump, and in addition yields some interesting information about the total pump modulation on the beam. The gain expression reduces to that of Wade and Adler for the special case which they treated.

2.2 The Basic Assumptions and a Description of the Model

The conventional one-dimensional assumptions that electron motion is constrained to the z direction and that the z components of the electric fields over the cross section of the beam are constant are used. The fluid model of the electron stream is used in which velocity is a single-valued function of position. The pump quantities are assumed to be large compared to the signal quantities, but much less than the d.c. quantities so that they may be described by linear theory. The finite geometry effects are included by use of the appropriate plasma-frequency reduction factor R (27).

The model to be considered consists of an electron beam, which has been premodulated by an input signal at frequency ω , passing through a

slow-wave propagating circuit such that the beam couples to the wave supported by the circuit. The premodulation on the beam will consist of the excitation of the fast signal space-charge wave only. The circuit wave will be the pumping signal, which will be assumed to be constant with distance along the beam. The validity of this assumption can be supported by two qualitative arguments. First, the circuit wave will travel faster than the fast space-charge wave at the pump frequency so that complete energy transfer to the beam will not occur. Secondly, the desired gain may be achieved in a short distance compared to that necessary for the transfer of the energy to the beam. This assumption is consistent with the one used by Wade and Adler. If necessary, it is possible to set up a single pump wave by proper adjustment of the initial conditions. The electric fields are assumed to be composed of the sum of the space-charge and circuit fields, i.e.,

$$E = E_{sc} - \frac{\partial V_c}{\partial z} \tag{2.1}$$

where E_{sc} represents the space charge fields and V_c the circuit voltage.

2.3 The Derivation of the Characteristic Equation

The three fundamental equations to be used in this one-dimensional analysis are Poisson's equation

$$\frac{\partial E_{sc}}{\partial z} = \frac{R^2(\omega)\rho}{\epsilon_o} \quad , \tag{2.2}$$

the equation of motion, which can be written

$$\frac{\partial v}{\partial t} + v \frac{\partial v}{\partial z} = - \eta E \qquad \left(\eta = \left|\frac{e}{m}\right|\right) \tag{2.3}$$

and the continuity equation

$$\frac{\partial \rho}{\partial t} + \frac{\partial i}{\partial z} = 0 \quad , \tag{2.4}$$

where ϵ_o = the permittivity of free space

v = velocity of the beam

ρ = charge density of the stream

i = current in the stream

and R is the plasma frequency reduction factor incorporated to account for the effects of the finite geometry of the beam. The plasma frequency for an infinite one-dimensional beam is obtained from

$$\omega_p^2 = - \frac{\eta \bar{\rho}_o}{\epsilon_o} \quad , \tag{2.5}$$

where $\bar{\rho}_o$ is the average charge density and the reduced plasma frequency for the cylindrical beam is given by

$$\omega_q = R \, \omega_p \quad . \tag{2.6}$$

The current is given by

$$i = \rho v \quad . \tag{2.7}$$

Differentiating equation 2.3 with respect to z and combining with equations 2.1 and 2.2 gives

$$\frac{\partial^2 v}{\partial z \partial t} + \frac{\partial^2}{\partial z^2}\left(\frac{v^2}{2}\right) + \frac{\eta R^2 \rho}{\epsilon_o} = \eta \frac{\partial^2 V_c}{\partial z^2} \quad . \tag{2.8}$$

Equations 2.4 and 2.7 are combined to give

$$\frac{\partial \rho}{\partial t} + v \frac{\partial \rho}{\partial z} + \rho \frac{\partial v}{\partial z} = 0 \quad . \tag{2.9}$$

The normal procedure in a wave analysis is to assume a solution of the form of a perturbed solution of the uncoupled system. The perturbation is usually a relatively slowly varying quantity. Since any growing wave results from coupling to other traveling waves and takes place with distance, the assumed perturbed solution is usually of the form $v_1(z)e^{j(\omega t - \beta z)}$. For each derivative with respect to z, the derivative of the product of two functions of z must be taken. To reduce the number of terms that must be handled, and also to facilitate physical interpretation of the results, the analysis will be performed in a frame of reference moving in the z direction at the average velocity of the electrons u_o. In this moving frame, the perturbation becomes a function of time and the number of product derivatives is reduced. The moving frame will be denoted with primed quantities (z') and the laboratory frame with unprimed quantities (z).

When a fast space charge wave at frequency ω is excited in the laboratory system, it has a dependence as

$$e^{j(\omega t - \beta z)} \tag{2.10}$$

where

$$\beta = \frac{\omega - R\omega_p}{u_o} \quad . \tag{2.11}$$

To change to the frame of reference moving at velocity u_o , the non-relativistic transformations

$$z = z' + u_o t \qquad (t' = t) \tag{2.12}$$

are used to substitute for z and t , and the wave solution becomes

$$e^{j[\omega - \beta u_o)t - \beta z']} \quad . \tag{2.13}$$

Thus it is seen that the time dependence in the moving frame is given by

$$\omega' = \omega - \beta u_o = R\,\omega_p = \omega_q \quad , \tag{2.14}$$

the reduced plasma frequency. Equations 2.11 and 2.6 were used in obtaining 2.14 .

From the physical arguments associated with Figure 1.4, it seems desirable to use a circuit pump wave which has a frequency about twice that of the signal frequency in the laboratory frame and propagates at a velocity in the vicinity of the phase velocity of the fast space-charge wave at the signal frequency. It will be assumed that the circuit wave is given by

$$V = V_c e^{j(\omega_c t - \Gamma z)} \tag{2.15}$$

which becomes

$$V = V_c e^{j[(\omega_c - \Gamma u_o)t - \Gamma z']} \tag{2.16}$$

In the moving frame of reference. The Doppler-shifted circuit-wave frequency in the moving frame will be defined as

$$\omega_c' \equiv \omega_c - \Gamma u_o \quad . \tag{2.17}$$

The solution for the velocity and charge density modulation induced on the beam due to the pumping signal will be sought first. These quantities will be the first order solution to the equations, and the signal modulation will later be introduced as first order perturbations of these quantities. In order to obtain particular solutions to equations 2.8 and 2.9, solutions of the form of the driving function V are assumed; thus

$$v_2 = v_c e^{j[\omega_c' t - \Gamma z]} \tag{2.18}$$

$$\rho_2 = \bar{\rho}_o + \rho_c e^{j[\omega_c' t - \Gamma z']} \tag{2.19}$$

After substituting into equations 2.8 and 2.9 and making the linear or small-signal approximation that terms involving the product of a.c. quantities can be neglected, the coefficients of the time-varying terms become

$$v_c \omega_c' \Gamma + \frac{\eta R_2^2 \rho_c}{\epsilon_o} = - \Gamma^2 \eta V_c \tag{2.20}$$

where R_2 is the plasma frequency reduction factor at the circuit wave frequency, and

$$\omega_c' \rho_c - \Gamma \bar{\rho}_o v_c = 0 \quad . \tag{2.21}$$

Solving simultaneously and using equation 2.5 gives

$$v_c = - \frac{\Gamma \eta V_c \omega_c'}{(\omega_c'^2 - R_2^2 \omega_p^2)} \quad . \tag{2.22}$$

$$\rho_c = - \frac{\Gamma^2 \eta \, \bar{\rho}_o \, V_c}{(\omega_c'^2 - R_2^2 \omega_p^2)} \quad . \tag{2.23}$$

The required complementary function solutions to the homogeneous form of equations 2.8 and 2.9 are simply the space charge wave solutions. Adding these to the particular solution just obtained, one can write for the total modulation on the beam due to the pump wave

$$v_2 = - \frac{\Gamma \eta V_c \omega_c'}{(\omega_c'^2 - R_2^2 \omega_p^2)} e^{j(\omega_c' t - \Gamma' z)} + \sum_i C_i e^{j(R_i \omega_p t - \beta_i z)} + \sum_j D_j e^{-j(R_j \omega_p t + \beta_j z')} \tag{2.24}$$

and

$$\rho_2 = - \frac{\Gamma^2 \eta \, \bar{\rho}_o \, V_c}{(\omega_c'^2 - R_2^2 \omega_p^2)} e^{j(\omega_c' t - \Gamma' z)} + \sum_i \frac{C_i \beta_i \bar{\rho}_o}{R_i \omega_p} e^{j(R_i \omega_p t - \beta_i z')} - \sum_j \frac{D_j \beta_j \bar{\rho}_o}{R_j \omega_p} e^{-j(R_j \omega_p t + \beta_j z')} \tag{2.25}$$

where equation 2.21 has been used for each of the superposed solutions. The summations represent the sum total of the infinite number of space-charge waves which can be excited; the wave numbers β_i and β_j and the reduction factors R_i and R_j are determined by the excitation signal wavelength. It will be assumed that both the fast and slow space-charge waves have the same reduction factor R_2 .

In the laboratory frame of reference the boundary condition is imposed that at $z = 0$, $v_2 = \rho_2 = 0$. This means that v_2 and $\rho_2 = 0$ for $z' \leq -u_o t$ in the moving coordinate system. Letting $t = -z'/u_o$

in equation 2.24 gives

$$v_2 = -\frac{\Gamma \eta V_c \omega_c'}{(\omega_c'^2 - R_2^2\omega_p^2)} e^{-j(\frac{\omega_c'}{u_o}+\Gamma)z'} + \sum_i C_i e^{-j(\frac{R_2\omega_p}{u_o} + \beta_i)z'} + \sum_j D_j e^{j(\frac{R_2\omega_p}{u_o} - \beta_j)z'} \quad . \qquad (2.26)$$

To meet the boundary conditions it is seen that the exponents must be made the same and then the condition at $z' = 0$ matched with the coefficients. From the i summation this requires that

$$\text{a)} \quad \frac{\omega_c'}{u_o} + \Gamma = \frac{R_2\omega_p}{u_o} + \beta_i , \qquad \text{or} \qquad \beta_i = \Gamma + \frac{1}{u_o}(\omega_c' - R_2\omega_p) \quad . \qquad (2.27)$$

Similarly for the j summation

$$\text{b)} \quad \frac{\omega_c'}{u_o} + \Gamma = -\frac{R_2\omega_p}{u_o} + \beta_j , \qquad \text{or} \qquad \beta_j = \Gamma + \frac{1}{u_o}(R_2\omega_p + \omega_c') \quad . \qquad (2.28)$$

Substituting for ω_c' from equation 2.7 yields

$$\beta_i = \frac{\omega_c - R_2\omega_p}{u_o} \qquad (2.29)$$

$$\beta_j = \frac{\omega_c + R_2\omega_p}{u_o} \quad . \qquad (2.30)$$

Thus β_i is the wave number of a fast space-charge wave excited at the pumping frequency and β_j that of a slow space-charge wave at the same frequency. Imposing the condition that at $t = z' = 0$, $v_2 = \rho_2 = 0$ gives

$$- \frac{\Gamma \eta V_c \omega'_c}{\omega'^2_c - R_2^2 \omega_p^2} + C_i + D_j = 0 \tag{2.31}$$

$$- \frac{\Gamma^2 \rho_o \eta V_c}{(\omega'^2_c - R_2^2 \omega_p^2)} + \frac{C_i \beta_i \rho_o}{R_2 \omega_p} - \frac{D_j \beta_j \rho_o}{R_2 \omega_p} = 0 \quad . \tag{2.32}$$

Solving simultaneously, the constants become

$$C_i = - \frac{v_c}{2} \left(1 + \frac{R_2 \omega_p}{\omega'_c}\right) \tag{2.33}$$

$$D_j = - \frac{v_c}{2} \left(1 - \frac{R_2 \omega_p}{\omega_c}\right) \tag{2.34}$$

where v_c is defined in equation 2.22. Substituting these expressions into equations 2.24 and 2.25 gives the a.c. modulation quantities on the beam due to the pump wave.

It is now desired to inquire into the possibility of amplification of a fast space-charge wave excited at a signal frequency ω in the laboratory frame. Noting that the phase velocities of the space-charge waves excited by the pump wave at the initial plane are quite far removed from that of a signal space-charge wave, it is expected that coupling between these and the signal wave will produce second-order effects resulting in some initial perturbation of the exponential growth curve. The amplitude will depend upon the relative velocity separation. Since the prime interest is in the exponential growth at present, these terms will be ignored in equations 2.24 and 2.25 and only the more nearly synchronous driven wave represented by the first term will be retained.

It should be noted that in the traveling-wave-tube theory of Pierce (28), in which the circuit wave is not assumed constant, a wave of approximately constant amplitude (characterized by Pierce's δ_3) is excited on the beam if the phase velocity of the circuit is greater than that of the fast space-charge wave. Also, its phase velocity is very close to that of the circuit wave. Since the first order wave solution obtained here has essentially the same properties and offers the possibility of comparison of results with Wade's theory, it is felt that these similarities further justify the use of the approximate procedures as previously outlined.

In the conventional small-signal analysis, the a.c. quantities are regarded as small perturbations of large d.c. quantities. After neglecting second-order terms, the resulting linearized differential equations have constant coefficients. In this analysis the signal frequency quantities are regarded as small perturbations of the larger pump frequency components as represented by the first terms in equations 2.24 and 2.25 written as real quantities. When this assumed solution is substituted and terms involving products of signal quantities are neglected, the resulting differential equations are linear with variable coefficients. Since the equations are linear, superposition holds and real physical variables can be represented by exponentials with the understanding that the real part signifies the physical quantity.

A fast signal space-charge wave varying as

$$v_1 \sim e^{j(\omega_q t - \beta z')} \tag{2.35}$$

is assumed to be excited on the beam. Note that nonlinear terms in the

differential equations will give rise to terms which vary as

$$e^{j[(\omega_q + \omega_c')t - (\Gamma + \beta)z']} \quad \text{and} \quad e^{j[(\omega_q - \omega_c) - (\Gamma - \beta)z']}.$$

These in turn will mix with the pump to give terms which vary as

$$e^{j[(\omega_q + 2\omega_c) - (\beta + 2\Gamma)\, z']} \quad \text{and} \quad e^{j[(\omega_q - 2\omega_c)t - (\beta - 2\Gamma)\, z']}, \text{ and}$$

these in turn mix until all sum and difference frequencies are present. Therefore it will be convenient to define

$$\omega_n \equiv \omega_q + n\omega_c' \qquad n = \cdots -2,-1,0,1,2 \cdots \tag{2.36}$$

and

$$\beta_n \equiv \beta + n\Gamma \qquad n = \cdots -2,-1,0,1,2 \cdots \tag{2.37}$$

and write the form of the perturbing solution as

$$v = \sum_{-\infty}^{\infty} v_n(t)\, e^{j(\omega_n t - \beta_n z')} \tag{2.38}$$

since growth in the moving reference frame will take place with time instead of distance. $n = 0$ then corresponds to the signal wave, and $n = -1$ to the idler wave. The other integral values of n correspond to the higher order idler waves.

Harmonics of the pump will not be considered in this analysis, so the following forms are assumed for the solutions for ρ and v which are to be substituted into equations 2.8 and 2.9

$$v = Me^{j(\omega_c' t - \Gamma z')} + Me^{-j(\omega_c' t - \Gamma z')} + \sum_{-\infty}^{\infty} v_n(t) e^{j(\omega_n t - \beta_n z')} \tag{2.39}$$

$$\rho = \bar{\rho}_o + Ne^{j(\omega_c' t - \Gamma z')} + Ne^{-j(\omega_c' t - \Gamma z')} + \sum_{-\infty}^{\infty} \rho_n(t) e^{j(\omega_n t - \beta_n z')} \tag{2.40}$$

where the constants M and N are defined by

$$M \equiv -\frac{1}{2} \frac{\eta \omega_c' V_c}{(\omega_c'^2 - R_2^2 \omega_p^2)} \tag{2.41}$$

$$N \equiv -\frac{1}{2} \frac{\Gamma^2 \rho_o \eta V_c}{(\omega_c'^2 - R_2^2 \omega_p^2)} \quad . \tag{2.42}$$

After substitution the first-order pump frequency solution is removed and second-order terms involving products of the small signal quantities are ignored. Equations 2.8 and 2.9 then become

$$\left[\beta_n(\omega_n - j\frac{d}{dt})v_n + \frac{\eta R_n^2 \rho_n}{\epsilon_o}\right] e^{j(\omega_n t - \beta_n z)} - M\beta_{n+1}^2 v_n e^{j(\omega_{n+1} t - \beta_{n+1} z)}$$

$$- M\beta_{n-1}^2 v_n e^{j(\omega_{n-1} t - \beta_{n-1} z)} = 0 \tag{2.43}$$

$$\left[\beta_n \bar{\rho}_o v_n + (j\frac{d}{dt} - \omega_n)\rho_n\right] e^{j(\omega_n t - \beta_n z)} + \left[N(\beta_n + \Gamma)v_n + M(\beta_n + \Gamma)\rho_n\right]$$

$$\cdot e^{j(\omega_{n+1} t - \beta_{n+1} z)} + \left[N(\beta_n - \Gamma)v_n + M(\beta_n - \Gamma)\rho_n\right] e^{j(\omega_{n-1} t - \beta_{n-1} z} = 0 \tag{2.44}$$

Making use of the orthogonality relation

$$\int_0^{2\pi/\Gamma} e^{-j\beta_n z} e^{j\beta_m z} dz = \delta_n^m (\frac{2\pi}{\Gamma}) \tag{2.45}$$

the equations become

$$-M\,\beta_m^2 v_{m-1} + (\omega_m\beta_m - j\beta_m\frac{d}{dt})v_m + \frac{R_m^2\,\rho_m}{\epsilon_o} - M\,\beta_m^2 v_{m+1} = 0 \qquad (2.46)$$

$$N(\beta_{m-1}+\Gamma)v_{m-1} + M(\beta_{m-1}+\Gamma)\rho_{m-1} + \beta_m\bar{\rho}_o v_m - (\omega_m - j\frac{d}{dt})\rho_m$$

$$+ N(\beta_{m+1}-\Gamma)v_{m+1} + M(\beta_{m+1}-\Gamma)\rho_{m+1} = 0 \ . \qquad (2.47)$$

Note that the $e^{j\omega_n t}$ dependence which was factored out in equation 2.38 has combined with the time dependence of the pump terms to cancel from the equations, and that as a result of this choice, the coefficients are constants.

Equations 2.46 and 2.47 represent a doubly infinite set of coupled equations. Note that for each ω_m, coupling to ω_{m+1} and ω_{m-1} terms occurs through the action of the pump. This is readily seen if one recalls that the constants M and N contain the pump wave amplitude V_c. If $V_c = 0$, the coupling vanishes. Thus the signal frequency ω_o is coupled to the principal idler frequency ω_{-1} and to another idler frequency ω_{+1} whose time dependence is the sum of the signal and pump frequencies.

It is now postulated that the strongest interaction takes place only with the ω_{-1} idler wave, and that the others can be neglected. This argument is made on the basis that it is the only wave that has about the same time dependence as the signal and also that it has about the same phase velocity as the signal wave. This reduces the problem to the familiar three-frequency case which has been solved for other types of parametric amplifiers. Coupling only to the idler wave means

that only the -1 and 0 terms in equations 2.46 and 2.47 are retained. Writing out the equations which remain, the following coupled equations are obtained:

$$(\omega_{-1}\beta_{-1} - j\beta_{-1}\frac{d}{dt})v_{-1} + \frac{\eta R_{-1}^2 \rho_{-1}}{\epsilon_o} - M\beta_{-1}^2 v_o = 0 \quad (2.48)$$

$$-M\beta_o^2 v_{-1} + (\omega_o\beta_o - j\beta_o\frac{d}{dt})v_o + \frac{R_o^2 \rho_o}{\epsilon_o} = 0 \quad (2.49)$$

$$\beta_{-1}\bar{\rho}_o v_{-1} + (j\frac{d}{dt} - \omega_{-1})\rho_{-1} + N(\beta_o - \Gamma)v_o + M(\beta_o - \Gamma)\rho_o = 0 \quad (2.50)$$

$$N(\Gamma + \beta_{-1})v_{-1} + M(\beta_{-1} + \Gamma)\rho_{-1} + \beta_o\bar{\rho}_o v_o + (j\frac{d}{dt} - \omega_o)\rho_o = 0 \quad (2.51)$$

These are four equations in the four unknowns v_{-1}, ρ_{-1}, v_o and ρ_o. Assuming dependence as $e^{j\mu\omega_q t}$, where μ is the complex incremental propagation constant, and setting the resulting determinant of the coefficients equal to zero yields the characteristic equation

$$\mu^4 + 2\mu^3 f' + \mu^2(2-f')\left[\frac{f'^2}{2-f'} - 2 + \frac{\epsilon^2}{2} + \frac{b'\epsilon^2}{2}\right] - \mu(2-f')\left[2f' - \frac{f'\epsilon^2}{2} - \frac{f'b'\epsilon^2}{2} - \frac{R_o^2 b'(b'+2)\epsilon^2}{2(2-f')}\right] + \epsilon^2(2-f')\left[\frac{f'}{4} + \frac{f'b'}{2} - \frac{(b'+2)^2}{4} - \frac{R_o^4(b'+2)}{4(2-f')^2} + \frac{R_o^2 b'(b'+2)}{2(2-f')} - \frac{R_o^2 b'(b'+2)}{2} - \frac{R_o^2(b'+2)}{2}\right] + \frac{1}{16}\epsilon^4(2-f')^2(b'+1)^2 = 0 \quad (2.52)$$

in which the parameters are defined by

$$f' \equiv \frac{2\omega_p - \omega_c'}{\omega_p} \quad (2.53)$$

$$b' \equiv \frac{\Gamma - 2\beta}{\beta} \tag{2.54}$$

$$\epsilon \equiv \frac{\Gamma\beta_n V_c}{(\omega'^2_c - R_2^2\omega_p^2)} \sqrt{\frac{\omega'_c}{\omega_q}} \tag{2.55}$$

In addition, the assumption that $(R_o/R_{-1})^2 \approx 1$ has been used. This is a good approximation since the signal and idler frequencies are almost equal in the normal operating range.

2.3 The Degenerate Case

It will be of interest at this point to investigate the behavior in the special limiting case in which the phase velocity of the circuit pump wave is exactly the same as that of the fast-signal space-charge wave and in which the pumping frequency is twice that of the signal frequency. The finite geometry effects will be ignored so all reduction factors are set equal to unity. This then corresponds to the case which has been treated by Wade and Adler through the use of a harmonic oscillator analog.

In this case the phase velocity of the fast-signal space-charge wave is given by

$$v_p = \frac{\omega}{\beta} = \frac{u_o}{1 - \frac{\omega_p}{\omega}} \tag{2.56}$$

while that of the circuit wave is given by

$$v_{p_c} = \frac{2\omega}{\Gamma} \quad . \tag{2.57}$$

Equating these, one finds that

$$\Gamma = 2\left(\frac{\omega - \omega_p}{u_o}\right) = 2\beta \quad . \tag{2.58}$$

Thus in equation 2.52 the phase velocities are made the same by letting $b' = 0$. The Doppler-shifted pump frequency as viewed in the moving frame of reference then becomes (using equation 2.17)

$$\omega_c' = 2\omega - 2\beta u_o = 2\omega_p \quad . \tag{2.59}$$

Therefore, the parameter f' must also be zero for this special case. Under these conditions, the characteristic equation 2.52 becomes

$$\mu^4 - \mu^2\left(4 - \frac{8}{9}\frac{\beta^4\eta^2 V_c^2}{\omega_p^4}\right) - 4\beta^4\eta^2 V_c^2 + \frac{16}{81}\frac{\beta^8\eta^4 V_c^4}{\omega_p^4} = 0 \tag{2.60}$$

Defining $\epsilon'^2 = \dfrac{\beta^4\eta^2 V_c^2}{\omega_p^4}$ and using the quadratic formula, one gets

$$\mu^2 \approx 2 - \frac{4}{9}\epsilon'^2 \pm 2\sqrt{1 + \frac{5}{9}\epsilon'^2} \tag{2.61}$$

where a term in ϵ'^4 has been neglected. This would correspond to the case of weak pumping fields.

For no pumping fields, the roots become:

$$\mu^2 = 0 \quad , \qquad \mu = \pm 2 \quad . \tag{2.62}$$

The latter pair of roots correspond to slow space-charge waves at the signal $(\mu = -2)$ and idler $(\mu = +2)$ frequencies, and are not influenced much by the pump strength.

Expanding the radical, it is noted that as ϵ' increases, the two

zero roots become

$$\mu = \pm j\epsilon' \quad . \tag{2.63}$$

These represent a growing wave and a decaying wave arising from the coupling of the fast space-charge waves at the signal and idler frequencies. Using the relation

$$\Gamma V_c = 2\beta V_c = E_z \tag{2.64}$$

one can write an expression for the growing wave in the laboratory frame of reference as

$$v_o = v_{oo} e^{\frac{\beta\eta E_z}{2\omega_p u_o}} \quad . \tag{2.65}$$

Using Pierce's definition (28) of the interaction impedance

$$K = \frac{E_z^2}{2\beta^2 P} \tag{2.66}$$

where P represents the power flow on the circuit, and the velocity relation

$$u_o = \sqrt{2\eta V_o} \tag{2.67}$$

equation 2.65 can be written as

$$v_o = v_{oo} e^{\frac{1}{2}\frac{\omega}{u_o}\frac{\sqrt{2KP}}{V_o}\frac{\omega}{\omega_p}\left(1 - \frac{\omega_p}{\omega}\right)^2} \tag{2.68}$$

which is in exact agreement with the results obtained by Wade and Adler. Thus it has been shown that in this special case the gain predicted from two completely different analytical approaches is the same.

2.4 Discussion of the Physical Nature of the Parameters

In the moving frame of reference, the parameters are

$$f' \equiv \frac{2\omega_q - \omega'_c}{\omega_p} \tag{2.69}$$

$$b' \equiv \frac{\Gamma - 2\beta}{\beta} \tag{2.70}$$

$$\epsilon \equiv \frac{\Gamma \beta \eta V_c}{(\omega'^2_c - R_2^2 \omega_p^2)} \sqrt{\frac{\omega'_c}{\omega_p}} \quad . \tag{2.71}$$

f' is a measure of the amount by which the Doppler-shifted pump frequency differs from twice the reduced plasma frequency. b' and ϵ are merely convenient mathematical parameters with no particular physical significance. ϵ will be referred to as the "pump strength" parameter, however, since it does contain the circuit field amplitude. It is felt that a set of parameters which are a measure of physical quantities in the laboratory frame of reference will be more useful.

The signal and idler frequencies in the laboratory frame can be written as

$$\omega = \omega_q + \beta u_o \tag{2.72}$$

$$\omega_i = \omega_q - \omega'_c + (\beta - \Gamma) u_o \tag{2.73}$$

By our definition

$$\omega_i = \omega - \omega_c \tag{2.74}$$

Combining these three equations and substituting b', one gets

$$b' \approx \frac{\omega_c - 2\omega}{\omega} \tag{2.75}$$

under the condition that $\omega_q/\omega \ll 1$. Thus the prime can be dropped and b becomes a frequency parameter which is a measure of the difference between the pump frequency and twice the signal frequency. Also $b = 0$ corresponds to degenerate operation.

Now let us examine the difference between the fast signal space-charge-wave velocity and the circuit or pump-wave velocity. This can be written in terms of the moving reference frame quantities as

$$v_s - v_p = \frac{\omega_q + \beta u_o}{\beta} - \frac{\omega' + \Gamma u_o}{\Gamma} \quad . \tag{2.76}$$

Dividing by v_p and substituting b' and f' , one gets

$$\frac{v_s - v_p}{v_p} = \frac{\omega_q}{\omega_c}(b' + f') \quad . \tag{2.77}$$

Next, define

$$f \equiv b' + f' \tag{2.78}$$

and write it as

$$f = \frac{\omega_c}{\omega_q}\left(\frac{v_s - v_p}{v_p}\right) \quad . \tag{2.79}$$

f is thus seen to be a parameter which is a measure of the difference in phase velocities of the two waves.

Another factor of prime importance is the depth of modulation index "m", which represents the magnitude of the total a.c. beam current induced on the beam at the pumping frequency normalized to the d.c. beam current. It determines the pump harmonic content of the beam and thus the number of idler waves which may couple noise to the beam. The

amplitude of the a.c. current due to the pumping signal can be written from equations 2.7, 2.24, and 2.25 as

$$i_c \cong \rho_2 u_o + v_2 \bar{\rho}_o \quad . \tag{2.80}$$

Substituting for ρ_2 and v_2 in this equation and using the definitions for C_i and D_j, one gets

$$i_c = \rho_c u_o \left[\left(1 + \frac{\omega_c'}{\Gamma u_o}\right) e^{j(\omega_c' t - \Gamma z')} - \frac{\omega_c' \beta_i}{2\Gamma R_2 \omega_p} \left(1 + \frac{R_2 \omega_p}{\omega_c'}\right)\left(1 + \frac{R_2 \omega_p}{\beta_i u_o}\right) e^{j(R_2 \omega_p - \beta_i z)} \right.$$

$$\left. + \frac{\omega_c' \beta_i}{2\Gamma R_2 \omega_p} \left(1 - \frac{R_2 \omega_p}{\omega_c'}\right)\left(1 - \frac{R_2 \omega_p}{\beta_j u_o}\right) e^{-j(R_2 \omega_p t + \beta_j z')} \right] \quad . \tag{2.81}$$

Several of the terms in this equation can be neglected. Since $\Gamma u_o \approx \omega_c$ and $\omega_c'/\omega_c \ll 1$, $\omega_c'/\Gamma u_o$ can be neglected. Also, $\frac{R_2 \omega_p}{\beta_i u_o} \approx \frac{R_2 \omega_p}{\beta_j u_o} \approx \frac{\omega_p}{\omega_c} \ll 1$, so these terms can be neglected. Since the d.c. current is given by

$$I_o = - \overline{\rho_o} \, u_o \tag{2.82}$$

one can write

$$m = \left| \frac{i_c}{I_o} \right| \approx \frac{\rho_c}{\overline{\rho_o}} \left[e^{j(\omega_c' t - \Gamma z')} - \frac{\omega_c' \beta_i}{2\Gamma R_2 \omega_p} \left(1 + \frac{R_2 \omega_p}{\omega_c'}\right) e^{j(R_2 \omega_p t - \beta_i z')} \right.$$

$$\left. + \frac{\omega_c' \beta_j}{2\Gamma R_2 \omega_p} \left(1 - \frac{R_2 \omega_p}{\omega_c'}\right) e^{-j(R_2 \omega_p t + \beta_j z')} \right] \quad . \tag{2.83}$$

Since only the first term in this expression has been retained in the analysis, it may prove of some interest to consider the depth of modulation of this wave only, which will be called m_1. From

equation 2.83

$$m_1 \approx \left| \frac{\rho_c}{\rho_o} \right| \quad . \tag{2.84}$$

Eliminating v_c in equations 2.20 and 2.21, one can write

$$\frac{\rho_c}{\rho_o} = \frac{\Gamma_n^2 V_c}{\omega_c'^2 - R_2^2 \omega_p^2} \tag{2.85}$$

Using the definitions 2.54, 2.55 and 2.17, and squaring, this can be written

$$\left| \frac{\rho_c}{\rho_o} \right|^2 = \frac{(b' + 2)^2 \epsilon^2 \omega_q}{\omega_c - \Gamma u_o} \quad . \tag{2.86}$$

Substituting for ω_c and Γ in terms of f' and b', one finally obtains

$$m_1 \approx \left| \frac{\rho_c}{\rho_o} \right| = \frac{(b' + 2)\epsilon}{\sqrt{2 - f'}} \quad . \tag{2.87}$$

This is an expression for the depth of modulation of the important wave in terms of the other parameters. f, b, m, and m_1 now represent a set of parameters which will allow interpretation of the results from a physical point of view in the laboratory frame.

2.5 Solutions of the Characteristic Equation

The fourth degree polynomial has been solved for the following ranges of parameters

ϵ	b'	f'
0.25	-1 to +2	-7 to +7
0.50	-1 to +3	"
0.75	-1 to +2	"

A typical plot of the roots is shown in Figure 2.1 . The dependence of the wave represented by these solutions is as

$$e^{x_i \beta_q z} \; e^{j[\omega t - (\beta - y_i \beta_q) z]} \tag{2.88}$$

for the signal frequency, and as

$$e^{x_i \beta_q z} \; e^{j[(\omega - \omega_c) t - (\beta - \Gamma - y_i \beta_q) z]} \tag{2.89}$$

which can be written

$$e^{x_i \beta_q z} \; e^{j[(\omega - \omega_c) t + (\beta(b' + 1 + y_i \beta_q) z]} \tag{2.90}$$

for the idler frequency. β_q is the reduced plasma wave number given by

$$\beta_q \equiv \frac{\omega_q}{u_o} \quad . \tag{2.91}$$

Substituting into equation 2.88 one can write for the growing-wave signal frequency velocity modulation

$$v_{out} = v_{in} \exp\left\{x_1 \beta_q L + j[\omega t - (\beta - y_1 \beta_q) z]\right\} \tag{2.92}$$

and

$$\text{Gain} = \left(\frac{v_{out}}{v_{in}}\right)^2 = 8.68 x_1 (2\pi N_q) \text{db} \tag{2.93}$$

where N_q is the length in reduced plasma wavelengths.

The nature of the waves outside the interaction region can be determined by substituting the roots of the equation into equations 2.88 and 2.90. One sees that $y_1 \approx 0$ and $y_3 \approx -2$ will represent one pair of waves. Upon substitution into 2.88, it is noted that these are fast and slow space-charge waves, respectively, at the signal frequency.

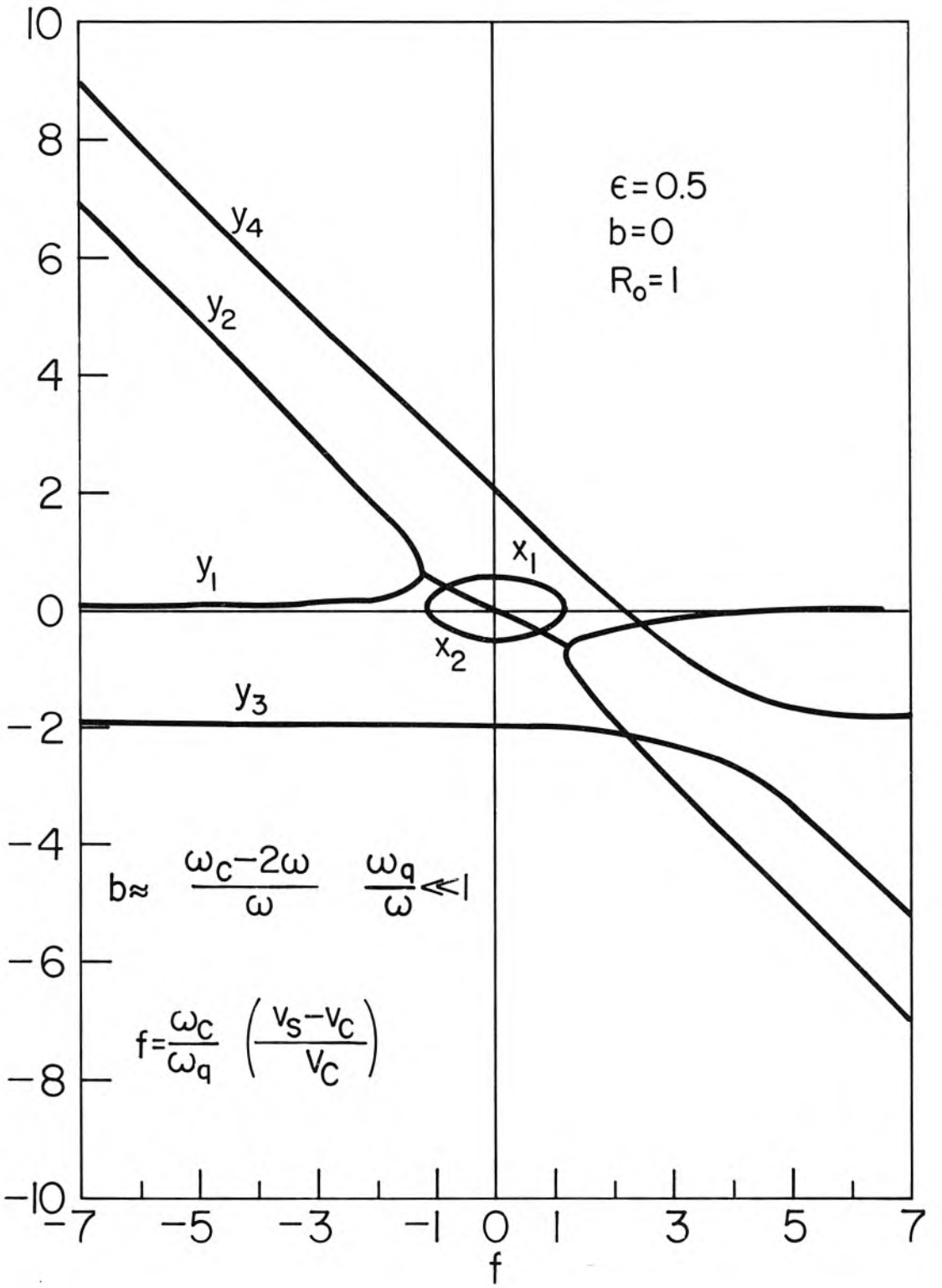

Fig. 2.1 A typical plot of the propagation constant $\mu = ix + y$. The dependence of the normal modes is given by

$$e^{x_i \beta_q z} \; e^{j[\omega t-(\beta - y_i \beta_q)z]}$$

Similarly, $y_2 \approx -f$, and $y_4 \approx -f+2$, and upon substitution into equation 2.90 they are seen to represent fast and slow space-charge waves respectively at the idler frequency. The gain is seen to arise from coupling of the fast signal and fast idler wave.

The case for $b = 0$ was chosen as an illustration because it also contains the special degenerate case treated in the last section. As can be seen in Figure 2.1, the roots at $f = 0$ are $\mu \approx \pm j\epsilon, \pm 2$ as were calculated in the last section for the case of exactly synchronous phase velocities and pumping at twice the signal frequency. From this figure, one can see the gain variation as a function of the relative phase velocities of the waves. An estimate of the accuracy of the adjustment of the phase velocity necessary to achieve gain can be gotten from equation 2.79. One can see that

$$\Delta v_s = \frac{\omega_q}{\omega_c} v_c \Delta f \tag{2.91}$$

is the allowed spread in signal space-charge-wave velocity where Δf is defined by the limiting f values at the extremities of the island of growth, as in Figure 2.1. Assuming $v_c \approx v_s$ gives

$$\frac{\Delta v_s}{v_s} \approx \frac{\omega_q}{\omega_c} \Delta f \tag{2.92}$$

which is about 5 to 10% for normal ω_q/ω_c and for $\Delta f \approx 2$, as in Figure 2.1 . Thus it is seen that the adjustment should not be extremely critical.

In Figure 2.2 the maximum growth factor x_1 is plotted as a function of b and m_1 or ϵ . Operating at $b = -1$ corresponds to pumping at the signal frequency, $b = 0$ corresponds to pumping at

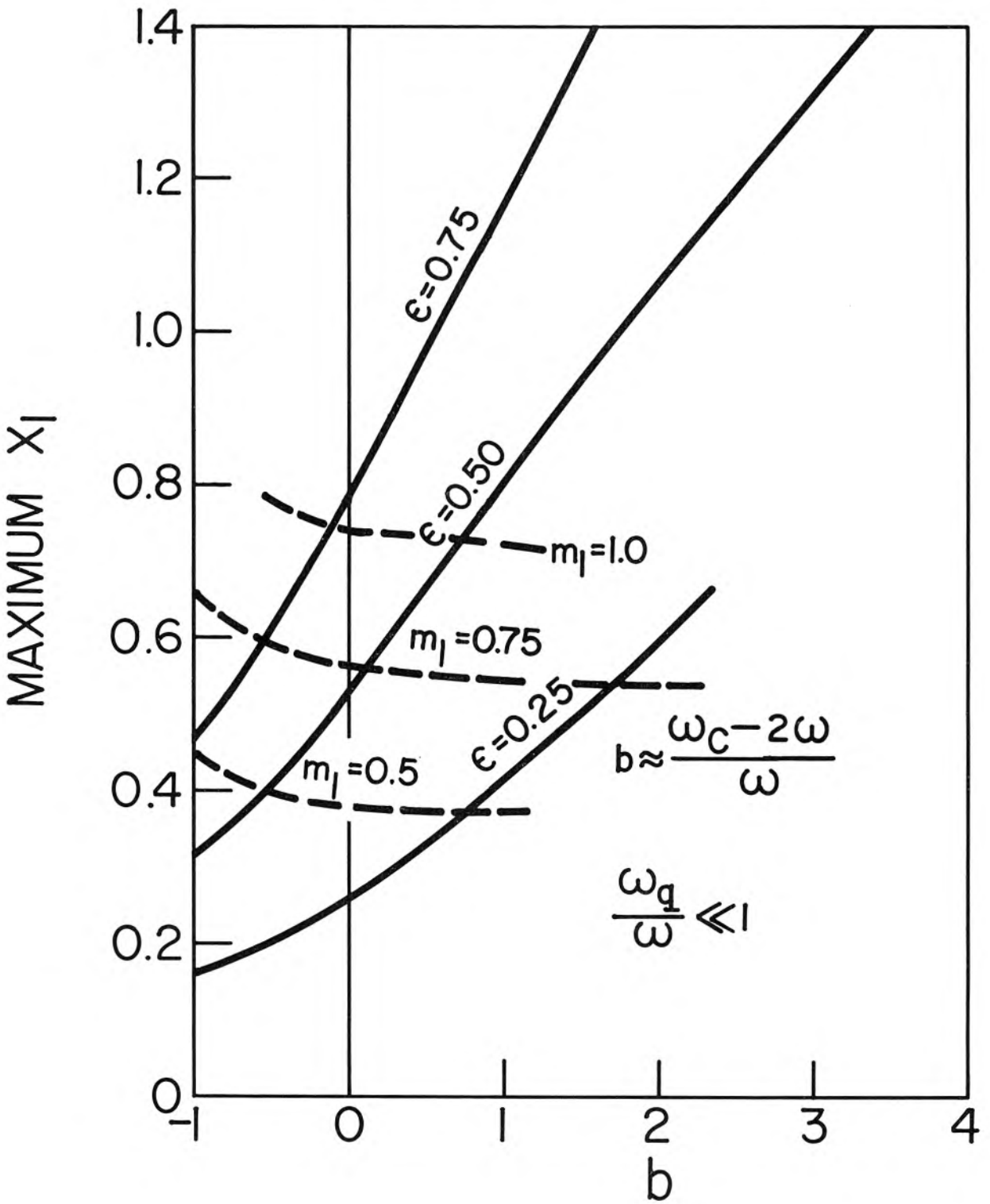

Fig. 2.2 The maximum value of the growth constant x_1 as a function of the frequency parameter b . b = 0 corresponds to the degenerate case.

twice the signal frequency, and higher b corresponds to higher relative pumping frequency. The ability to achieve gain at the low pump frequencies is explained by the fact that the Doppler-shifted pump frequency can still be adjusted to approximately twice the reduced plasma frequency in the moving reference frame by appropriate adjustment of the relative phase velocities. At $b = 0$ the growth factor for a given value of m_1 is the same as that obtained by Louisell and Quate ( ) for the same m for their thin-beam case in which the phase velocities are exactly synchronous and the pump frequency is twice the signal frequency. The agreement in this analogous case provides a check on the validity of the analysis under the limitations of the assumptions involved.

2.6 Consideration of the Total Depth of Modulation

As has been mentioned, the necessity for driving the beam to the saturation region results in the generation of pump harmonics and as a consequence a complete set of idlers for each harmonic. It is of prime importance, therefore, to determine what degree of saturation is needed to achieve reasonable gains per unit length. The natural unit of length to use for comparison with other devices is the plasma wavelength.

In equation 2.83 an expression was derived for the depth of modulation on the beam. For simplicity, let us again study the degenerate case ($f' = b' = 0$, $R_n = 1$) . Under these conditions equation 2.83 becomes

$$m \approx \frac{\beta^2 \eta V_c}{\omega_p^2} \left[\frac{4}{3} e^{j(2\omega_p t - 2\beta z')} - \frac{\beta_i}{\beta} e^{j(\omega_p t - \beta_i z')} + \frac{1}{3} \frac{\beta_j}{\beta} e^{-j(\omega_p t + \beta_j z')} \right] . \tag{2.93}$$

Using the definition of ϵ' for this special case, i.e.,

$$\epsilon' = \frac{\beta^2 \eta V_c}{\omega_p^2} \tag{2.94}$$

and the approximations

$$\frac{\beta_i}{\beta} \approx \frac{\beta_j}{\beta} \approx 2 \tag{2.95}$$

m can be written

$$m \approx \epsilon' \left[\frac{4}{3} e^{j(2\omega_p t - 2\beta' z)} - 2e^{j(\omega_p t - \beta_i' z)} + \frac{2}{3} e^{-j(\omega_p t + \beta_j' z)} \right] \tag{2.96}$$

Shifting to the laboratory frame of reference, this becomes

$$m \approx \epsilon' \left[\frac{4}{3} e^{j(2\omega t - 2\beta z)} - 2e^{j(2\omega t - \beta_i z)} + \frac{2}{3} e^{j(2\omega t - \beta_j z)} \right] . \tag{2.97}$$

Factoring out the time varying component and the rapidly varying z component $(e^{j2\omega t - (2\omega/u_o)z})$, and taking the magnitude of the slowly varying envelope, this reduces to

$$m = \epsilon' \left[\frac{56}{9} - \frac{16}{3} \cos \beta_p z - \frac{8}{3} \cos 2\beta_p z + \frac{16}{9} \cos 3\beta_p z \right]^{1/2} . \tag{2.98}$$

This quantity is plotted in Fig. 2.3 for $\epsilon' = 0.75$, 0.37, and 0.18, which correspond to approximately 40, 20, and 10 db gain per plasma wavelength respectively. For comparison, the dashed lines represent the corresponding values for m_1, or for the total m of Louisell

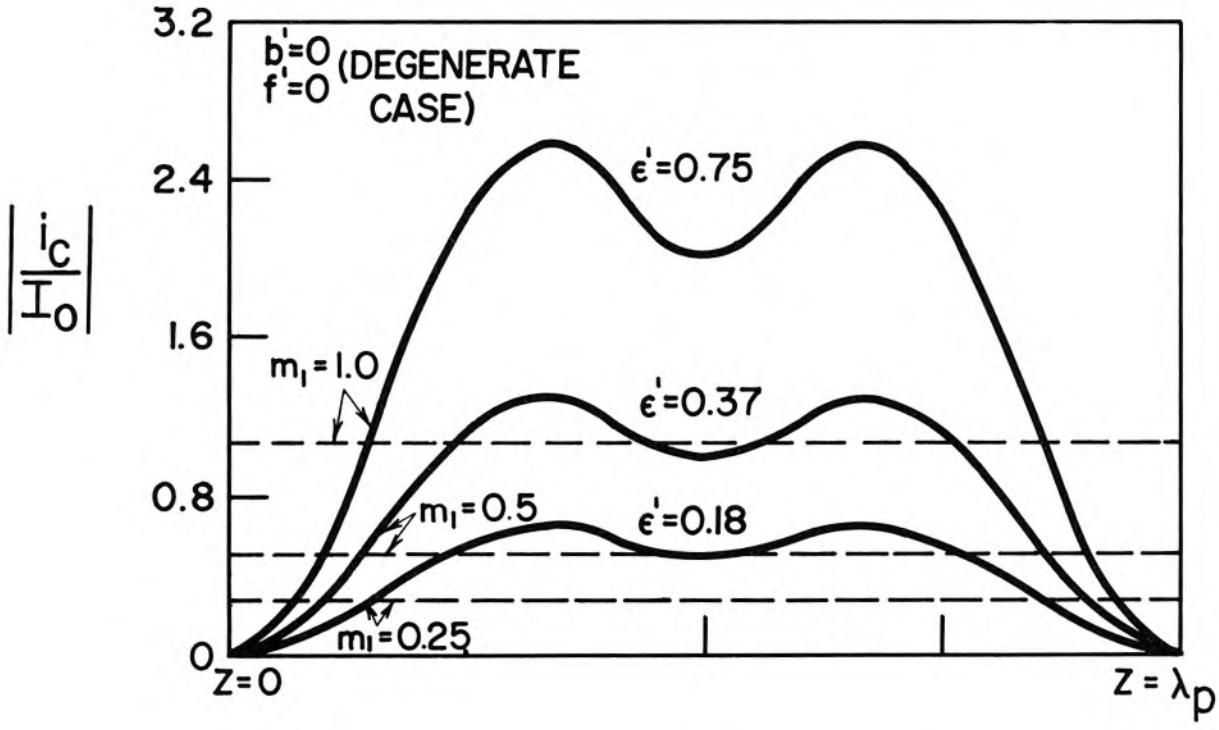

Fig. 2.3 The saturation characteristics of the beam in the pumping region of a circuit-pumped amplifier. It is evident that operation only for $m_1 < 0.5$ can be physically realized unless measures are taken to excite only a single pump mode.

and Quate (1) .

Since an electron beam is normally assumed saturated when $m = 1$, it is obvious that the 40 db gain curve not only violates the small signal assumptions but cannot be realized physically. The 20 db curve is felt to be realizable but in violation of the assumptions. It is seen that the only apparent advantage to be gained using the circuit-pumped amplifier is a short region where the beam is unsaturated in which up to 5 db of signal gain may be achieved. However, there follows a longer region in which the beam becomes more saturated than the beam in the space-charge pumped amplifier for the same gain per plasma wavelength.

2.7 Limitations of the Analysis

The neglect of the effects of higher order idler waves in this analysis casts some doubt upon the validity of the predicted gain behavior, but even more serious is the neglect of the noise which is undoubtedly coupled in from these waves. The assumption of a single pumping wave, although drastic, is necessary if one is to obtain differential equations with constant coefficients. The effect of the other pump waves in saturating the beam will be to render the small-signal analysis invalid except for the cases of weaker pumping. The latter difficulty can be circumvented in practice by devising a method to excite only the desired pumping wave (Pierce's δ_3 mode). In Chapters III and IV the higher order idler waves and multiple pump waves will be included in more sophisticated treatments.

CHAPTER III

A COUPLED-MODE TREATMENT OF THE MULTIPLE-FREQUENCY ELECTRON BEAM FOR A SINGLE PUMPING WAVE

3.1 Introduction

In this chapter general equations are obtained which can be used to predict the performance of a large class of devices employing electron beams and involving multiple frequencies. Again, the single-pumping-wave assumption is made, but the effects of all higher order idlers are included. The equations are written in coupled-mode formalism since, in many cases, a considerable reduction in the complexity of the problem can be achieved. As an example, the slow space-charge waves which were included in the three-frequency analysis, but which did not contribute to the gain mechanism, could have been separated out and ignored if equations 2.45 and 2.46 had been in coupled-mode form. The characteristic equation would have been quadratic and the need for resorting to computer calculation avoided. A discussion of the properties of a system which can be determined from an examination of the coupled-mode equations describing that system is included before the analysis is undertaken.

3.2 General Discussion of Coupled Modes

The first objective in the formulation of the problem is to find a new set of equations which describe the elements of the uncoupled system in terms of separately excitable normal mode amplitudes. The variable quantities in these new equations are the normalized mode amplitudes and are linear combinations of physical variables in the original equations describing the uncoupled system elements. When coupling is introduced between the elements, new terms representing coupling to

other normal modes of the elements appear in the equations.

A typical set of equations representing the coupling of two traveling-wave modes is written

$$(\frac{d}{dz} + j\beta_1)A_1 + jk_{12}A_2 = 0 \tag{3.1}$$

$$jk_{21}A_1 + (\frac{d}{dz} + j\beta_2)A_2 = 0 \tag{3.2}$$

where the A_i are the mode amplitudes and the k's the coupling coefficients. If no coupling exists ($k_{12} = k_{21} = 0$), and if the time dependence of the mode amplitudes is $e^{j\omega t}$, it is seen that the solutions of the equations are two traveling waves

$$A_1 = C_1 e^{j(\omega t - \beta_1 z)} \tag{3.3}$$

$$A_2 = C_2 e^{j(\omega t - \beta_2 z)} \tag{3.4}$$

which propagate on the uncoupled system elements. Solutions of the coupled system will cause perturbations of the propagation constants β_i. If one assumes a solution of the form $e^{j\mu z}$ the solutions for μ are given by

$$\mu = -\frac{(\beta_1 + \beta_2)}{2} \pm \frac{(\beta_1 - \beta_2)}{2} \sqrt{1 + \frac{4k_{12}k_{21}}{(\beta_1 - \beta_2)^2}} \tag{3.5}$$

Again for zero coupling, it is seen that the solutions are the propagation constants β_1 and β_2. If the signs of k_{12} and k_{21} are the same, and the inequality

$$k_e = \left| \frac{4k_{12}k_{21}}{(\beta_1 - \beta_2)^2} \right| \gtrsim 1 \tag{3.6}$$

holds, the difference between the values for the propagation constants describing the coupled system increases as the coupling is increased. This means that the phase velocities of the waves are diverging. This will be referred to as "passive"* coupling. Excitation of either A_1 or A_2 in a passively coupled system will cause beating, i.e., partial or total periodic transfer of energy between the two modes.

On the other hand, if the signs are opposite and $k_e > 1$, the μ's become complex and an unstable condition resulting in an exponentially growing wave develops. This will be known as "active" coupling and is the type of behavior sought in all traveling-wave amplifiers. Note from equation 3.6 that the effective coupling parameter k_e is very sensitive to the difference in the β's of the uncoupled system modes, and that modes with similar values of β tend to be tightly coupled. If, however, the difference in the β's is large or the product of the k's is small such that $k_e \ll 1$, the effect of the coupling can be ignored. This argument usually reduces the complexity by reducing the number of equations that must be solved.

It might be well to note that these concepts are the same as those used in discussions of the problem of diagonalizing a matrix, and that the term pairs "mode amplitude" and "eigenvector", "normal propagation constant" and "eigenvalue", and "uncoupled system" and "normal coordinate system", respectively, may be used interchangeably.

---

*The terms "active" and "passive" coupling were first used by Cook and Louisell at the Western Electronics Show and Convention, San Francisco, 1959.

3.3 Formulation of the Basic Equations

Under the same assumptions that were made in the three-frequency analysis of the circuit-pumped amplifier, equations 2.1, 2.2, and 2.3 can be combined to give

$$\frac{\partial^2 v}{\partial t^2} + \frac{\partial^2}{\partial z \partial t}\left(\frac{v^2}{2}\right) - R^2 \omega_p^2 \frac{u_o}{I_o} i = \eta \frac{\partial^2 V}{\partial z \partial t} \tag{3.7}$$

Equations 2.4 and 2.7 are combined to give

$$v^2 \frac{\partial i}{\partial z} + v \frac{\partial i}{\partial t} - i \frac{\partial v}{\partial t} = 0 \tag{3.8}$$

Note that the charge density has been eliminated instead of the current as in the three-frequency analysis. As before, the nonlinear terms in the differential equations will give rise to a series of terms whose time dependence is given by

$$\omega_n = \omega + n\,\omega_c \qquad n = \cdots -2,-1,0,1,2, \cdots \tag{3.9}$$

An appropriate form for the solution to the equations is then written

$$i = -I_o + \frac{i_c(z)}{2} e^{j\omega_c t} + \frac{i_c^*(z)}{2} e^{-j\omega_c t} + \sum_n i_n(z) e^{j\omega_n t} \tag{3.10}$$

and

$$v = u_o + \frac{v_c(z)}{2} e^{j\omega_c t} + \frac{v_c^*(z)}{2} e^{-j\omega_c t} + \sum_n v_n(z) e^{j\omega_n t} \tag{3.11}$$

It is understood that the physical variables are represented by the real parts of the exponentials in the last terms. Allowing coupling to a slow wave circuit at all frequencies requires the inclusion of the circuit equations for forward circuit waves[28]

$$\left(\frac{\partial}{\partial z} + j\Gamma_c\right)V_c = -\frac{K_c\sigma}{2}\frac{\partial i_c}{\partial z} \tag{3.12}$$

and

$$\left(\frac{\partial}{\partial z} + j\Gamma_n\right)V_n = -\frac{K_n\sigma}{2}\frac{\partial i_n}{\partial z}, \quad n = \cdots -2,-1,0,1,2, \cdots \tag{3.13}$$

where Γ_i and K_i represent the circuit propagation constant and interaction impedance respectively at the i^{th} frequency. An appropriate form for the total circuit voltage V in equation 3.7 is

$$V = V_c(z)e^{j\omega_c t} + \sum_n V_n(z)e^{j\omega_n t} \tag{3.14}$$

Substituting equations 3.10, 3.11 and 3.14 into 3.7 and 3.8, and neglecting products of pump quantities as compared to d.c. quantities* and also terms involving products of signal quantities, the following equations are obtained

$$e^{j\omega_n t}\left[-\omega_n^2 v_n + j\omega_n u_o \frac{dv_n}{dz} - \frac{R_n^2\omega_p^2 u_o i_n}{I_o} - j\eta\omega_n \frac{dv_n}{dz}\right] + e^{j(\omega_n+\omega_c)t}\left[j\frac{(\omega_n+\omega_c)}{2}\left(v_n\frac{dv_c}{dz} + v_c\frac{dv_n}{dz}\right)\right] + e^{j(\omega_n-\omega_c)t}\left[j\frac{(\omega_n-\omega_c)}{2}\left(v_n\frac{dv_c^*}{dz} + v_c^*\frac{dv_n}{dz}\right)\right]$$
$$+e^{j\omega_c t}\left[j\frac{\omega_c u_o}{2}\frac{dv_c}{dz} - \frac{\omega_c^2}{2}v_c - R_c^2\frac{\omega_p^2}{I_o}\frac{u_o i_c}{2} - j\eta\omega_c\frac{dv_c}{dz}\right] + e^{-j\omega_c t}\left[-\frac{\omega_c^2 v_c^*}{2} - j\omega_c u_o\frac{dv_c^*}{dz} - R_c^2\frac{\omega_p^2}{I_o}\frac{u_o i_c^*}{2} + j\omega_c\eta\frac{dv_c^*}{dz}\right] = 0 \tag{3.15}$$

$$e^{j\omega_n t}\left[u_o^2\frac{di_n}{dz} + j\omega_n u_o i_n + j\omega_n v_n I_o\right] + e^{j(\omega_n+\omega_c)t}\left[u_o v_c\frac{di_n}{dz} + u_o v_n\frac{di_c}{dz} + j\frac{\omega_n v_c i_n}{2} + j\frac{\omega_c i_c v_n}{2} - j\frac{\omega_n v_c i_n}{2} - j\frac{\omega_c v_c i_n}{2}\right]$$
$$+e^{j(\omega_n-\omega_c)t}\left[u_o v_c^*\frac{di_n}{dz} + u_o v_n\frac{di_c^*}{dz} + j\frac{\omega_n i_c v_c^*}{2} - j\frac{\omega_c i_c^* v_n}{2} - j\frac{\omega_n v_c i_c^*}{2} + j\frac{\omega_c v_c^* i_n}{2}\right] + e^{j\omega_c t}\left[\frac{u_o^2}{2}\frac{di_c}{dz} + j\frac{\omega_c u_o i_c}{2} + j\frac{\omega_c v_c I_o}{2}\right] \tag{3.16}$$
$$+e^{-j\omega_c t}\left[\frac{u_o^2}{2}\frac{di_c^*}{dz} - j\frac{\omega_c u_o i_c^*}{2} - j\frac{\omega_c v_c^* I_o}{2}\right] = 0$$

*In essence, this is the neglect of pump harmonics which may be of the order of some of the signal quantities which are retained.

After applying the orthogonality relation

$$\int_0^{\frac{2\pi}{\omega_c}} e^{j\omega_n t}\, e^{-j\omega_s t}\, dt = \delta_n^s\left(\frac{2\pi}{\omega_c}\right) \tag{3.17}$$

the equations become

$$\frac{1}{2u_o}\left(v_c\frac{d}{dz}+\frac{dv_c}{dz}\right)v_{s-1}+\left(\frac{d}{dz}+j\frac{\omega_s}{u_o}\right)v_s+j\frac{R^2\omega_p^2 i_s}{\omega_s I_o}-\frac{\eta}{u_o}\frac{dv_s}{dz}+\frac{1}{2u_o}\left(\frac{dv_c^*}{dz}+v_c^*\frac{d}{dz}\right)v_{s+1}=0 \tag{3.18}$$

$$\left(\frac{1}{u_o}\frac{di_c}{dz}+j\frac{\omega_c i_c}{2u_o^2}-j\frac{\omega_{s-1} i_c}{2u_o^2}\right)v_{s-1}+\left(\frac{v_c}{u_o}\frac{d}{dz}+j\frac{\omega_{s-1} v_c}{2u_o^2}-j\frac{\omega_c v_c}{2u_o^2}\right)i_{s-1}+j\frac{\omega_s I_o v_s}{u_o^2}+$$

$$+\left(\frac{d}{dz}+j\frac{\omega_s}{u_o}\right)i_s+\left(\frac{1}{u_o}\frac{di_c^*}{dz}-j\frac{\omega_c i_c^*}{2u_o^2}-j\frac{\omega_{s+1} i_c^*}{2u_o^2}\right)v_{s+1}+\left(\frac{v_c^*}{u_o}\frac{d}{dz}+j\frac{\omega_{s+1} v_c^*}{2u_o^2}+j\frac{\omega_c v_c^*}{2u_o^2}\right)i_{s+1}=0 \tag{3.19}$$

for signal and idler frequencies, and

$$j\frac{\omega_c u_o}{2}\frac{dv_c}{dz}-\frac{\omega_c^2}{2}v_c-R_c^2\omega_p^2\frac{u_o}{I_o}\frac{i_c}{2}-j\eta\omega_c\frac{dv_c}{dz}=0 \tag{3.20}$$

$$\frac{u_o^2}{2}\frac{di_c}{dz}+j\frac{\omega_c u_o i_c}{2}+j\frac{\omega_c v_c I_o}{2}=0 \tag{3.21}$$

for the pump frequency. The subscript c has been retained for simplicity. The complex conjugates of equations 3.20 and 3.21 are also obtained as a consequence of the assumption of the pump solution in real form.

The next step is to put these equations, together with equations 3.12 and 3.13, into coupled-mode form. The first step will be to write equations 3.18 and 3.19 in terms of normal modes of the uncoupled system.

To accomplish this let v_c and $i_c \to 0$, and consider only the terms involving v_s and i_s. It is desired to express v_s and i_s in terms of new variables a_s^i which are linear combinations of these quantities, and which when substituted into the equations, allow them to be written in the form

$$(\frac{d}{dz} + j\beta_s^i)a_s^i = 0 \tag{3.22}$$

These new variables are the normal mode amplitudes, and the resulting equations for the uncoupled system are diagonalized.

Multiply equation 3.19 by some arbitrary constant C_1, and add to equation 3.18 to get

$$(\frac{d}{dz} + j\frac{\omega_s}{u_o})(v_s + C_1 i_s) + j\frac{I_o\omega_s}{u_o^2} C_1 v_s + j\frac{R_s^2\omega_s^2}{I_o\omega_s} i_s = 0 \tag{3.23}$$

For any wave which propagates as $e^{j(\omega t-\beta z)}$ on the beam, the following relation between the current and velocity modulation can be obtained from the continuity equation

$$i = \frac{\omega \bar{\rho}_o v}{(\omega-\beta u_o)} \tag{3.24}$$

To put equation 3.23 into the form of 3.22, let $\beta_s = \frac{\omega_s}{u_o} + \alpha$, and equate the undesired terms to zero, letting $(v_s + C_1 i_s) = a_s$.

$$\frac{I_o\omega_s}{u_o^2} C_1 v_s + \frac{R_s^2\omega_s^2 i_s}{J_o\omega_s} - \alpha(v_s + C_1 i_s) = 0 \tag{3.25}$$

Substituting for i_s in terms of v_s by equation 3.24, and using $I_o = -\rho_o u_o$, the coefficient of the C_1 term drops out, leaving

$$\alpha^2 = \frac{R_s^2 \omega_p^2}{u_o^2} \tag{3.26}$$

or

$$\alpha = \pm \frac{R_s \omega_p}{u_o} \tag{3.27}$$

These propagation constants are simply those of the fast and slow space charge waves on the electron beam. Choosing the upper sign for α, let

$$v_s = a_s - C_1 i_s \tag{3.28}$$

and substitute into equation 3.25. Equating the coefficients of a_s and $i_s = 0$, it is found that the equation is satisfied for

$$C_1^+ = \frac{R_s \omega_p u_o}{I_o \omega_s} \tag{3.29}$$

Choosing the negative sign for α results in

$$C_1^- = -\frac{R_s \omega_p u_o}{I_o \omega_s} \tag{3.30}$$

Recalling the original operation on equations 3.18 and 3.19, it is seen that multiplying 3.19 by $R_s \omega_p u_o / I_o \omega_s$ and adding and subtracting from equation 3.18 will give

$$\left[\frac{d}{dz} + j\left(\frac{\omega_s + R_s \omega_p}{u_o}\right)\right] a_s^- = 0 \tag{3.31}$$

$$\left[\frac{d}{dz} + j\left(\frac{\omega_s - R_s \omega_p}{u_o}\right)\right] a_s^+ = 0 \tag{3.32}$$

where

$$a_s^- \equiv \left(v_s + \frac{R_s \omega_p u_o}{I_o \omega_s} i_s\right) \tag{3.33}$$

$$a_s^+ \equiv \left(v_s - \frac{R_s \omega_s u_o}{I_o \omega_s} i_s\right) \tag{3.34}$$

which are recognized as the amplitudes of the slow and fast space-charge modes respectively.

Performing this operation on equations 3.18 and 3.19 for v_c and $i_c \neq 0$, the equations become

$$\left[\frac{1}{2u_o}\left(v_c \frac{d}{dz} + \frac{dv_c}{dz}\right) + \frac{R_s \omega_s p}{I_o \omega_s}\left(\frac{di_c}{dz} - j\frac{i_c}{2u_o}\{\omega_{s-1} - \omega_c\}\right)\right] v_{s-1} + \frac{R_s \omega_s p}{I_o \omega_s}\left[v_c \frac{d}{dz} + j\frac{v_c}{2u_o}(\omega_{s-1} - \omega_c)\right] i_{s-1} + \left[\frac{d}{dz} + j\beta_s^-\right] a_s^- - \frac{\eta}{u_o}\frac{dV_s}{dz}$$
$$+ \left[\frac{1}{2u_o}\left(v_c^* \frac{d}{dz} + \frac{dv_c^*}{dz}\right) + \frac{R_s \omega_s p}{I_o \omega_s}\left(\frac{di_c^*}{dz} - j\frac{i_c^*}{2u_o}\{\omega_{s+1} + \omega_c\}\right)\right] v_{s+1} + \frac{R_s \omega_s p}{I_o \omega_s}\left[v_c^* \frac{d}{dz} + j\frac{v_c^*}{2u_o}(\omega_{s+1} + \omega_c)\right] i_{s+1} = 0 \tag{3.35}$$

$$\left[\frac{1}{2u_o}\left(v_c \frac{d}{dz} + \frac{dv_c}{dz}\right) - \frac{R_s \omega_s p}{I_o \omega_s}\left(\frac{di_c}{dz} - j\frac{i_c}{2u_o}\{\omega_{s-1} - \omega_c\}\right)\right] v_{s-1} - \frac{R_s \omega_s p}{I_o \omega_s}\left[v_c \frac{d}{dz} + j\frac{v_c}{2u_o}(\omega_{s-1} - \omega_c)\right] i_{s-1} + \left[\frac{d}{dz} + j\beta_s^+\right] a_s^+ - \frac{\eta}{u_o}\frac{dV_s}{dz}$$
$$+ \left[\frac{1}{2u_o}\left(v_c^* \frac{d}{dz} + \frac{dv_c^*}{dz}\right) - \frac{R_s \omega_s p}{I_o \omega_s}\left(\frac{di_c^*}{dz} - j\frac{i_c^*}{2u_o}\{\omega_{s+1} + \omega_c\}\right)\right] v_{s+1} - \frac{R_s \omega_s p}{I_o \omega_s}\left[v_c^* \frac{d}{dz} + j\frac{v_c^*}{2u_o}(\omega_{s+1} + \omega_c)\right] i_{s+1} = 0 \tag{3.36}$$

At this point it becomes necessary to discuss the nature of the z dependence of the pumping quantities v_c and i_c.

3.4 Coupled Mode Formulation for a Single Pump Wave

Assume that the pump wave propagates as $e^{j(\omega_c t - \beta_c z + \phi)}$. To get a relation between i_c and v_c, ignore the effects on the pump wave due to the small ω_n quantities, and write

$$i = -I_o + i_c e^{j(\omega_c t - \beta_c z + \phi)} \tag{3.37}$$

$$v = u_o + v_c e^{j(\omega_c t - \beta_c z + \phi)} \tag{3.38}$$

Making the small signal assumptions, one obtains from the continuity equation 3.8

$$\frac{v_c}{u_o} = - \frac{i_c}{I_o} \left(1 - \frac{\beta_c u_o}{\omega_c}\right) \tag{3.39}$$

Defining $u \equiv \left(1 - \frac{\beta_c u_o}{\omega_c}\right)$ and recalling that the phase velocity of the pump wave is given by

$$v_{p_c} = \frac{\omega_c}{\beta_c} \tag{3.40}$$

one gets

$$v_{p_c} = \frac{u_o}{1-u} \approx u_o(1+u) \tag{3.41}$$

The parameter u will remain arbitrary and will be a measure of the deviation of v_{p_c} from the average velocity u_o. Under normal conditions u will be $\ll 1$. Using equation 3.39, β_c is now written

$$\beta_c = \frac{\omega_c}{u_o}(1-u) \tag{3.42}$$

Using the inverse relations from equations 3.33 and 3.34

$$v_s = \frac{a_s^- + a_s^+}{2} \tag{3.43}$$

$$i_s = \frac{a_s^- - a_s^+}{\frac{2R_s \omega_p u_o}{I_o \omega_s}} \tag{3.44}$$

to substitute for the $s+1$ and $s-1$ current and velocity modulation, and factoring out part of the z dependence in the a_i by redefining the mode amplitudes as

$$a_s^{\pm}(z) = A_s^{\pm'}(z) e^{-j(\beta_o^+ + s\beta_c)z} \tag{3.45}$$

the equations become

$$-j\left[\frac{\omega_s \tilde{v}_c}{u_o}+\frac{R_s \omega \tilde{i}_c}{I_o}+\frac{R_s \omega_{s-1} \tilde{v}_c}{R_{s-1} u_o}\right]\frac{A_{s-1}^{-'}}{4u_o}-j\left[\frac{\omega_s \tilde{v}_c}{u_o}+\frac{R_s \omega \tilde{i}_c}{I_o}-\frac{R_s \omega_{s-1} \tilde{v}_c}{R_{s-1} u_o}\right]\frac{A_{s-1}^{+'}}{4u_o}+j\frac{\eta \omega_s}{u_o^2}\sqrt{2K_s}\,A_s^c+\left[\frac{d}{dz}+j(\beta_s^- - \beta_o^+ - s\beta_c)\right]A_s^{-'}$$
$$-j\left[\frac{\omega_s v_c^*}{u_o}+\frac{R_s \omega \tilde{i}_c^*}{I_o}+\frac{R_s \omega_{s+1} \tilde{v}_c^*}{R_{s+1} u_o}\right]\frac{A_{s+1}^{-'}}{4u_o}-j\left[\frac{\omega_s \tilde{v}_c^*}{u_o}+\frac{R_s \omega \tilde{i}_c^*}{I_o}-\frac{R_s \omega_{s+1} \tilde{v}_c^*}{R_{s+1} u_o}\right]\frac{A_{s+1}^{+'}}{4u_o}=0 \qquad (3.46)$$

$$-j\left[\frac{\omega_s \tilde{v}_c}{u_o}-\frac{R_s \omega \tilde{i}_c}{I_o}-\frac{R_s \omega_{s-1} \tilde{v}_c}{R_{s-1} u_o}\right]\frac{A_{s-1}^{-'}}{4u_o}-j\left[\frac{\omega_s \tilde{v}_c}{u_o}-\frac{R_s \omega \tilde{i}_c}{I_o}+\frac{R_s \omega_{s-1} \tilde{v}_c}{R_{s-1} u_o}\right]\frac{A_{s-1}^{+'}}{4u_o}+j\frac{\eta \omega_s}{u_o^2}\sqrt{2K_s}\,A_s^c+\left[\frac{d}{dz}+j(\beta_s^+ - \beta_o^+ - s\beta_c)\right]A_s^{+'}$$
$$-j\left[\frac{\omega_s \tilde{v}_c^*}{u_o}-\frac{R_s \omega \tilde{i}_c^*}{I_o}-\frac{R_s \omega_{s+1} \tilde{v}_c^*}{R_{s+1} u_o}\right]\frac{A_{s+1}^{-'}}{4u_o}-j\left[\frac{\omega_s v_c^*}{u_o}-\frac{R_s \omega \tilde{i}_c}{I_o}+\frac{R_s \omega_{s+1} \tilde{v}_c^*}{R_{s+1} u_o}\right]\frac{A_{s+1}^{+'}}{4u_o}=0 \qquad (3.47)$$

where the circuit mode amplitude has been defined by

$$V_s \equiv \sqrt{2K_s}\;A_s^c(z)e^{-j(\beta_o^+ + s\beta_c)z} \qquad (3.48)$$

and the following approximations have been made in the coupling coefficients to the off diagonal mode amplitudes.

$$\frac{d}{dz}\,v_c,\,i_c \approx -\,j\,\frac{\omega_c}{u_o}\,v_c,\,i_c \qquad (3.49)$$

$$\frac{dA_i(z)}{dz} \approx -\,j\left(\frac{\omega+s\omega_c}{u_o}\right)A_i(z)e^{-j(\beta_o^+ + s\beta_c)z} = -\,j\,\frac{\omega_s}{u_o}\,A_i(z)e^{-j(\beta_o^+ + s\beta_c)z} \qquad (3.50)$$

The approximations are made under the assumptions that $R_o\omega_p/\omega \ll 1$, and $u \ll 1$. The z dependence has been removed from the pump quantities by redefining them as

$$v_c, i_c \equiv \tilde{v}_c, \tilde{i}_c e^{-j\beta_c z} \tag{3.51}$$

The complex conjugate notation has been retained since $\tilde{v}_c$ and $\tilde{i}_c$ still contain an arbitrary initial phase factor $e^{j\phi}$. Note that the z dependence which has been removed from v_c and i_c, together with that removed from the circuit and space-charge modes, has combined to drop out of the equations, and that the coupling coefficients are now constants and no longer z dependent. This is the sole reason for using this form of the mode amplitude definitions.

Substituting for v_c/u_o in terms of i_c/I_o from equation 3.39 and defining m_1 as in the three-frequency analysis

$$m_1 \equiv \left| \frac{i_c}{I_o} \right| \tag{3.52}$$

and after redefining the mode amplitudes in the manner suggested by Haus and Robinson (17) such that their absolute square gives the power flow associated with the modes, i.e.,

$$A_s^- e^{-j(\beta_o^+ + s\beta_c)z} e^{jn\phi} \equiv \frac{1}{2\sqrt{2|W_s|}} \left(\frac{u_o}{\eta} v_s - W_s I_s\right) \tag{3.53}$$

$$A_s^+ e^{-j(\beta_o^+ + s\beta_c)z} e^{jn\phi} \equiv \frac{1}{2\sqrt{2|W_s|}} \left(-\frac{u_o}{\eta} v_s + W_s I_s\right) \tag{3.54}$$

where

$$W_s \equiv \frac{2V_o}{I_o} \frac{R_s \omega_p}{\omega_s} \tag{3.55}$$

and

$$I_s = \sigma i_s \tag{3.56}$$

the equations become

$$-jD_1(s)A_{s-1}^- - jD_2(s)A_{s-1}^+ - jk_sA_s^c + \left[\frac{d}{d\zeta} + j\left(1+\frac{R_s}{R_o}+\frac{s\omega_c}{\omega_o}\nu\right)\right] A_s^- - jD_3(s)A_{s+1}^- - jD_4(s)A_{s+1}^+ = 0 \qquad (3.57)$$

$$jD_5(s)A_{s-1}^- + jD_6(s)A_{s-1}^+ - jk_sA_s^c + \left[\frac{d}{d\zeta} + j\left(1-\frac{R_s}{R_o}+\frac{s\omega_c}{\omega_o}\nu\right)\right] A_s^+ + jD_7(s)A_{s+1}^- + jD_8(s)A_{s+1}^+ = 0 \qquad (3.58)$$

The phase factor $e^{jn\phi}$ combines with the initial phase of the pump to drop out of the equations. The mode amplitude change is made by the simple substitutions

$$A_s^{\pm\prime} = -\frac{2\eta\sqrt{2W_s}}{u_o} A_s^{\pm}$$

The velocity parameter ν is defined by letting

$$u \equiv \nu \frac{R_o\omega_p}{\omega_o} \qquad (3.59)$$

The distance parameter ζ is defined by

$$\zeta = \frac{R_o\omega_p}{u_o} z = R_o\beta_p z \qquad (3.60)$$

and k_s is given by

$$k_s \equiv \frac{1}{2R_o}\frac{\omega_s}{\omega_p}\sqrt{\frac{K_s}{W_s}} \cong \frac{R_s}{4R_o}\frac{1}{(Q_sC_s)^{3/4}} \qquad (3.61)$$

where C_s and Q_s are the C and Q of Pierce (28) evaluated at frequency ω_s.

The coupling coefficients are given by

$$D_1(s) = \frac{m_1}{4}\left[\frac{R_s}{R_o} - \nu\frac{\omega_s}{\omega_o}\left\{1+\frac{R_s}{R_{s-1}}\frac{\omega_{s-1}}{\omega_s}\right\}\right]\sqrt{\frac{R_{s-1}\omega_s}{R_s\omega_{s-1}}} \qquad (3.62)$$

$$D_2(s) = \frac{m_1}{4}\left[\frac{R_s}{R_o} - \nu\frac{\omega_s}{\omega_o}\left\{1-\frac{R_s}{R_{s-1}}\frac{\omega_{s-1}}{\omega_s}\right\}\right]\sqrt{\frac{R_{s-1}\omega_s}{R_s\omega_{s-1}}} \tag{3.63}$$

$$D_3(s) = \frac{m_1}{4}\left[\frac{R_s}{R_o} - \nu\frac{\omega_s}{\omega_o}\left\{1+\frac{R_s}{R_{s+1}}\frac{\omega_{s+1}}{\omega_s}\right\}\right]\sqrt{\frac{R_{s+1}\omega_s}{R_s\omega_{s+1}}} \tag{3.64}$$

$$D_4(s) = \frac{m_1}{4}\left[\frac{R_s}{R_o} - \nu\frac{\omega_s}{\omega_o}\left\{1-\frac{R_s}{R_{s+1}}\frac{\omega_{s+1}}{\omega_s}\right\}\right]\sqrt{\frac{R_{s+1}\omega_s}{R_s\omega_{s+1}}} \tag{3.65}$$

$$D_5(s) = \frac{m_1}{4}\left[\frac{R_s}{R_o} + \nu\frac{\omega_s}{\omega_o}\left\{1-\frac{R_s}{R_{s-1}}\frac{\omega_{s-1}}{\omega_s}\right\}\right]\sqrt{\frac{R_{s-1}\omega_s}{R_s\omega_{s-1}}} \tag{3.66}$$

$$D_6(s) = \frac{m_1}{4}\left[\frac{R_s}{R_o} + \nu\frac{\omega_s}{\omega_o}\left\{1+\frac{R_s}{R_{s-1}}\frac{\omega_{s-1}}{\omega_s}\right\}\right]\sqrt{\frac{R_{s-1}\omega_s}{R_s\omega_{s-1}}} \tag{3.67}$$

$$D_7(s) = \frac{m_1}{4}\left[\frac{R_s}{R_o} + \nu\frac{\omega_s}{\omega_o}\left\{1-\frac{R_s}{R_{s+1}}\frac{\omega_{s+1}}{\omega_s}\right\}\right]\sqrt{\frac{R_{s+1}\omega_s}{R_s\omega_{s+1}}} \tag{3.68}$$

$$D_8(s) = \frac{m_1}{4}\left[\frac{R_s}{R_o} + \nu\frac{\omega_s}{\omega_o}\left\{1+\frac{R_s}{R_{s+1}}\frac{\omega_{s+1}}{\omega_s}\right\}\right]\sqrt{\frac{R_{s+1}\omega_s}{R_s\omega_{s+1}}} \tag{3.69}$$

Note that D_2, D_4, D_5 and D_7 couple slow space-charge waves to fast space-charge waves and that they all have minus signs in the curl brackets. In the limit of large s, $\omega_c/\omega_s \to 0$ and R_s/R_{s+1}, $R_s/R_{s-1} \to 1$, so that the coupling coefficients become smaller. Also D_6 and D_8 couple fast space-charge waves and become larger for $\nu > 0$, while D_1 and D_3 couple slow waves and become larger for $\nu < 0$. This behavior is in qualitative agreement with what might be expected since $\nu > 0$ corresponds

to a pump wave velocity near that of fast space-charge waves, while $\nu < 0$ corresponds to a velocity nearer that of slow space-charge waves.

It is also easy to prove the following identities using only equation 3.9.

$$\frac{D_1(s)}{\omega_s} = \frac{D_3(s-1)}{\omega_{s-1}} \tag{3.70}$$

$$\frac{D_2(s)}{\omega_s} = \frac{D_7(s-1)}{\omega_{s-1}} \tag{3.71}$$

$$\frac{D_5(s)}{\omega_s} = \frac{D_4(s-1)}{\omega_{s-1}} \tag{3.72}$$

$$\frac{D_6(s)}{\omega_s} = \frac{D_8(s-1)}{\omega_{s-1}} \tag{3.73}$$

These relations are also expected since they are merely statements that the coupling between waves is reciprocal for waves with the same time dependence.

Since equations 3.57 and 3.58 also include coupling to a slow-wave circuit mode A_s^c at each frequency, equation 3.13 must be put into coupled mode form to complete the set. This can be done by solving 3.53 and 3.54 for the inverse relation

$$i_s = \sqrt{\frac{2}{W_s}} \left(\frac{A_s^+ - A_s^-}{\sigma}\right) e^{-j(\beta_o^+ + s\beta_c)z} \tag{3.74}$$

and substituting this relation and equation 3.48 into 3.13 to get

$$\left[\frac{d}{d\zeta} + j\left(1 - \frac{\omega_s}{\omega_o}\lambda_s + \frac{s\omega_c}{\omega_o}\nu\right)\right] A_s^c + jk_s A_s^- - jk_s A_s^+ = 0 \tag{3.75}$$

The cold circuit phase velocity has been defined

$$v_p \equiv \frac{\omega_s}{\Gamma_s} = \frac{u_o}{1-\lambda_s \frac{R_o \omega_p}{\omega_o}} \tag{3.76}$$

and the k_s is given by equation 3.61. Circuit losses have been ignored in this formulation.

Equations 3.57, 3.58 and 3.75 represent three infinite sets of simultaneous linear differential equations with constant coefficients. Certain assumptions will be necessary in order to achieve solutions. In particular, it is hoped that it will be possible to show that the solutions will converge fairly rapidly and that only a few of the equations from each set involving frequencies near the signal frequency will be needed.

As a consequence of the form of the assumed solutions 3.10, 3.11 and 3.14, many of the equations will involve negative frequencies. As an example, consider a fast space-charge wave at frequency $\omega_{-1} = \omega - \omega_c$. The general solution for a fast space-charge mode is written

$$\frac{1}{2\sqrt{2|W_s|}} \left(-\frac{u_o}{\eta} v_s + W_s I_s\right) e^{j(\omega_s t - \frac{\omega_s - R_s \omega_p}{u_o} z)} \tag{3.77}$$

If $\omega_c > \omega$, and $s = -1$, then $\omega_{-1} < 0$. Substitution of a negative frequency for ω_s in the expression above will result in a wave which has the properties of a slow space-charge wave, since W_s in the mode amplitude definition will change sign and correspond to equation 3.53 and the phase velocity will become

$$v_p = \frac{-\omega}{\frac{-\omega - R_{-1}\omega_p}{u_o}} = \frac{u_o}{1 + \frac{R_{-1}\omega_p}{\omega}} \tag{3.78}$$

The $|W_s|$ in the radical is written as the magnitude since it is a normalization constant to put the mode amplitude into dimensions of the square root of power. Thus it is seen that for negative frequencies, the waves switch roles and + modes become slow modes, and vice-versa. To avoid this awkward situation it is noted that the association with R_s of the sign of the frequency involved (ω_s) will remedy this situation. The consequence of this association is that whenever one considers a negative frequency, he must associate with it a negative reduced plasma frequency. This artifice will be adopted and used throughout the remainder of this analysis.

3.5 The Degenerate Case

As has been done for the three-frequency analysis, a special limiting case which was treated by Louisell and Quate (1) will be used to compare the results predicted by these equations with those obtained from other treatments. This special case is one in which pumping is achieved by a strong fast-space-charge wave traveling at the same velocity as the fast signal-space-charge wave, and in which the pump frequency is twice that of the signal frequency. This was also shown to be a special case of the three-frequency analysis and the discussion of Fig. 2.1 showed that the gain is achieved through coupling of fast signal and idler space-charge waves. As a consequence, it may be well to consider the degenerate case in which only the fast space-charge waves are considered, and then to include the slow space-charge waves to correlate the theory with that of Louisell and Quate.

Special Case No. 1, Coupling of Fast Space-Charge Waves Only. For coupling of the fast waves, only the $s = -1$ and $s = 0$ equations from

3.58 are used.

$$s = -1 \qquad \left[\frac{d}{d\zeta} + j\left(1 - \frac{R_{-1}}{R_o} - \nu\,\frac{\omega_c}{\omega_o}\right)\right] A^+_{-1} + jD_8(-1)A^+_o = 0 \tag{3.79}$$

$$s = 0 \qquad jD_6(0)A^+_{-1} + \frac{d}{d\zeta} A^+_o = 0 \tag{3.80}$$

The condition for the velocity of the pump wave to be equal to that of the fast signal space-charge wave is obtained from 3.41 and is given by

$$\nu = 1 \tag{3.81}$$

For degenerate operation $R_{-1} = -R_o$, and $\omega_c = 2\omega_o$. Substituting these relations into 3.67 and 3.69 to obtain the coupling coefficients, the equations become

$$\frac{d}{d\zeta} A^+_{-1} - j\,\frac{3m_1}{4} A^+_o = 0 \tag{3.82}$$

$$j\,\frac{3m_1}{4} A^+_{-1} + \frac{d}{d\zeta} A^+_o = 0 \tag{3.83}$$

Assuming solutions of the form $e^{j\mu\zeta}$, and setting the determinant of the coefficients equal to zero, the roots of the characteristic equation are

$$\mu = \pm\, j\,\frac{3m_1}{4} \tag{3.84}$$

The character of the signal and idler waves are maintained, as can be seen by substituting the roots into the form of the solution given by

$$e^{j\left[\omega_s t - (\beta^+_o - s\beta_c)z + \mu\zeta\right]} \tag{3.85}$$

However, each is allowed to grow or decay as $e^{\pm \frac{3m_1}{4} \beta_q z}$, and this is exactly the gain behavior predicted by Louisell and Quate. The amount of excitation for each wave is dependent upon the phase of m_1 as determined by matching boundary conditions.

This check on the solutions obtained from the equations substantiates the theory that the gain arises from coupling of only the fast waves. Inherent in the analysis of Louisell and Quate, however, is the inclusion of the slow space-charge waves. Including the slow space-charge waves from equation 3.57 will allow complete comparison with the results obtained from the aforementioned theory.

Special Case No. 2, Inclusion of the Slow Space-Charge Waves. Under the same conditions that were assumed for Case No. 1, the equations 3.57 and 3.58 become

$$\left[\frac{d}{d\zeta} - j2\right]A_{-1}^{-} \qquad -j\frac{m_1}{4}A_o^{-} \qquad +j\frac{m_1}{4}A_o^{+} \qquad = 0 \qquad (3.86)$$

$$\frac{d}{d\zeta}A_{-1}^{+} \qquad -j\frac{m_1}{4}A_o^{-} \qquad -j\frac{3m_1}{4}A_o^{+} \qquad = 0 \qquad (3.87)$$

$$j\frac{m_1}{4}A_{-1}^{-} \qquad -j\frac{m_1}{4}A_{-1}^{+} \qquad +\left[\frac{d}{d\zeta} + j2\right]A_o^{-} \qquad = 0 \qquad (3.88)$$

$$j\frac{m_1}{4}A_{-1}^{-} \qquad +j\frac{3m_1}{4}A_{-1}^{+} \qquad +\frac{d}{d\zeta}A_o^{+} \qquad = 0 \qquad (3.89)$$

Again assuming a solution of the form $e^{j\mu\zeta}$, substituting, and setting the determinant of the coefficients equal to zero, the characteristic equation becomes

$$\mu^4 - 4\left(1 - \frac{m_1^2}{8}\right)\mu^2 - \frac{9m_1^2}{4} + \frac{m_1^4}{16} = 0 \qquad (3.90)$$

and its approximate roots are $\pm j\frac{3m}{4}$, ± 2 . These results are in exact agreement with those obtained by Louisell and Quate.

Thus far the validity of equations 3.57 and 3.58 seems to be verified insofar as coupling between space-charge waves is concerned. There remain in these equations terms representing coupling to a circuit which, together with equation 3.75, have yet to be verified. Suffice it to say that upon letting $m_1 = 0$ (i.e., no pumping), redefining the mode amplitudes, and using the traveling wave tube parameters (28), it is easy to show that equations 3.57, 3.58 and 3.75 reduce to the three coupled-mode equations used by Gould (21) in his analysis of space-charge-wave couplers. It is evident, therefore, that the equations are valid and can be used for numerical computations to investigate the effects of coupling to higher order idlers and to various circuit modes.

3.6 Kinetic Power Theorem

An interesting power theorem can be derived from equations 3.57, 3.58 and 3.75. Multiplying equation 3.75 by A_s^{c*} and multiplying the conjugate of 3.75 by A_s^{c} , and then adding the two resulting equations gives

$$\frac{d}{d\zeta} A_s^c A_s^{c*} + jk_s(A_s^- A_s^{c*} - A_s^{-*} A_s^c) - jk_s(A_s^+ A_s^{c*} - A_s^{+*} A_s^c) = 0 \qquad (3.91)$$

In a similar manner, after multiplying equation 3.57 by A_s^{-*} and the conjugate of equation 3.57 by A_s^- , one obtains

$$jD_1^{*}A_{s-1}^{c*}A_s^{-} - jD_1A_{s-1}^{-}A_m^{-*} + jD_2^{*}A_{s-1}^{+*}A_s^{-} - jD_2A_{s-1}^{+}A_s^{-*} + jk_s\left[A_s^{c*}A_s^{-} - A_s^{c}A_s^{-*}\right] + \frac{d}{d\zeta}A_s^{-}A_s^{-*} + jD_3^{*}A_{s+1}^{-*}A_s^{-} - jD_3A_{s+1}^{-}A_s^{-*} + jD_4^{*}A_{s+1}^{+*}A_s^{-} - jD_4A_{s+1}^{+}A_s^{-*} = 0 \qquad (3.92)$$

Similarly from equation 3.58

$$jD_5A_{s-1}^{-}A_s^{+*} - jD_5^{*}A_{s-1}^{-*}A_s^{+} + jD_6A_{s-1}^{+}A_s^{+*} - jD_6^{*}A_{s-1}^{+*}A_s^{+} + jk_s\left[A_s^{c*}A_s^{+} - A_s^{c}A_s^{+*}\right] + \frac{d}{d\zeta}A_s^{+}A_s^{+*} + jD_7A_{s+1}^{-}A_s^{+*} - jD_7^{*}A_{s+1}^{-*}A_s^{+} + jD_8A_{s+1}^{+}A_s^{+*} - jD_8^{*}A_{s+1}^{+*}A_s^{+} = 0 \qquad (3.93)$$

where all of the D's are of argument s (i.e., $D_i \equiv D_i(s)$. The next step is to subtract equation 3.92 from equation 3.91 and then add equation 3.93 to the result. This equation represents an infinite set of equations for $s = \cdots -2,-1,0,1,2, \cdots$. If it is now postulated that adequate solutions are obtained for a finite set $s = -\ell \cdots -1,0,1,2 \cdots n$, and the equation written out for each of these integers, it will be found that upon addition of the resulting set of equations and application of the relations 3.70 through 3.73, the following equation results

$$\sum_{s=-\ell}^{n} \frac{1}{\omega_s}\frac{d}{d\zeta}\left[A_s^{c}A_s^{c*} - A_s^{-}A_s^{-*} + A_s^{+}A_s^{+*}\right] = 0 \qquad (3.94)$$

Letting $\ell = n \to \infty$, it is seen that this is in effect a statement of the Manley-Rowe relation (7). It will be recognized in the more familiar form for the three-frequency case where $\ell = 1$ and $n = 0$. The resulting equation becomes

$$\frac{1}{\omega_o}\frac{d}{d\zeta}P_o = -\frac{1}{\omega_{-1}}\frac{d}{d\zeta}P_{-1} \qquad (3.95)$$

where P_s is the sum of the power flows on the various uncoupled modes at frequency ω_s . Integrating 3.95 and assuming $P_{-1}(0) = 0$ one obtains

$$\frac{P_o(\zeta) - P_o(0)}{\omega_o} = - \frac{P_{-1}(\zeta)}{\omega_{-1}} \tag{3.96}$$

which is the more familiar form of the Manley-Rowe (7) relation. One should recall that ω_{-1} is negative in this formulation.

3.7 Discussion of the Coupled-Mode Equations

Certain general observations can be made from consideration of the form of equations 3.57, 3.58 and 3.75 which apply to special cases. For example, for the case of zero pumping fields ($m_1 = 0$), the equations describe the traveling wave tube. Note that the k_s terms coupling the A_s^c mode to the A_s^- mode are of opposite sign, and, as has been shown, this leads to exponentially growing waves. Note also that the k_s terms coupling the fast mode A_s^+ to the circuit modes have the same sign and thus beating occurs. This effect leads to the Kompfner dip condition (29,30) which is exploited in the noise removal couplers which were mentioned in Chapter I.

Now let us shift our attention to a beam which has a pump wave present ($m_1 \neq 0$) and is coupled to a circuit ($k_s \neq 0$). A schematic representation of the coupling expressed by the equations is shown in Figure 3.1.

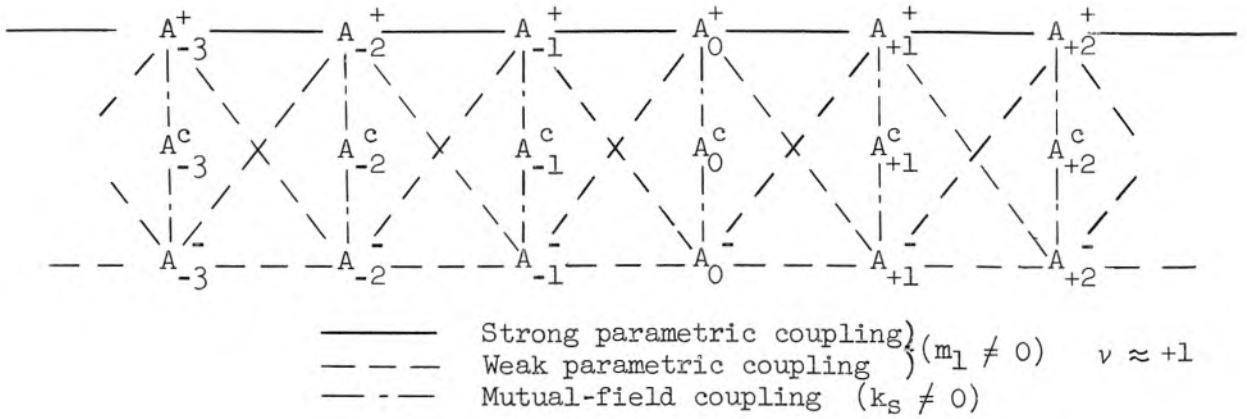

Fig. 3.1 Coupling as expressed by the general equations for a fast-wave parametric amplifier.

The coupling represented by the solid and uniformly dashed lines is due to the presence of the pumping wave, and disappears for $m_1 = 0$. The other lines represent mutual field coupling to forward waves on a circuit and disappear for $k_s = 0$. The uniformly dashed lines are used to represent effective coupling which becomes weak when the phase velocity of the pump wave is fast, i.e., $\nu \approx +1$. This is determined by substitution of the appropriate coupling coefficients (D's) and propagation constants of the uncoupled modes into equation 3.6. The solid lines represent parametric coupling which is strong under these conditions. For the drifting-beam ($k_s = 0$) parametric amplifier, the coupling to the slow space-charge waves and circuit waves is negligible, and, as a result, only equation 3.58 need be considered for solution of this problem.

If it is assumed that an adequate solution can be obtained from an ordered finite set of equations represented by indices $s = -n$ to $+n+1$, it is readily seen that they can be written in the matrix form

$$jHA = -\frac{d}{d\zeta} A \tag{3.96}$$

where the derivative terms have been transposed. The diagonal elements of the matrix H are the propagation constants of the uncoupled modes and the off-diagonal elements are the coupling coefficients. If solutions of the form

$$A = \bar{A} e^{j\mu\zeta} \tag{3.97}$$

are sought, the equation becomes

$$H\bar{A} = -\mu\bar{A} \tag{3.98}$$

which is in the form associated with the general problem class known as "eigenvalue problems". In this case, the solutions are the normal propagation constants of the coupled system and are obtained as the eigenvalues of the matrix H.

From an examination of the signs of the coupling coefficients in the matrix H in conjunction with the considerations of Section 3.2, the table in Fig. 3.2 has been prepared to summarize the behavior to be expected from parametric and mutual-field coupling of various combinations of wave pairs. Some minor modifications of the behavior predicted in this table occur when coupling of many waves is considered simultaneously. These will be noted in Chapters V and VI in which the equations are solved. However, the first order behavior of Fig. 3.2 outlines completely the more conventional performance of the various combinations. The most significant features to be noted are: a) active coupling of two positive a.c. energy carriers is obtained through parametric pumping and b) passive coupling of one positive and one negative carrier can also be achieved. The applications of these mechanisms as indicated in the last column are the subjects of further detailed discussions in Chapters V and VI.

COUPLED PAIR	ENERGY CARRIER	COUPLING METHOD	CONDITIONS ν	CONDITIONS k_s	CONDITIONS m_1	RESULTANT COUPLING	COMMENTS	DEVICE APPLICATION
Circuit Slow Space-Charge	+ -	mutual field	-	$\neq 0$	0	active		TWT
Circuit Fast Space-Charge	+ +	mutual field	-	$\neq 0$	0	passive	Kompfner Dip	fast-wave couplers
a) fast space-charge fast space-charge	+ +	parametric pumping	$\approx +1$	0	$\neq 0$	active	A_{-1}^{+} to A_{0}^{+} only	fast-wave parametric amplifier
b) fast space-charge fast space-charge	+ +	"	$\approx +1$	0	$\neq 0$	passive	all other combinations	
a) slow space-charge slow space-charge	- -	parametric pumping	≈ -1	0	$\neq 0$	active	A_{-1}^{-} to A_{0}^{-} only	slow-wave parametric amplifier (noisy)
b) slow space-charge slow space-charge	- -	"	≈ -1	0	$\neq 0$	passive	all other combinations	
slow space-charge fast space-charge	- +	"	0	0	$\neq 0$	passive	Strongest Coupling A_{0}^{+} to A_{-1}^{-} A_{-1}^{+} to A_{0}^{-}	slow space-charge wave cooling

1) Parametric coupling of circuit waves to space-charge waves does not occur.

2) Space-charge waves are not coupled by mutual fields because they are by definition orthogonal modes.

3) See Gould (31) for coupling to backward circuit waves.

Fig. 3.2 A summary of the behavior to be expected from the coupling of various pair combinations of forward circuit waves and space-charge waves by mutual fields and parametric pumping.

CHAPTER IV

COUPLED-MODE TREATMENT OF THE MULTIPLE-FREQUENCY ELECTRON BEAM FOR THE GENERAL CASE OF CIRCUIT-WAVE PUMPING

4.1 Introduction

In this chapter, the single-pumping-wave approximation is avoided by solving a set of coupled-mode traveling-wave-tube equations for the amplitudes of the pump space-charge modes, and then formulating the general equations so that the coupling coefficients contain these mode amplitudes. Since these mode amplitudes vary with ζ the coefficients in the differential equations are variable.

The principal use for this more complex formalism will probably be to get estimates of the validity of the results obtained from the single-wave theory. One cannot ignore the presence of additional pump waves and it would certainly be presumptive to treat each pump wave separately and then superpose the results. If it should turn out that the additional waves cause trouble, methods can be studied to get rid of them. However, if they do not prove to be troublesome, a considerable amount of complexity, both theoretical and experimental, can be avoided. Solutions for these equations are not obtained here because the more extensive computing facilities which are required are not readily available.

4.2 Formulation of the Equations for the General Case

As stated previously, equations 3.35 and 3.36 contain no assumptions about the z dependence of the pumping quantities v_c and i_c. Since they will now represent combinations of a slow and a fast space-

charge wave at the pump frequency, and since these waves have different z dependence in both phase and amplitude, it will be impossible to completely remove the z dependence from the coefficients in the differential equations. Nevertheless, it will still be advantageous to factor out some of the rapidly varying dependence in the definitions of the mode amplitudes.

As a consequence, the mode amplitudes definitions for the signal quantity waves are written as

$$a_s^{\pm}(z) \equiv \underline{A}_s^{\pm}(z)\, e^{-j\frac{\omega_s}{u_o}z} \quad , \quad V_s \equiv \sqrt{2K_s}\, \underline{A}_s^{c}(z)\, e^{-j\frac{\omega_s}{u_o}} \tag{4.1}$$

The definitions to be used in this formulation will be differentiated from those in the single-wave theory by underlining analogous quantities here. Using these definitions and the relations

$$\frac{d}{dz}\, v_c, i_c \cong -\, j\, \frac{\omega_c}{u_o}\, \underline{v}_c(z),\ \underline{i}_c(z)\, e^{-j\frac{\omega_c}{u_o}z} \tag{4.2}$$

(note that some z dependence is still present in the pump quantities in this case) and substituting into equations 3.35 and 3.36, a set of equations very similar to 3.46 and 3.47 are obtained

$$-J\left[\frac{\omega_s}{u_o}\underline{\tilde{v}}_c + \frac{R_s\omega_p}{I_o}\underline{\tilde{i}}_c + \frac{R_s\omega_{s-1}}{R_{s-1}u_o}\underline{\tilde{v}}_c\right]\frac{\underline{A}_{s-1}^{-'}}{4u_o} - J\left[\frac{\omega_s}{u_o}\underline{\tilde{v}}_c + \frac{R_s\omega_p}{I_o}\underline{\tilde{i}}_c - \frac{R_s\omega_{s-1}}{R_{s-1}u_o}\underline{\tilde{v}}_c\right]\frac{\underline{A}_{s-1}^{+'}}{4u_o} + J\frac{\eta\omega_s}{u_o}\sqrt{2K_s}\,\underline{A}_s^{c} + \left[\frac{d}{dz} + J\frac{R_s\omega_p}{u_o}\right]\underline{A}_s^{-'}$$

$$- J\left[\frac{\omega_s\underline{\tilde{v}}_c^{*}}{u_o} + \frac{R_s\omega_p}{I_o}\underline{\tilde{i}}_c + \frac{R_s\omega_{s+1}}{R_{s+1}u_o}\underline{\tilde{v}}_c^{*}\right]\frac{\underline{A}_{s+1}^{-'}}{4u_o} - J\left[\frac{\omega_s}{u_o}\underline{\tilde{v}}_c + \frac{R_s\omega_p}{I_o}\underline{\tilde{i}}_c^{*} - \frac{R_s\omega_{s+1}}{R_{s+1}u_o}\underline{\tilde{v}}_c^{*}\right]\frac{\underline{A}_{s+1}^{+'}}{4u_o} = 0 \tag{4.3}$$

$$-j\left[\frac{\omega_s}{u_o}\tilde{\underline{v}}_c - \frac{R_s\omega_p}{I_o}\tilde{\underline{i}}_c - \frac{R_s\omega_{s-1}}{R_{s-1}u_o}\tilde{\underline{v}}_c\right]\frac{A_{-s-1}^{-'}}{4u_o} - j\left[\frac{\omega_s}{u_o}\tilde{\underline{v}}_c - \frac{R_s\omega_p}{I_o}\tilde{\underline{i}}_c + \frac{R_s\omega_{s-1}}{R_{s-1}u_o}\tilde{\underline{v}}_c\right]\frac{A_{-s-1}^{+'}}{4u_o} + j\frac{\omega_s}{u_o^2}\sqrt{2K_s}\,\underline{A}_s^c + \left[\frac{d}{dz} - j\frac{R_s\omega_p}{u_o}\right]\underline{A}_s^{+'}$$

$$- j\left[\frac{\omega_s}{u_o}\tilde{\underline{v}}_c^* - \frac{R_s\omega_p}{I_o}\tilde{\underline{i}}_c^* - \frac{R_s\omega_{s+1}}{R_{s+1}u_o}\tilde{\underline{v}}_c^*\right]\frac{A_{-s+1}^{-'}}{4u_o} - j\left[\frac{\omega_s}{u_o}\tilde{\underline{v}}_c^* - \frac{R_s\omega_p}{I_o}\tilde{\underline{i}}_c^* + \frac{R_s\omega_{s+1}}{R_{s+1}u_o}\tilde{\underline{v}}_c^*\right]\frac{A_{-s+1}^{+'}}{4u_o} = 0 \qquad (4.4)$$

Note that the z dependence which was removed in the definitions of the signal modes has combined with that removed from the pump quantities to drop out of the equations.

The pump quantities must now be written in terms of amplitudes of the uncoupled modes which are defined as

$$A_c^- = \frac{1}{2\sqrt{2W_c}}\left(-\frac{u_o}{\eta}\tilde{\underline{v}}_c - W_c\tilde{\underline{I}}_c\right) \qquad (4.5)$$

$$A_c^+ = \frac{1}{2\sqrt{2W_c}}\left(-\frac{u_o}{\eta}\tilde{\underline{v}}_c + W_c\tilde{\underline{I}}_c\right) \qquad (4.6)$$

where

$$W_c \equiv \frac{2V_o}{I_o}\frac{R_c\omega_p}{\omega_c} \qquad (4.7)$$

$$\tilde{\underline{I}}_c = \sigma\,\tilde{\underline{i}}_c \qquad (4.8)$$

These amplitudes are normalized as previously mentioned such that $A_i A_i^*$ is the power flow associated with the mode. To normalize the signal space-charge modes in the same manner, the substitution

$$\underline{A}_s^{\pm'} = -\frac{2\eta}{u_o}\sqrt{2W_s}\,\underline{A}_s^{\pm} \qquad (4.9)$$

is made. After some straightforward algebraic manipulations, the following equations are obtained.

$$JB_1(s)\frac{A_c^+}{\sqrt{P_o}}\underline{A}_{s-1}^- + JB_2(s)\frac{A_c^-}{\sqrt{P_o}}\underline{A}_{s-1}^- + JB_3(s)\frac{A_c^+}{\sqrt{P_o}}\underline{A}_{s-1}^+ + JB_4(s)\frac{A_c^-}{\sqrt{P_o}}\underline{A}_{s-1}^+ - Jk_s\underline{A}_s^c + \left[\frac{d}{d\zeta} + J\frac{R_s}{R_o}\right]\underline{A}_s^- + JB_5(s)\frac{A_c^+}{\sqrt{P_o}}\underline{A}_{s+1}^- + JB_6(s)\frac{A_c^-}{\sqrt{P_o}}\underline{A}_{s+1}^- + JB_7(s)\frac{A_c^+}{\sqrt{P_o}}\underline{A}_{s+1}^+ + JB_8(s)\frac{A_c^-}{\sqrt{P_o}}\underline{A}_{s+1}^+ = 0 \tag{4.10}$$

$$JB_4(s)\frac{A_c^+}{\sqrt{P_o}}\underline{A}_{s-1}^- + JB_3(s)\frac{A_c^-}{\sqrt{P_o}}\underline{A}_{s-1}^- + JB_2(s)\frac{A_c^+}{\sqrt{P_o}}\underline{A}_{s-1}^+ + JB_1(s)\frac{A_c^-}{\sqrt{P_o}}\underline{A}_{s-1}^+ - Jk_s\underline{A}_s^c + \left[\frac{d}{d\zeta} - J\frac{R_s}{R_o}\right]\underline{A}_s^+ + JB_8(s)\frac{A_c^+}{\sqrt{P_o}}\underline{A}_{s+1}^- + JB_7(s)\frac{A_c^-}{\sqrt{P_o}}\underline{A}_{s+1}^- + JB_6(s)\frac{A_c^+}{\sqrt{P_o}}\underline{A}_{s+1}^+ + JB_5(s)\frac{A_c^-}{\sqrt{P_o}}\underline{A}_{s+1}^+ = 0 \tag{4.11}$$

k_s is defined by equation 3.61 and ζ by equation 3.60. P_o is the d.c. beam power and is given by $I_o V_o$. The remaining constants are defined by

$$B_1(s) \equiv Q_s\left[1 + \frac{R_s}{R_{s-1}} - \frac{\omega_c}{\omega_s}\left(\frac{R_s}{R_{s-1}} + \frac{R_s}{R_c}\right)\right]$$

$$B_2(s) \equiv Q_s\left[1 + \frac{R_s}{R_{s-1}} - \frac{\omega_c}{\omega_s}\left(\frac{R_s}{R_{s-1}} - \frac{R_s}{R_c}\right)\right]$$

$$B_3(s) \equiv Q_s\left[1 - \frac{R_s}{R_{s-1}} + \frac{\omega_c}{\omega_s}\left(\frac{R_s}{R_{s-1}} - \frac{R_s}{R_c}\right)\right]$$

$$B_4(s) \equiv Q_s\left[1 - \frac{R_s}{R_{s-1}} + \frac{\omega_c}{\omega_s}\left(\frac{R_s}{R_{s-1}} + \frac{R_s}{R_c}\right)\right]$$

$$B_5(s) \equiv S_s\left[1 + \frac{R_s}{R_{s+1}} + \frac{\omega_c}{\omega_s}\left(\frac{R_s}{R_{s+1}} - \frac{R_s}{R_c}\right)\right]$$

$$B_6(s) \equiv S_s\left[1 + \frac{R_s}{R_{s+1}} + \frac{\omega_c}{\omega_s}\left(\frac{R_s}{R_{s+1}} + \frac{R_s}{R_c}\right)\right]$$

$$B_7(s) \equiv S_s \left[1 - \frac{R_s}{R_{s+1}} - \frac{\omega_c}{\omega_s}\left(\frac{R_s}{R_{s+1}} + \frac{R_s}{R_c}\right)\right]$$

$$B_8(s) \equiv S_s \left[1 - \frac{R_s}{R_{s+1}} - \frac{\omega_c}{\omega_s}\left(\frac{R_s}{R_{s+1}} - \frac{R_s}{R_c}\right)\right] \tag{4.12}$$

where

$$Q_s \equiv \frac{\omega_s}{4R_o\omega_p}\sqrt{\frac{R_c\omega_p}{\omega_c}\frac{R_{s-1}\omega_s}{R_s\omega_{s-1}}} \tag{4.13}$$

$$S_s \equiv \frac{\omega_s}{4R_o\omega_p}\sqrt{\frac{R_c\omega_p}{\omega_c}\frac{R_{s+1}\omega_s}{R_s\omega_{s+1}}} \tag{4.14}$$

The equation expressing the coupling of the circuit wave to the two signal space-charge modes is obtained in an analogous manner to that used in deriving equation 3.75. The inverse relation to be used in equation 3.13 for the current modulation is

$$i_s = \sqrt{\frac{2}{W_s}}\left(\frac{\underline{A}_s^+ - \underline{A}_s^-}{\sigma}\right)e^{-j\frac{\omega_s}{u_o}z} \tag{4.15}$$

Using this expression together with the definition of V_s in equation 4.1 allows equation 3.13 to be written

$$\left[\frac{d}{d\zeta} - j\frac{\omega_s}{\omega_o}\lambda_s\right]\underline{A}_s^c + jk_s\,\underline{A}_s^- - jk_s\,\underline{A}_s^+ = 0 \tag{4.16}$$

Again the $\underline{A}_s^i$ are regarded as slowly varying functions of z and terms involving their derivatives with respect to z have been dropped in the coupling coefficients. The constant λ_s is defined by equation 3.76.

Equations 4.10, 4.11 and 4.16 are three infinite sets of simultaneous linear differential equations with variable coefficients in which

coupling to idler space-charge waves is provided through action of the pump space-charge waves, which in turn are allowed to vary with distance z . The behavior of the pump space-charge waves is determined from a separate set of equations. The pumping quantities are assumed large with respect to the signal quantities so that effects on the pump mode amplitudes due to the signal modes can be neglected. Equations 3.12, 3.20 and 3.21 were derived under these assumptions and are the equations to be used to determine the behavior of the various pump-mode amplitudes. They must first be put into coupled-mode form and normalized to the common distance parameter ζ .

After defining the mode amplitude

$$V_c \equiv \sqrt{2K_c}\ A_c^c(z)\ e^{-j\frac{\omega_c}{u_o}z} \tag{4.17}$$

and noting the form of the definitions of A_c^+ and A_c^- from equations 4.2, 4.5 and 4.6, it is seen that equation 3.12 can be written directly by analogy to equation 4.16 as

$$\left[\frac{d}{d\zeta} - j\frac{\omega_c}{\omega_o}\lambda_c\right] A_c^c + jk_c A_c^- - jk_c A_c^+ = 0 \tag{4.18}$$

where λ_c is defined by

$$v_{p_c} \equiv \frac{\omega_c}{\Gamma_c} = \frac{u_o}{1 - \lambda_c \frac{R_o\omega_p}{\omega_o}} \tag{4.19}$$

and k_c is of the same form as k_s , i.e.,

$$k_c \cong \frac{R_c}{4R_o}\frac{1}{(Q_c C_c)^{3/4}} \tag{4.20}$$

To put equations 3.20 and 3.21 into coupled-mode form, it is necessary merely to note that they are of exactly the same form as 3.18 and 3.19 if the pump quantities v_c and i_c in these latter equations are allowed to become zero. Proceeding in exactly the same manner as that used to derive equations 3.31 and 3.32, except that the circuit voltage V_c is retained, and then using the normalized mode amplitudes of 4.5, 4.6 and 4.17, equations 3.20 and 3.21 become

$$\left[\frac{d}{d\zeta} + j\frac{R_c}{R_o}\right] A_c^- - jk_c A_c^c = 0 \tag{4.21}$$

$$\left[\frac{d}{d\zeta} - j\frac{R_c}{R_o}\right] A_c^+ - jk_c A_c^c = 0 \tag{4.22}$$

Equations 4.18, 4.21 and 4.22 are the traveling-wave tube equations in coupled-mode form and are the same as those used by Gould (21) when put into the notation of Pierce (28) and normalized to $\frac{\omega_c}{u_o} C_c z$ instead of ζ. When these three equations are used in conjunction with 4.10, 4.11 and 4.16 they should be written in dimensionless form by normalizing the mode amplitudes to $\sqrt{P_o}$.

4.3 A Discussion of a Typical Application of the Equations

This formidable set of equations which is necessary to describe the general case can usually be simplified considerably for most practical cases. As a typical example, consider a parametric amplifier in which a beam is being pumped by a circuit wave traveling with a velocity near that of the fast-space-charge wave at the signal frequency. Assume that the circuit supporting the pump wave is dispersive so that it does not interact with the signal space-charge modes. This means

that $K_s \approx 0$ and from equation 3.61 it is seen that the terms coupling the space charge waves to the circuit waves in 4.10 and 4.11 can be dropped. For the same reason equation 4.16 need not be considered. Furthermore, in the practical case the parameter $Q_c C_c$ may be quite large. Under these conditions the coupling to the slow pump-space-charge wave is very weak (31), and equation 4.21 is not needed. Consideration of the magnitudes of the coupling coefficients B_3, B_4, B_7 and B_8, together with the appropriate uncoupled mode propagation constants, shows that only weak coupling exists between the slow idler waves and the fast signal waves, so that equation 4.10 need not be considered. As a consequence of these arguments it is seen that only the coupling terms involving B_2 and B_6 remain in equation 4.11 and only 4.22 and the part of 4.18 expressing coupling between A_c^c and A_c^+ are needed to form a simple set of equations which very adequately describes the system. The simplified set of equations becomes

$$jB_2(s)\frac{A_c^+}{\sqrt{P_o}}\underline{A}_{s-1}^+ + \left[\frac{d}{d\zeta} - j\frac{R_s}{R_o}\right]\underline{A}_s^+ + jB_6(s)\frac{A_c^+}{\sqrt{P_o}}\underline{A}_{s+1}^+ = 0 \qquad (4.23)$$

$$\left[\frac{d}{d\zeta} - j\frac{\omega_c}{\omega_o}\,{}_c\right]\frac{A_c^c}{\sqrt{P_o}} - jk_c\frac{A_c^+}{\sqrt{P_o}} = 0 \qquad (4.24)$$

$$-jk_c\frac{A_c^c}{\sqrt{P_o}} + \left[\frac{d}{d\zeta} - j\frac{R_c}{R_o}\right]\frac{A_c^+}{\sqrt{P_o}} = 0 \qquad (4.25)$$

These equations can be simulated on a differential analyzer if a sufficient number of multipliers are available to allow continuous computation of the varying coefficients in 4.23.

4.4 Some General Observations on the Form and Use of the Equations

Because of the symmetry of the problem one would expect certain reciprocal interaction processes to be evident in the form of the equations. This is indeed the case. Note for example in equation 4.10 that the constant part of the coupling coefficient representing coupling between $\underline{A}_s^-$ and $\underline{A}_{s-1}^-$ through A_c^+ is B_1. Intuitively, one might expect that the coupling of the fast wave $\underline{A}_s^+$ to $\underline{A}_{s-1}^+$ through A_c^- to have the same coefficient; examination of equation 4.11 shows that the appropriate constant is B_1. Careful examination of each pair of coefficients in these equations involving the same B reveals similar symmetries.

Note also that in neither of the formulations of the equations does the coupling to circuit modes involve the pumping action. This implies that direct coupling of space-charge modes by circuit fields does not occur, but that coupling is only accomplished through modulation of the beam. It is a direct consequence of the fact that the term in the equation of motion which contains the circuit fields is linear.

In summary, equations 4.10, 4.11, 4.16, 4.18, 4.21 and 4.22 form a set of coupled-mode equations which allows treatment of the general problem of a multiple-frequency electron beam coupled to a circuit whose fields interact with the beam at any or all of the frequencies ω_c and ω_s. For any nontrivial case there must be present an initial set of conditions consisting of an initial normalized amplitude on one of the pump modes (or combination of initial pump mode amplitudes) and an initial amplitude on any one of the modes of arbitrary frequency ω_s. These initial conditions are necessary in order that all of the other idler frequency components can be generated through the coupling of the waves.

Careful examination of the equations will usually result in a considerable reduction in the number of equations needed for a solution of a particular problem. Of course, a sufficient number of equations from the infinite sets represented by 4.10, 4.11 and 4.16 must be used in order to arrive at a solution which converges.

CHAPTER V

SOLUTIONS OF THE SINGLE-PUMPING-WAVE EQUATIONS FOR THE PARAMETRIC AMPLIFIER

5.1 Introduction

In this chapter the single-wave equations are applied to the fast-space-charge-wave parametric amplifier with an eye to understanding the low gain and poor noise performance which has been observed experimentally and in hopes of finding new areas of operation which are more promising. The theory is shown to agree with that of Roe and Boyd (32) for traveling-wave parametric amplifiers with synchronous velocities for all waves. The equations are solved for the case of space-charge-wave pumping and for several cases of circuit-wave pumping in which the pump phase velocity is varied. Coupling of a circuit to the signal and idler space-charge waves is also considered.

5.2 Method of Solution

The equations were solved for the normal mode propagation constants of the coupled system on a digital computer. In lieu of matching the boundary conditions with the attendant need for solution of large numbers of simultaneous algebraic equations, the equations were programmed for an analog computer. The absolute square of each of the mode amplitudes can then be plotted directly as a function of the independent distance variable ζ for unit excitation at $\zeta = 0$ on any one of the modes. All computations were carried out for the near-degenerate case in which

$$\omega_c \approx 2\omega_o \tag{5.1}$$

In both digital and analog computer solutions, successive pairs of idler waves of increasing frequency $[\omega + (r-1)\omega_c$ and $\omega - r\,\omega_c$, beginning at $r = 0]$ are added until the solution converges. In general the solutions converge for $m_1 < 0.5$ when mode indices from $s = -5$ to $+4$ are included (i.e., 11 frequencies including the pump frequency). More idlers are necessary for solutions in the range $0.5 < m_1 < 1$, but since the analysis is valid only for small m_1 and, as will be shown, operation in this large m_1 range is undesirable, it was felt that further effort in this area was unnecessary.

5.3 Matrix Formulation of the Solutions

The analog computer solutions can be represented in the matrix form

$$|A_i(\ell)|^2 = M_{ij}|A_j(o)|^2 \qquad i,j = 1,2,\cdots 2n \tag{5.2}$$

for the case in which only fast space-charge waves are considered, the column matrices are written in the form

$$\begin{bmatrix} |A^+_{-n}|^2 \\ |A^+_{-(n-1)}|^2 \\ \vdots \\ |A^+_{-1}|^2 \\ |A^+_{o}|^2 \\ \vdots \\ |A^+_{n-1}|^2 \end{bmatrix} = \begin{bmatrix} |A_1|^2 \\ |A_2|^2 \\ \vdots \\ |A_n|^2 \\ |A_{n+1}|^2 \\ \vdots \\ |A_{2n}|^2 \end{bmatrix} \tag{5.3}$$

where n pairs of waves are considered adequate for solution and M is

a 2n x 2n square matrix. Examples of the notation to be used for the magnitudes of the matrix elements are $M^{+\,+}_{o,o}$, which relates the power on the A^{+}_{o} mode to that at the input on the same mode, and $M^{+\,+}_{o,+2}$, which relates the power output on the A^{+}_{o} mode due to that at the input on the A^{+}_{+2} mode. $M^{+\,+}_{o,o}$ is therefore the power gain of a fast space-charge-wave amplifier and $M^{+\,+}_{o,+2}$ is the conversion gain of the noise power from the A^{+}_{+2} mode. The M_{ij} of equation 5.2 is used to designate the position of a particular element $M^{\pm\,\pm}_{r,s}$ (or $M^{c\,c}_{r,s}$). The latter specification is used most frequently since it readily allows interpretation of the physical significance of the element. Since the analog computer results are all normalized to unit excitation, the data curves are direct plots of the matrix elements.

Noise Temperature. The noise temperature T_e of an amplifier is simply the internally-generated noise power of the amplifier referred to the input terminals, i.e., regarded as if it were excess noise present at the input terminals over and above the thermal noise coming in with the signal. It is defined by the equation

$$N_a \equiv Gk\,T_e B \tag{5.6}$$

where Na is the noise power generated in the amplifier, k is the Boltzmann constant, B is the bandwidth, and G the power gain. In contrast to the well-known "noise figure" of an amplifier, which depends for its value on the specification of some reference temperature, the noise temperature is an absolute figure of merit and will be used exclusively in discussions of the theoretical results.

It will be assumed that the thermal noise excitation of each

noise-contributing mode in the electron beam is given by

$$|A_i(0)|^2 = kT_K B \tag{5.7}$$

where T_K is the cathode temperature in ^oK. This assumption can be justified to some extent by noting that the minimum noise temperature of a traveling-wave tube is given by (33)

$$T_{e_{min}} \approx 0.8\, T_K \tag{5.8}$$

and recognizing that most of the noise contributed by the tube is due to amplification of the slow-wave noise. Since the $M^{c\,c}_{o,o}$ and $M^{c\,-}_{o,o}$ matrix elements are approximately equal, the noise temperature is roughly equal to the thermal excitation of the slow wave. Furthermore, since there is no net a.c. power flow on the beam, the positive flow of noise power on the fast wave must be of the same magnitude. The excitation of the fast wave in the cathode region and the optimization of the transformation to be undergone before entering the circuit region is a separate problem which will not be treated here.

Under the aforementioned assumption, the internal noise of the amplifier can be written

$$N_a = kT_K B \sum_{i \neq 0,-1} M^{+}_{o,i} \tag{5.9}$$

Note that all of the beam noise on the A^{+}_{o} and A^{+}_{-1} modes has been assumed to be completely removed in the input coupler. Combining equation 5.9 with 5.6 one can write

$$T_e = \frac{T_k}{G} \sum_{i \neq 0,-1} M^+_{o,i} = \frac{T_K}{M^+_{o,o}} \sum_{i \neq 0,-1} M^+_{o,i} \tag{5.10}$$

Thus, from a plot of the matrix elements $M^+_{o,i}$, the noise temperature of the amplifier is readily determined.

Accuracy of Solutions. Two independent methods are used to check the analog computer solutions. The first is a comparison of the growth constant of the dominant wave which is obtained from the digital computer with that inferred from the asymptotic rate of growth for large ζ as predicted in the analog computer results. The second method is a check to see whether or not equation 3.94 is satisfied.

Again considering the case of the coupling of 2n fast space-charge waves, equation 3.94 can be integrated to give

$$\frac{|A^+_{-n}|^2}{\omega_{-n}} + \cdots + \frac{|A^+_{-1}|^2}{\omega_{-1}} + \frac{|A^+_o|^2 - |A^+_o(0)|^2}{\omega_o} + \cdots \frac{|A^+_{n-1}|^2}{\omega_{n-1}} = 0 \tag{5.11}$$

After dividing by $|A^+_o(0)|^2$ and using equations 5.1, 3.9 and 5.2, this can be written for the near-degenerate case as

$$-\frac{M^+_{-n,o}\,{}^+}{(2n-1)} - \cdots - M^+_{-1,o}\,{}^+ + M^+_{o,o}\,{}^+ - 1 + \cdots + \frac{M^+_{n-1,o}\,{}^+}{(2n-1)} = 0 \tag{5.12}$$

Since each of the $M^+_{i,o}$ were plotted for each case studied, substitution into this equation provided an excellent check on the computer program.

In all cases in which the slow space-charge waves were included, their effects on the behavior of the fast waves was negligible. This behavior is in accordance with the expectations discussed in Chapter III

and can be expressed thus:

$$M^{+\,-}_{i,j} \ll M^{+\,+}_{i,j} \tag{5.13}$$

for all i and j in the equations needed to obtain convergence. For convenience, therefore, all mode amplitudes discussed in the remainder of this chapter are fast modes or circuit modes and the + superscripts on the matrix elements will be understood when none are shown.

5.4 The Synchronous Velocity or Thin-Beam Case

In Fig. 5.1 a plot of the plasma-frequency reduction factor R for confined beams is shown as a function of the parameter $\beta_e b$ where β_e is the electronic wave number and b the radius of the beam. a is the radius of the metal tube surrounding the beam. Note that for small $\beta_e b$ the curve is linear and

$$R(n\omega) \cong n\,R(\omega) \qquad n = 1,2,3 \cdots \tag{5.14}$$

Recalling that the phase velocity of a fast space-charge wave is given by

$$v_p^+ \approx u_o\left(1 + \frac{R(\omega)\,\omega_p}{\omega}\right) \tag{5.15}$$

it is seen that the phase velocities of all the waves of frequency $n\omega$ are the same if equation 5.14 holds.

Since this condition can hold for several waves on very thin beams (small $\beta_e b$) and since a comparison of results obtained from this theory with those obtained by Roe and Boyd (32) for nondispersive traveling-wave parametric amplifiers was desired, the equations were solved under the artificial constraint given by equation 5.14.

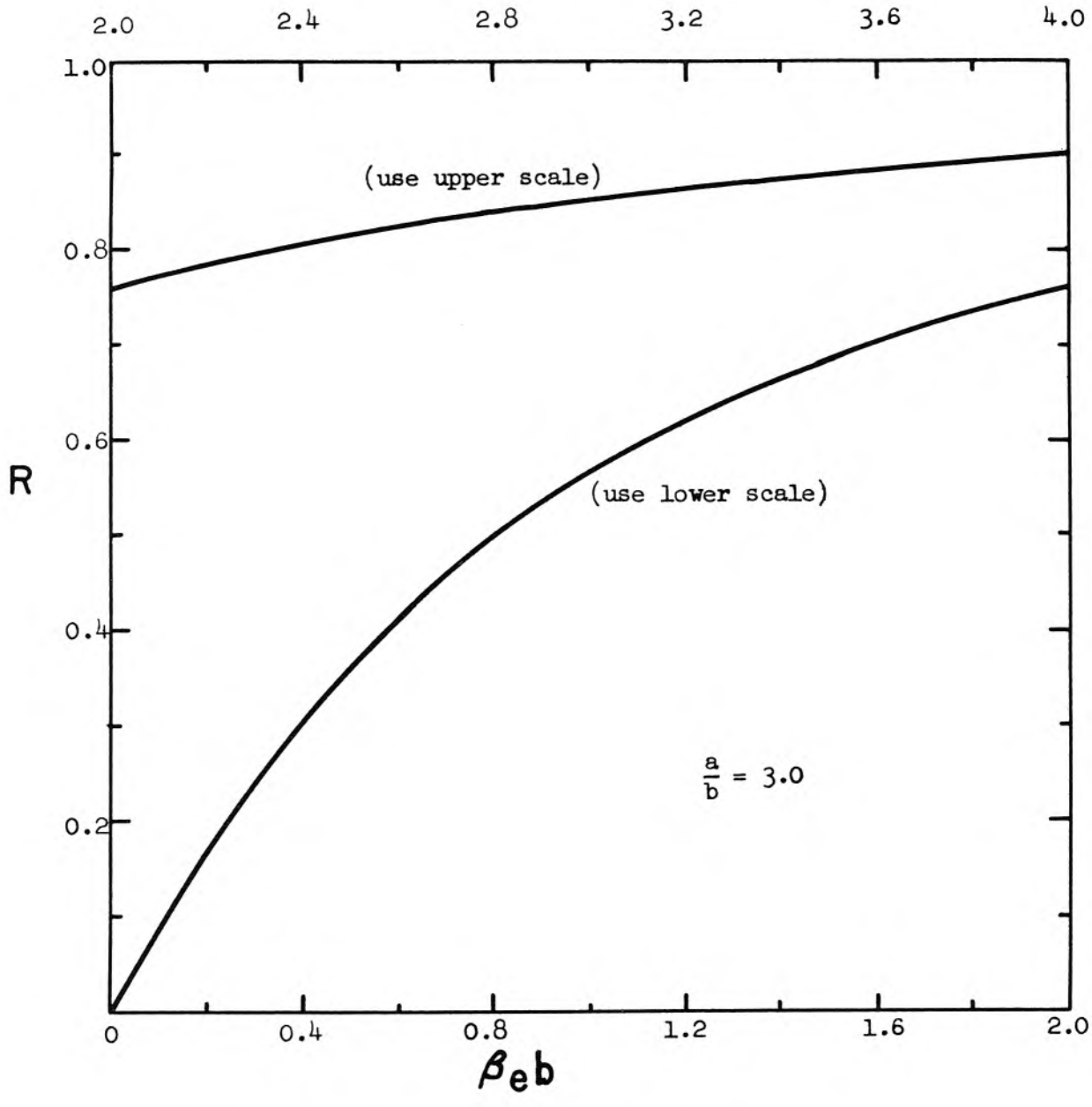

Fig. 5.1 The reduction factor curve for the beam which is used in the parametric amplifiers which are discussed in this chapter.

Under these conditions the constant terms inside the brackets in equation 3.58 are zero and after dividing through by m_1, a new distance parameter $\xi = \frac{m_1 R_o \omega_p}{u_o}$ can be defined. In Fig. 5.2 the behavior of the fast-wave signal power is shown for various numbers of idler pairs. The behavior in the region $\xi \lesssim 1$ is almost exactly that predicted by Roe and Boyd and, as they have pointed out, the rate of convergence by successive approximation is very slow. It is interesting to note the oscillatory nature of the curves when even numbers of pairs of idler waves are present. This same behavior is noted later in this chapter for dispersive beams (thick beams) when a pair of circuit waves with synchronous velocities is coupled to the signal waves. Roe and Boyd have obtained an exact solution for the nondispersive amplifier and have shown that the energy fed into the system by the pump wave is continuously converted to harmonic power, and that the fundamental does not experience exponential growth.

Plots of both the $M_{i,o}$ and the $M_{o,i}$ matrix elements were made for the 11 frequency case as a function of ξ. In the former case, it was found that $M_{0,0}$, $M_{-1,0}$, $M_{+2,0}$, $M_{-3,0}$, $M_{+4,0}$, $M_{-5,0}$ were all of the same order of magnitude, and in turn were more than an order of magnitude greater than $M_{+1,0}$, $M_{-2,0}$, $M_{+3.0}$, $M_{-4,0}$. This means that most of the energy was carried in the odd idler pairs of frequencies $\pm\omega$, $\pm 5\omega$, $\pm 9\omega$, while the even pairs ($\pm 3\omega$, $\pm 7\omega$) were hardly excited. In the $M_{o,i}$ case, $M_{o,o}$ and $M_{0,-1}$ were an order of magnitude greater than all others, but the tendency for the odd idler pairs to couple energy to the signal wave was still much stronger than that for the even pairs.

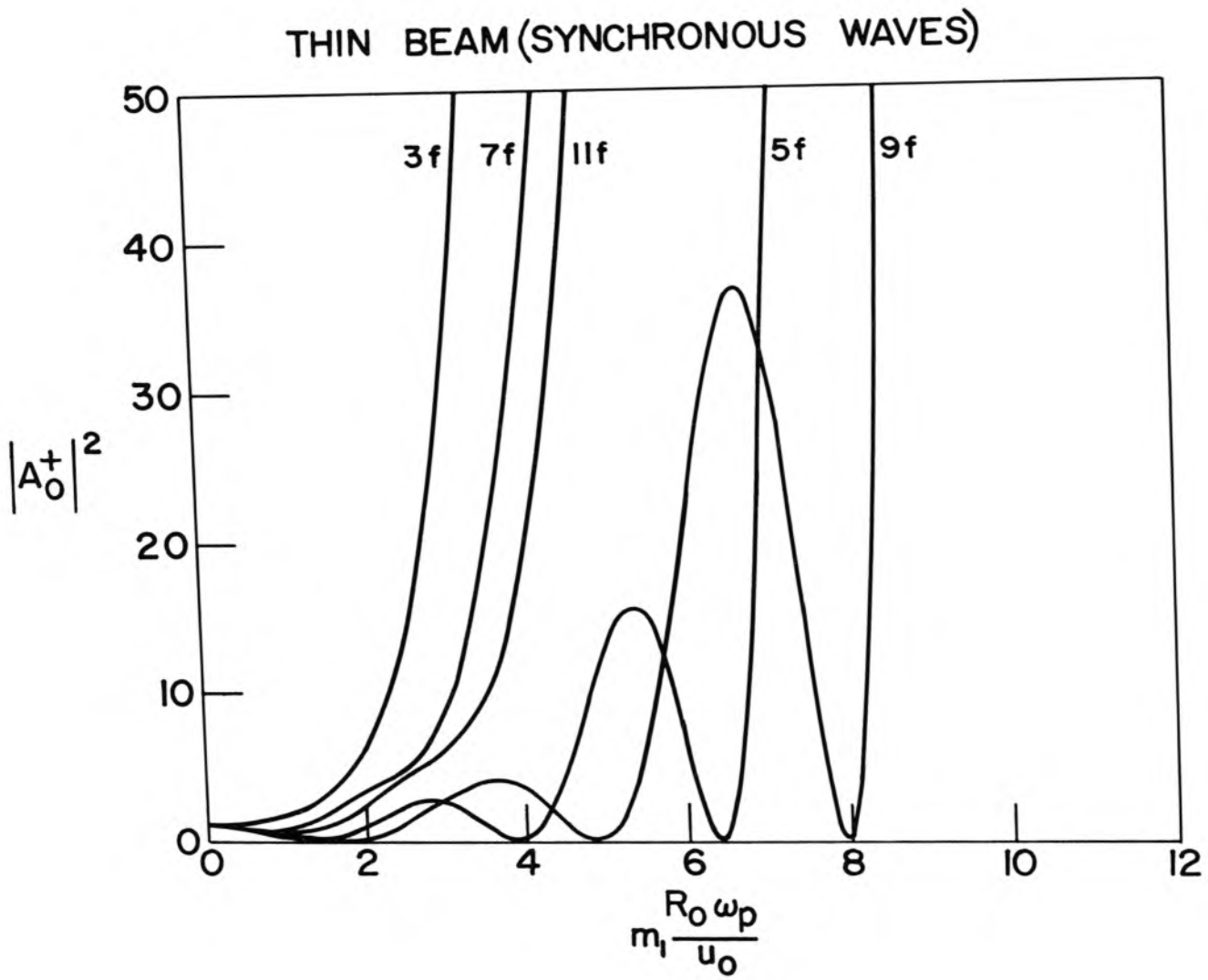

Fig. 5.2 The power flow on the fast signal wave in a thin beam, or nondispersive, parametric amplifier.

These considerations show definitely that the nondispersive amplifier is undesirable and that hope for successful traveling-wave amplification in which all harmonics are present lies in the use of dispersive media.

5.5 Space-Charge-Wave Pumping of the Drifting Thick Beam

An examination of the shape of the reduction factor curve (Fig. 5.1) indicates that equation 5.14 does not hold for $\beta_e b > 0.5$ and that a considerable amount of dispersion of the phase velocities of the higher-order idler waves will occur for $\beta_{e_o} b > 0.6$. The remainder of the cases to be considered in this chapter are for $\beta_{e_o} b = 0.7$ and $a/b = 3.0$. The dispersion characteristics of such a beam are plotted to scale in Fig. 5.3.

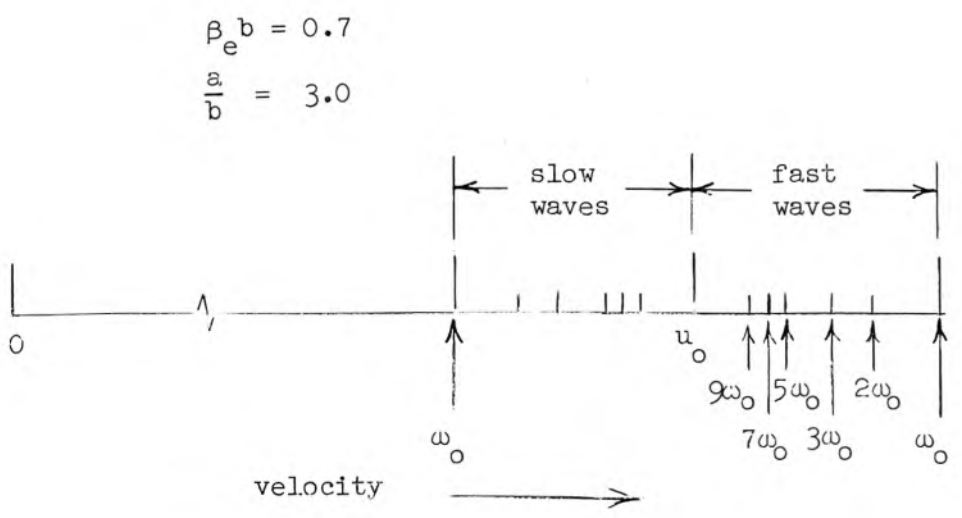

Fig. 5.3 The dispersion of the space-charge waves on the thick beam ($\beta_{e_o} b = 0.7$, $\frac{a}{b} = 3$) to be used in the model.

To simulate the case in which the pumping is achieved by the fast space-charge wave at the pump frequency, as treated by Louisell and Quate (1) one simply allows the parameter ν to become

$$\nu = \frac{\omega_o}{\omega_c} \frac{R_c}{R_o} \tag{5.16}$$

The single-wave theory yields an exact solution for this special case.

In Fig. 5.4 the real part of the normal propagation constants of the coupled system are plotted for 11 frequencies. The solutions have converged only for $m_1 < 0.5$. Because the roots occur in conjugate pairs, negative real roots of the same magnitude also occur. The imaginary parts of the roots are plotted in Fig. 5.5, in which the modes of the uncoupled system are identified in the limit of weak coupling $(m_1 \rightarrow 0)$.

The first growth region occurs at about $m_1 = 0.3$. From Fig. 5.5, the unstable condition is seen to arise from the coupling of the signal and idler to A^+_{-2} and A^+_{+1} respectively. This is evident in Fig. 5.6 where the $\pm 3\omega$ mode amplitudes are shown to grow as rapidly as the signal modes. Since these noise-carrying modes are so tightly coupled, the noise elements $M_{0,-2}$ and $M_{0,+1}$ are quite large. Because of the passive coupling of the signal and idler in this case, a strong oscillatory component is evident in the exponential growth of all the modes. The summation of matrix elements to be used in equation 5.10 to determine T_e is approximately 100 when $M^{c\,c}_{o,o} = 100$; thus $T_e \approx T_K$. This is considerably less than has been measured. However, it is noted that the length of the interaction region must be $\approx 7\lambda_q$ to achieve 20 db gain, and indicates that the experimental tubes must

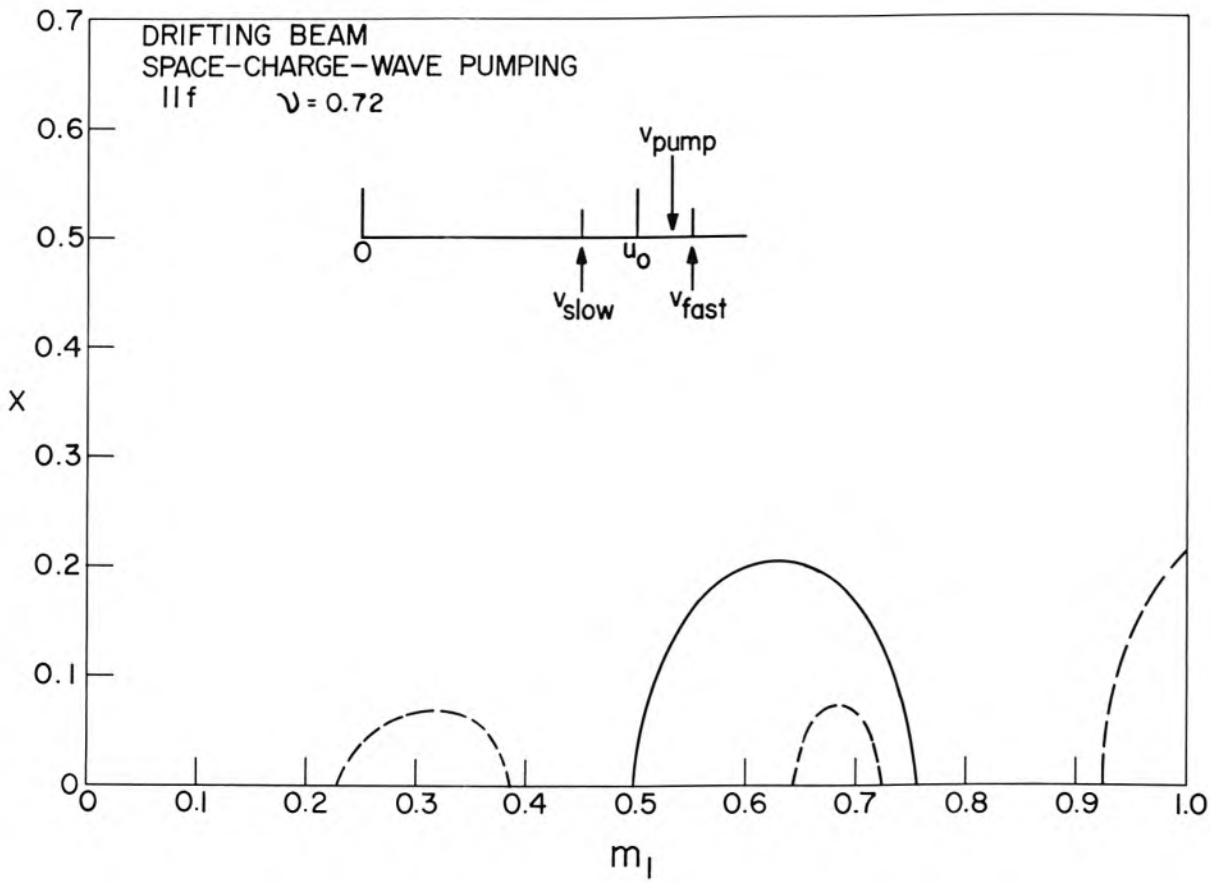

Fig. 5.4 The real parts (x_i) of the incremental propagation constants for the space-charge pumped parametric amplifier. Double roots are represented by dashed lines. The dependence of each wave is given by

$$e^{j[\omega_s t-(\beta_o^+ - S\beta_c - y\beta_q)z]}\ e^{x\beta_q z}$$

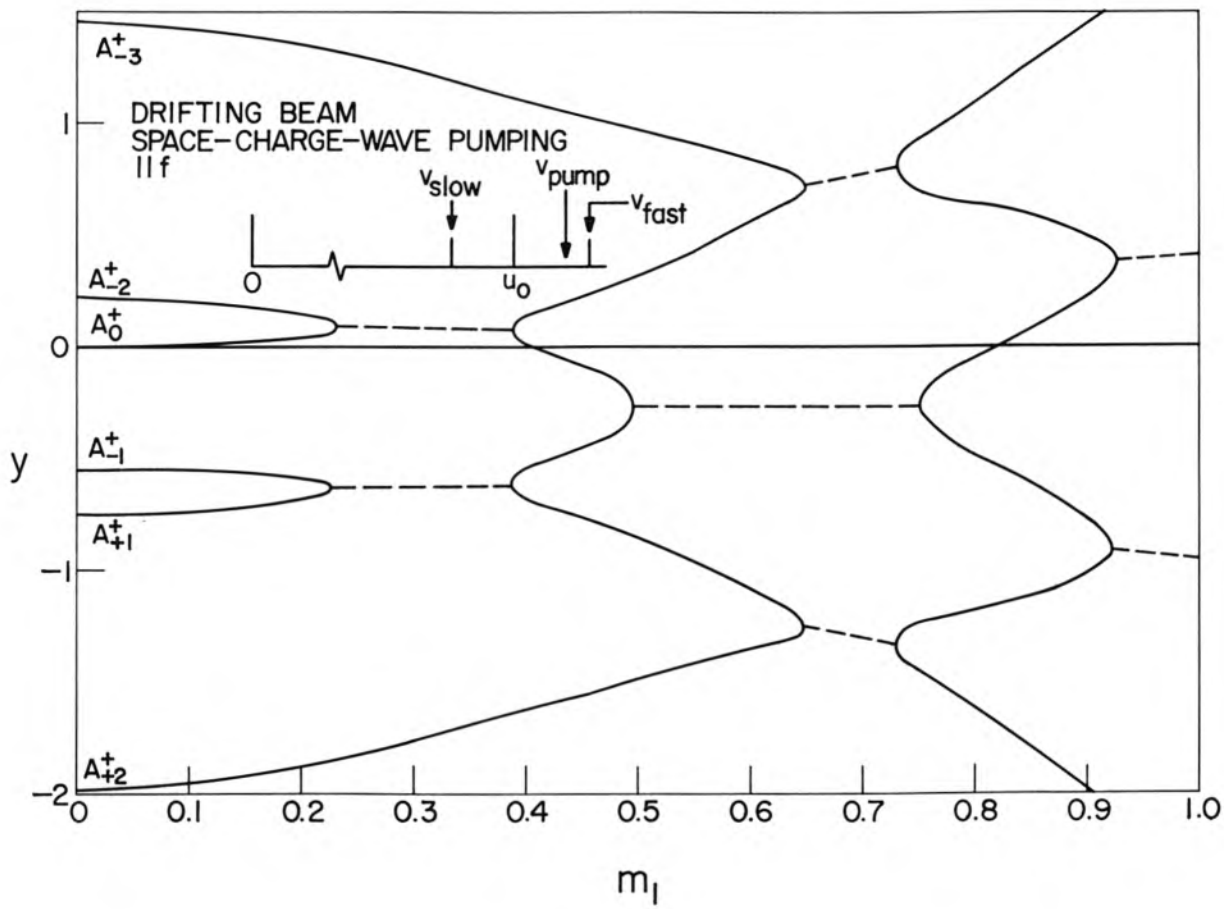

Fig. 5.5 The imaginary parts of the incremental propagation constants for the space-charge-pumped amplifier. Roots of the characteristic equation which do not converge to complex roots are not shown. They are disposed symmetrically about the roots which are plotted but lie off the graph.

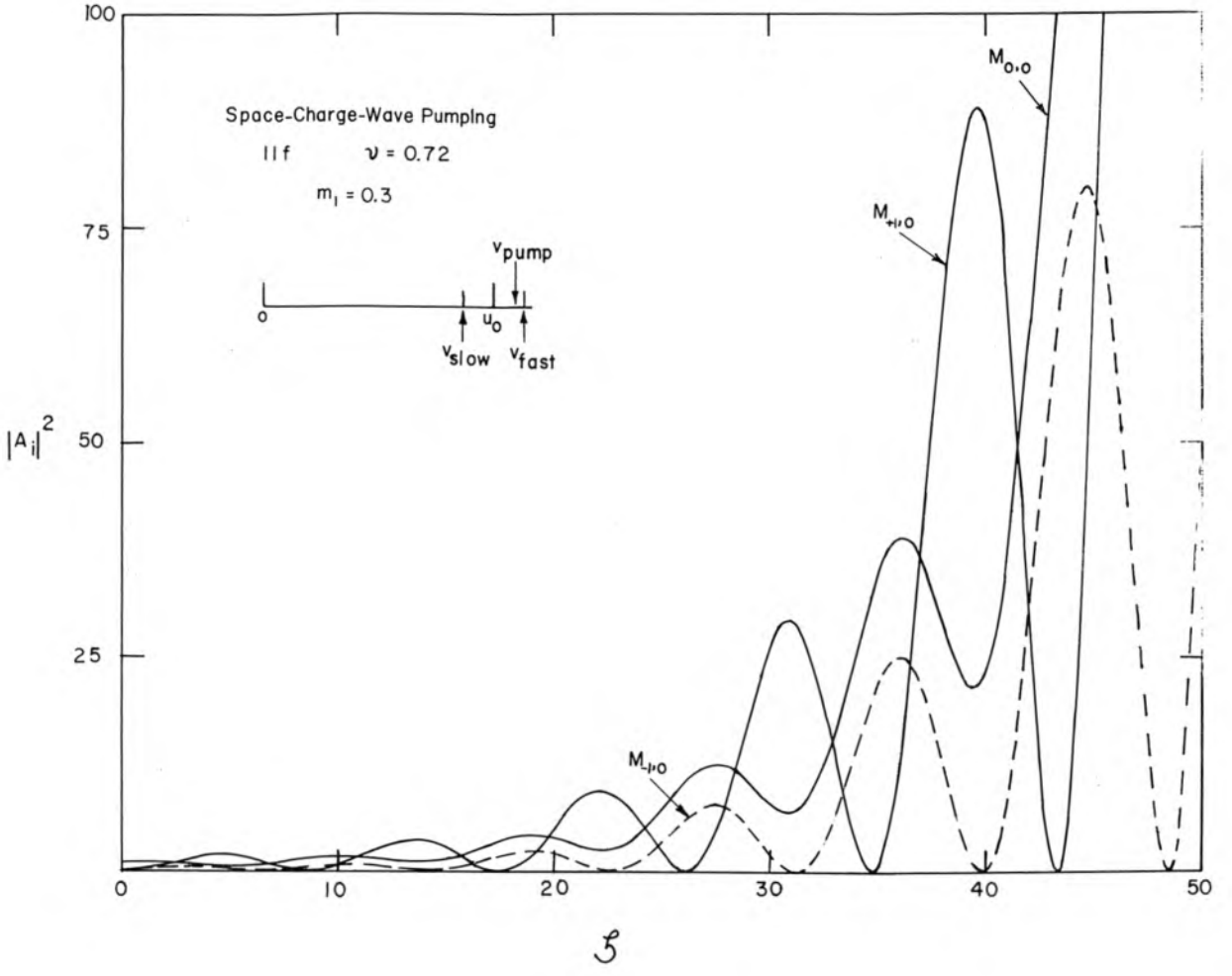

Fig. 5.6 Behavior of several of the modes in the space-charge-pumped amplifier due to unit excitation of the A_o^+ fast signal mode. The oscillatory behavior is due to passive coupling of the signal and principal idler mode. Note that a length of approximately $7\lambda_q$ is required for a gain of 20 db.

have operated at much larger m_1.

The solutions do not converge for 11 frequencies at $m_1 \approx 0.6$. However, data taken for this case indicates that all of the modes which have been included contribute noise. The trend is toward lower gain and higher noise as more modes are included. The conclusion which can be drawn for this case is that the gain per unit length is too low unless beam saturation is approached, at which stage the noise contributions from the tightly coupled higher idlers gets large.

5.6 Circuit-Wave Pumping of the Drifting Thick Beam

In this section the pumping wave is assumed to be set up by a dispersive circuit which interacts with the beam only at the pump frequency; thus the retention of the term "drifting" to differentiate from the case in which the circuit can also couple at signal and idler frequencies. Three cases are treated in which the pump phase velocity is first set equal to the signal space-charge-wave velocity and then slightly higher in two successive jumps.

Case I, Synchronous Pumping; $\nu = 1$ As indicated in Fig. 5.7 the phase velocity of the pump wave is equal to that of A_o^+ when $\nu = 1$. This again is a plot of the real parts of the normal propagation constants. The curves are shown for each successive approximation to the solution by the addition of idler pairs and are seen to converge for $m_1 < 0.5$. In this case there is no threshold value for m_1 which must be reached before growing waves occur. The peak asymptotic gain near $m_1 = 0.3$ is about 9.5 db per plasma wavelength. In Fig. 5.8, the positive imaginary propagation constants are plotted.

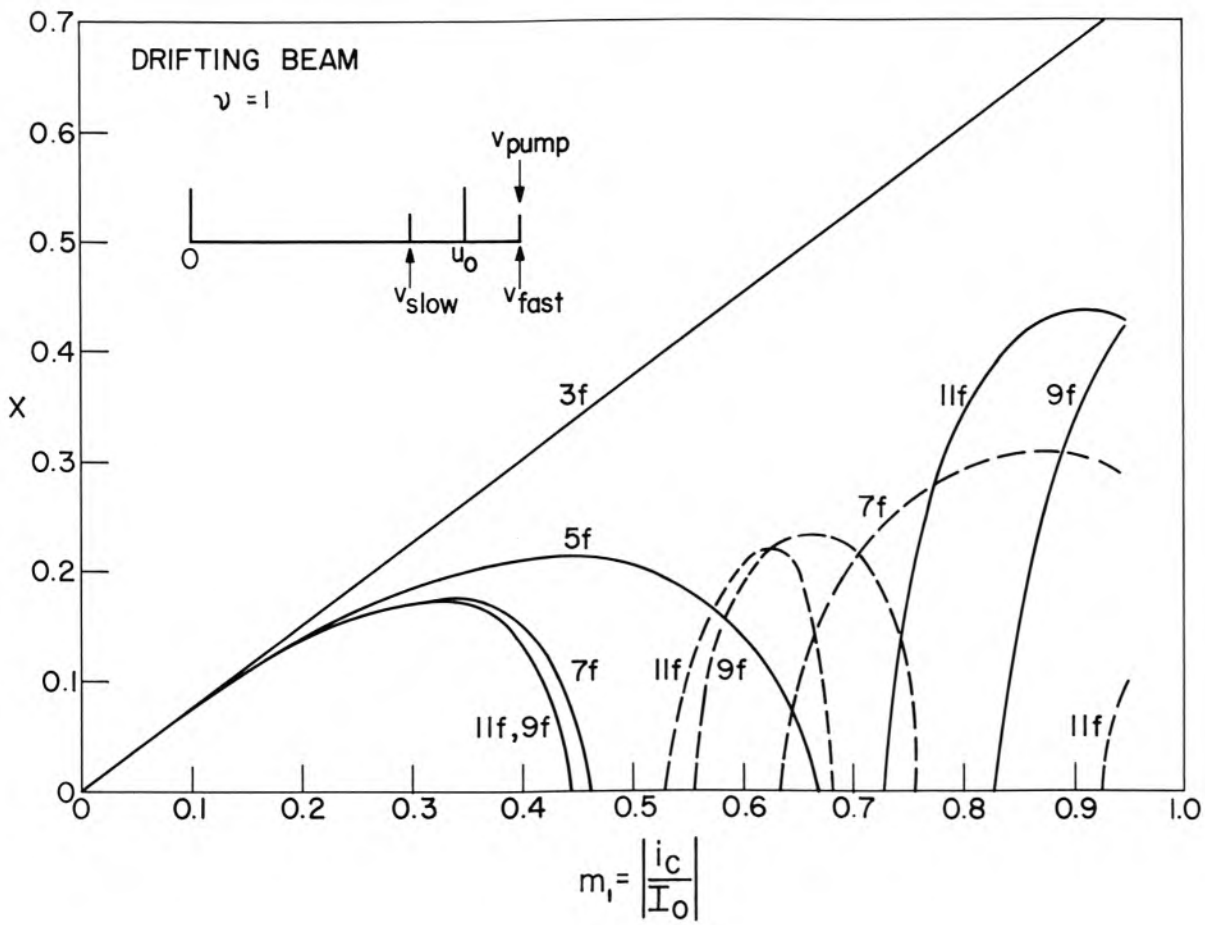

Fig. 5.7 The real parts of the incremental propagation constants for a circuit-pumped amplifier in which the pump wave has the same velocity as the fast signal wave. Curves for various numbers of idler pairs are included to illustrate the convergence of the solution for $m_1 < 0.5$.

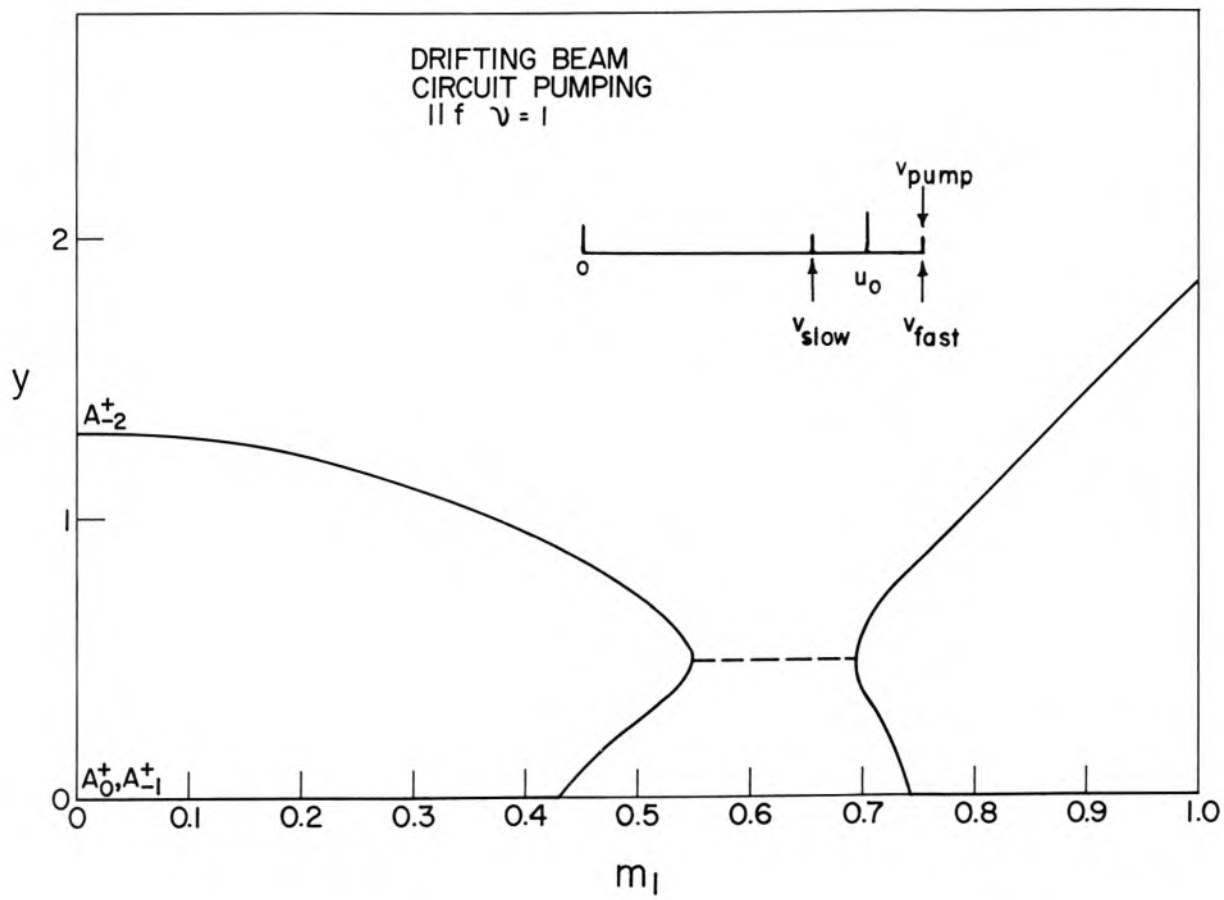

Fig. 5.8 The imaginary parts of the incremental propagation constants for the synchronous-pump-wave case. The signal and idler are coupled for $0 < m < 0.43$ and $0.74 < m \leq 1$, giving rise to the real parts shown in Fig. 5.7 .

In this case, corresponding negative or mirror image plots exist for both Figures 5.7 and 5.8. The dashed lines in Fig. 5.7 represent double roots, and are seen to arise from the coupling of the $\pm 3\omega$ pair of idlers to the signal and principal idler. Again, noisier operation is anticipated in this region due to tight coupling to these higher idlers.

In Fig. 5.9 the $M_{i,o}$ elements are plotted for $m_1 = 0.3$. A gain of 70, or 18.5 db, is achieved in about $2\text{-}1/2\ \lambda_q$. The higher idler waves are loosely coupled for this small value of m_1 and are seen to be considerably lower in amplitude than the signal wave. $M_{-5,0}$ and $M_{+4,0}$ were negligible and therefore not plotted. The values obtained for the $M_{o,i}$ elements at $\zeta = 15.5$ are: a) $M_{0,+1} = 2.2$, b) $M_{0,-2} = 2.5$, c) $M_{0,+2} = 0.15$, d) $M_{0,-3} = 0.20$, and e) the rest negligible. Substitution into equation 5.10 yields a noise temperature of

$$T_e \approx .072\ T_K$$

This is a very good noise temperature at any frequency, and would be unheard of at the higher microwave frequencies. However, the gain per reduced-plasma wavelength is still low.

Case II, Fast-Wave Pumping; $\nu = 1.25$ The improvement in the performance of the amplifier when the velocity of the pump wave is moved from that of the spump space-charge wave to that of the signal wave leads naturally to the speculation that more might be gained by following this trend. Accordingly, the phase velocity of the pump has been increased as illustrated in Fig. 5.10, the plot of the real part of the propagation constants for this case. The imaginary parts are in

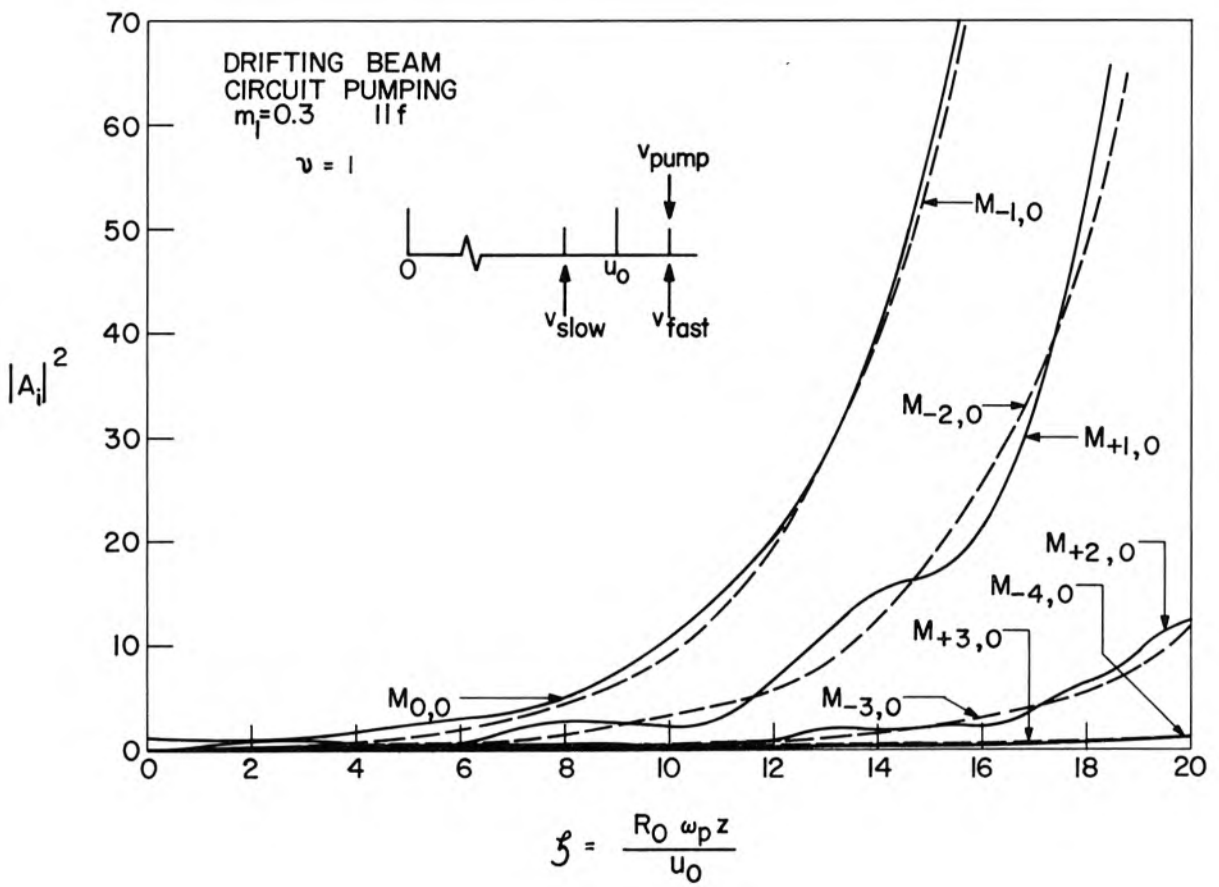

Fig. 5.9 The behavior of the various modes due to unit excitation of the A_0^+ mode for the synchronous-pump-wave case.

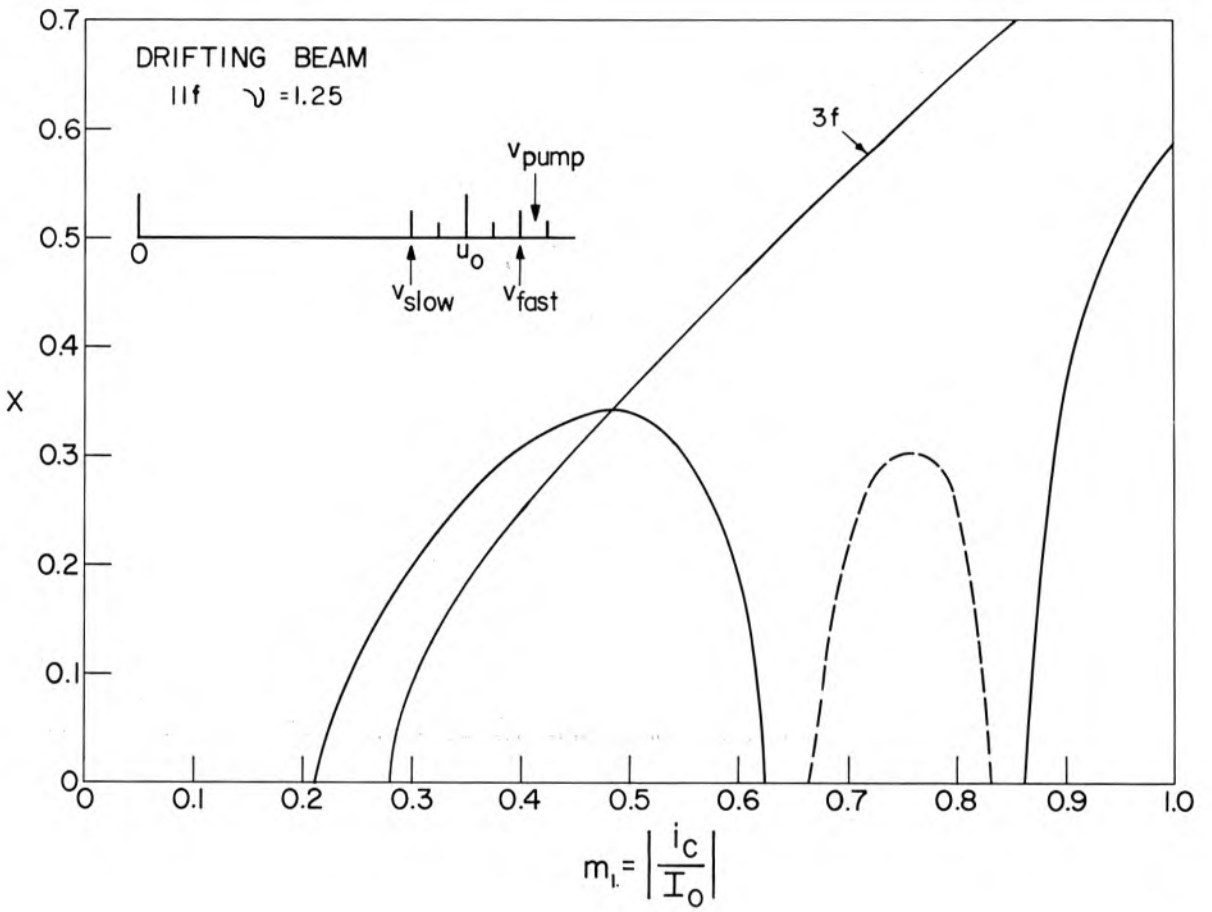

Fig. 5.10 The real parts of the incremental propagation constants for fast-wave pumping (ν = 1.25).

Fig. 5.11. Comparison of the growth constants for this case with the previous case shows that the peak asymptotic gain has almost doubled (now 18.5 db/λ_q), but that stronger pumping is necessary to achieve this gain. In addition, a threshold value for pump power again appears. Unexpectedly the gain in the small m_1 region is higher than that predicted in the three-frequency analysis, as shown in Fig. 5.10. The double roots again arise from coupling to the next idler pair as seen in Fig. 5.11.

The remaining question to be answered is whether or not the requirement for operating at $m_1 \approx 0.4$ causes the coupling to the higher idlers to affect the noise temperature. In Fig. 5.12 the $M_{i,o}$ elements are plotted for $m = 0.4$. The gain is seen to be 18.5 db at about $1.5\ \lambda_q$ and the idler amplitudes are well below the signal amplitude. In Fig. 5.13 the $M_{o,i}$ elements that are not negligible are plotted and the indicated noise temperature at $\zeta = 9.4$ is

$$T_e = 0.055\ T_K$$

Complete curves are presented for this case because it is felt to be near the region of optimum operation. More gain can be achieved as indicated in Fig. 5.10 by increasing m_1, but the noise temperature also increases. Decreasing m_1 yields a lower noise temperature but at the expense of increased length for fixed gain.

Case III, Fast-Wave Pumping; $\nu = 1.5$ Much higher gain can be achieved by further increasing the pump-wave phase velocity as shown in Figure 5.14. However, it is achieved at still higher pump strength. Data was taken for $m_1 = 0.5$ which predicted a noise temperature of $0.07\ T_K$ and a gain of 18.5 db at $1.1\ \lambda_q$. This minor degradation in performance indicates that there is a broad region of operation bracketed by Cases II

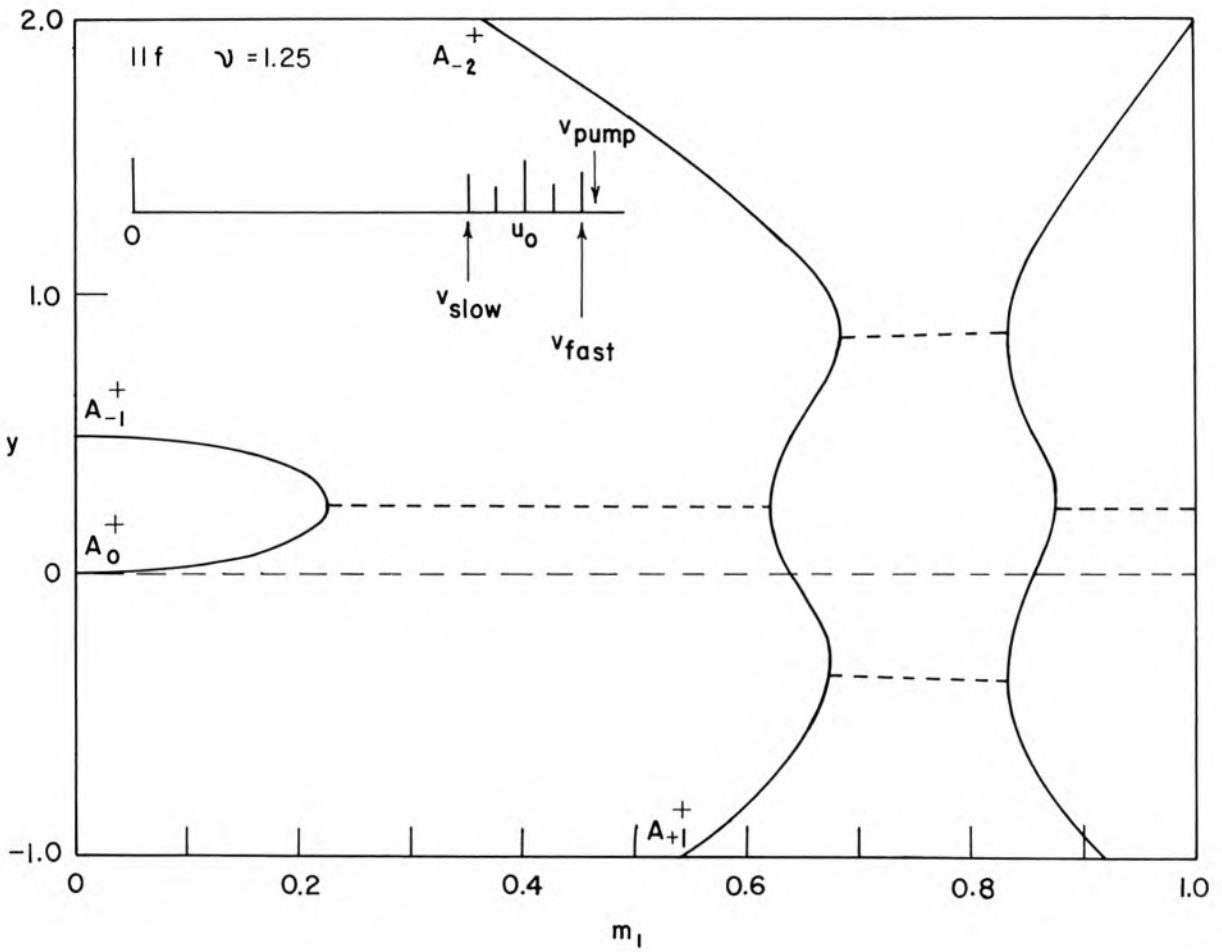

Fig. 5.11 The imaginary parts of the incremental propagation constants for fast-wave pumping ($\nu = 1.25$). Note that the gain at small m_1 still arises from coupling of the noise-free signal and idler wave.

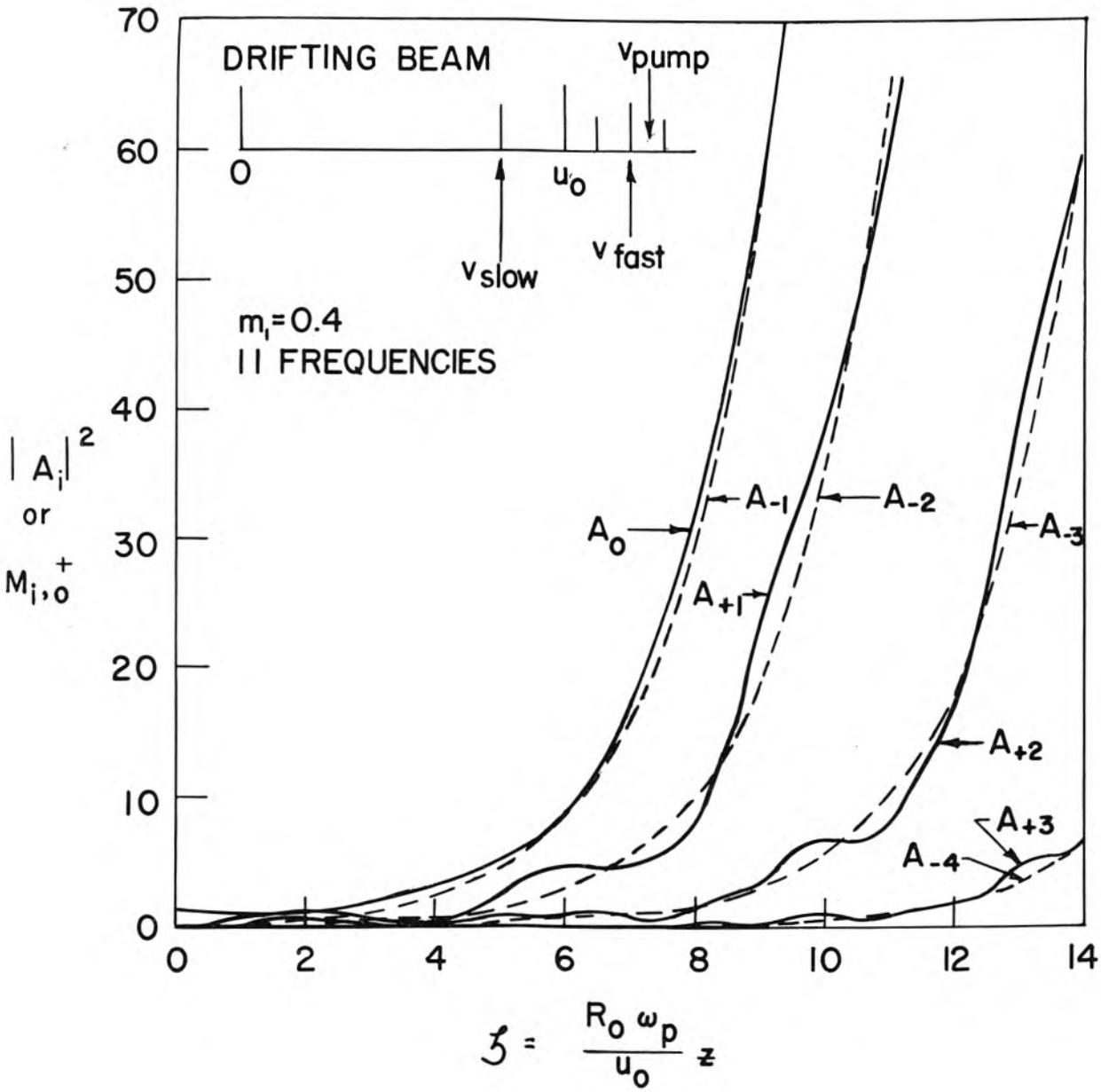

Fig. 5.12 Behavior of the various modes due to unit excitation of the A_o^+ mode for $\nu = 1.25$. Note that the amplitude of the higher order idlers is far below that of the signal and principal idler modes.

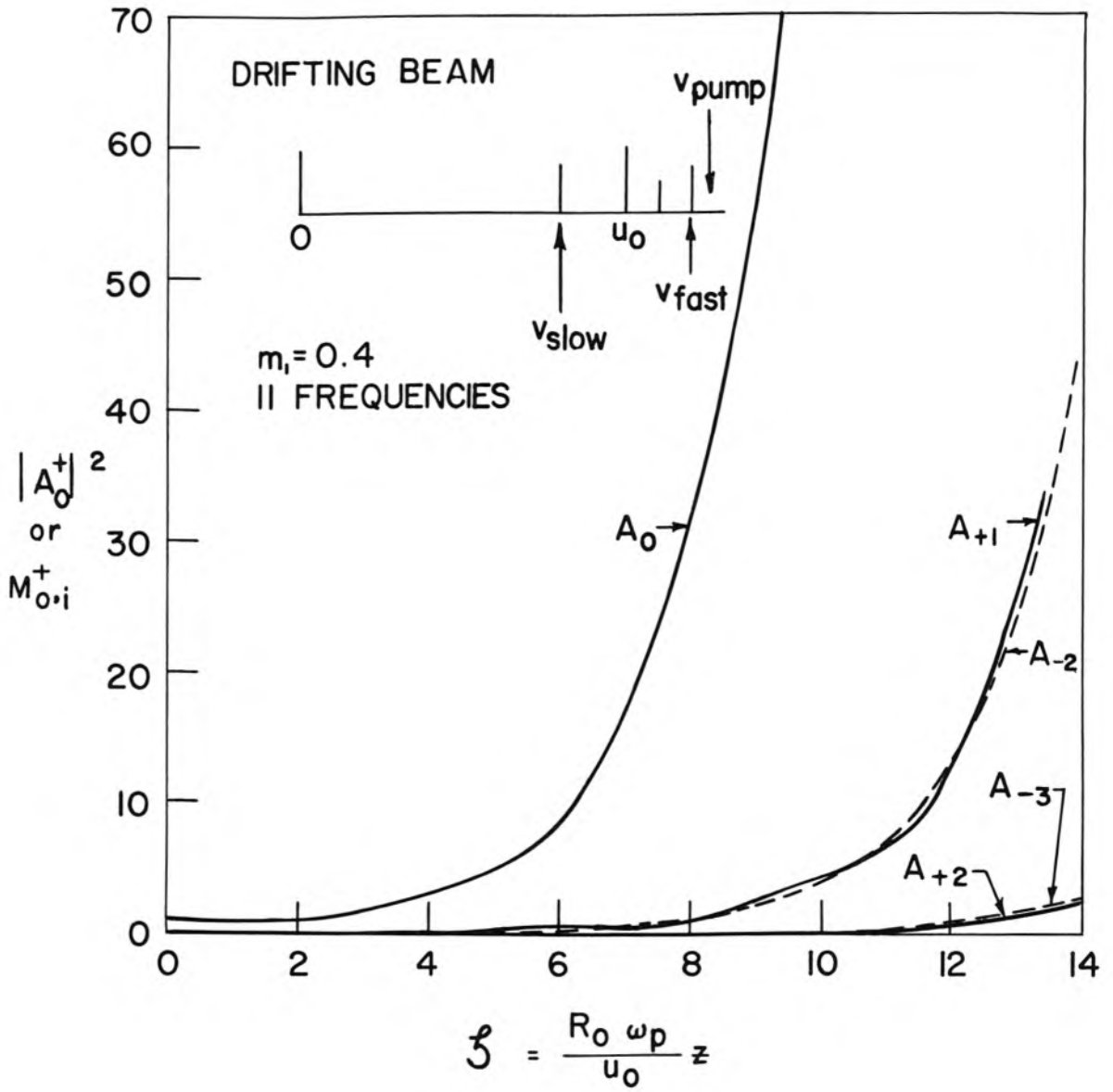

Fig. 5.13 The contribution to the signal mode amplitude due to unit excitation of each mode individually. Note that the contribution due to the noise-carrying higher idler modes is quite small.

and III in which excellent noise performance may be realized.

5.7 Inclusion of Circuit Coupling to Signal and Idler Waves of a Thick Beam

Many cases were studied in an attempt to determine the effects of allowing the circuit to couple to the beam at the signal and principal idler frequencies. In this study the phase velocities of the circuit and of the pump wave were programmed in various combinations in an effort to achieve some beneficial effect. The circuit coupling coefficient k_s was also varied. Only in one case were the results of sufficient interest to present.

In this case the phase velocities of the pump wave and the circuit waves at signal and idler frequencies were set equal to the fast-signal space-charge wave by setting $\nu = \lambda_o = \lambda_{-1} = 1$. k_s was set to 1/4, which corresponds to $QC = 1.0$. As was noted for the thin beam case, the inclusion of even numbers of idler pairs of the same phase velocities gives oscillatory exponential growth. In this case the addition of the pair of circuit waves at the signal wave velocity results in the same type of growth behavior as seen in Fig. 5.15, where some of the more interesting matrix elements are plotted for $m_1 = 0.3$. From Fig. 5.16, which shows the real parts of the propagation constants, it is seen that two growing waves with the same growth constant are present. Since the corresponding imaginary parts of the propagation constants (Fig. 5.17) are different, the phase velocities are different. However, since the matrix elements in Fig. 5.15 go through zero-value nulls, it is evident that the amplitudes of the pair of growing waves are excited equally at the initial plane. Moreover, it is noted that the oscillatory parts of all the $M^c_{o,i}$

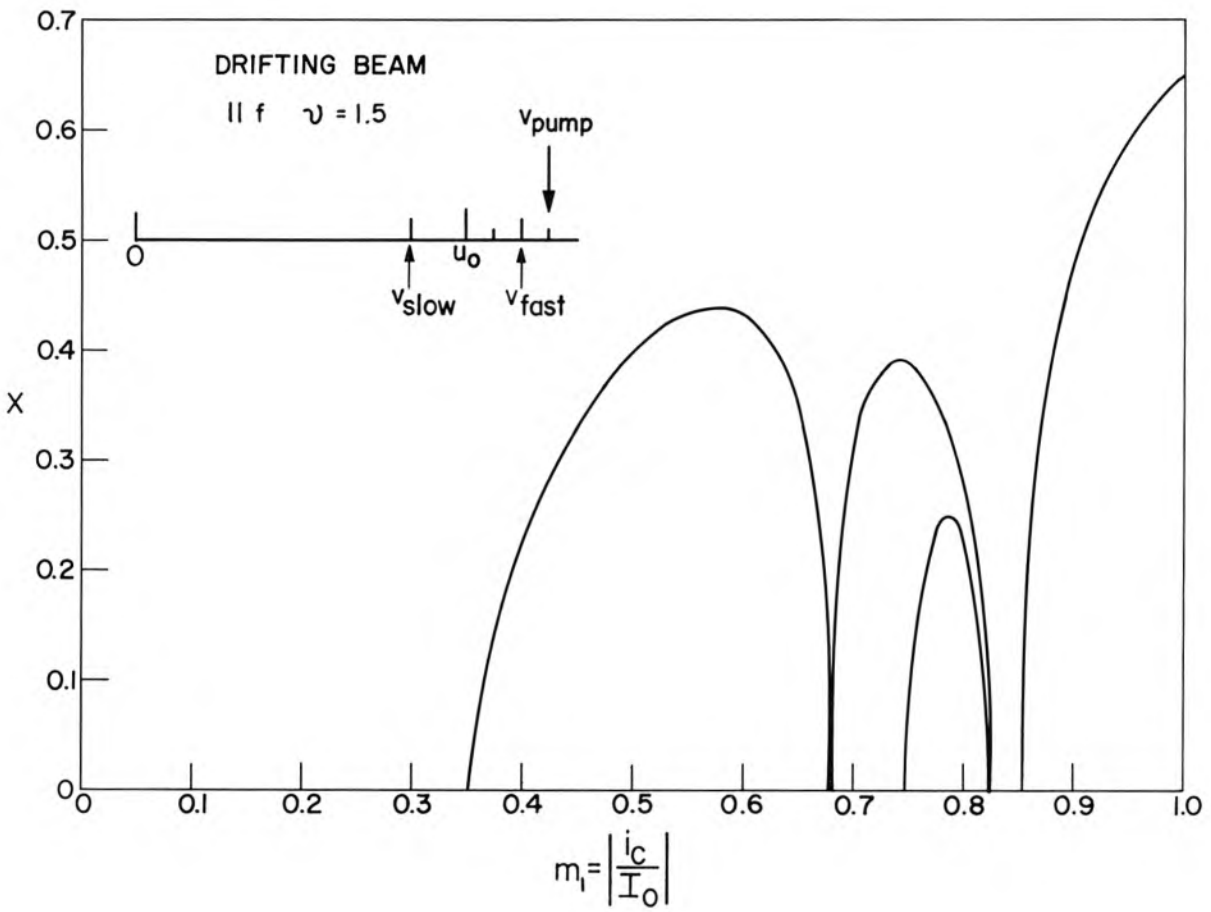

Fig. 5.14 The real parts of the incremental propagation constants for $\nu = 1.5$. Coupling to higher order idlers is quite weak so that relatively high gains are possible.

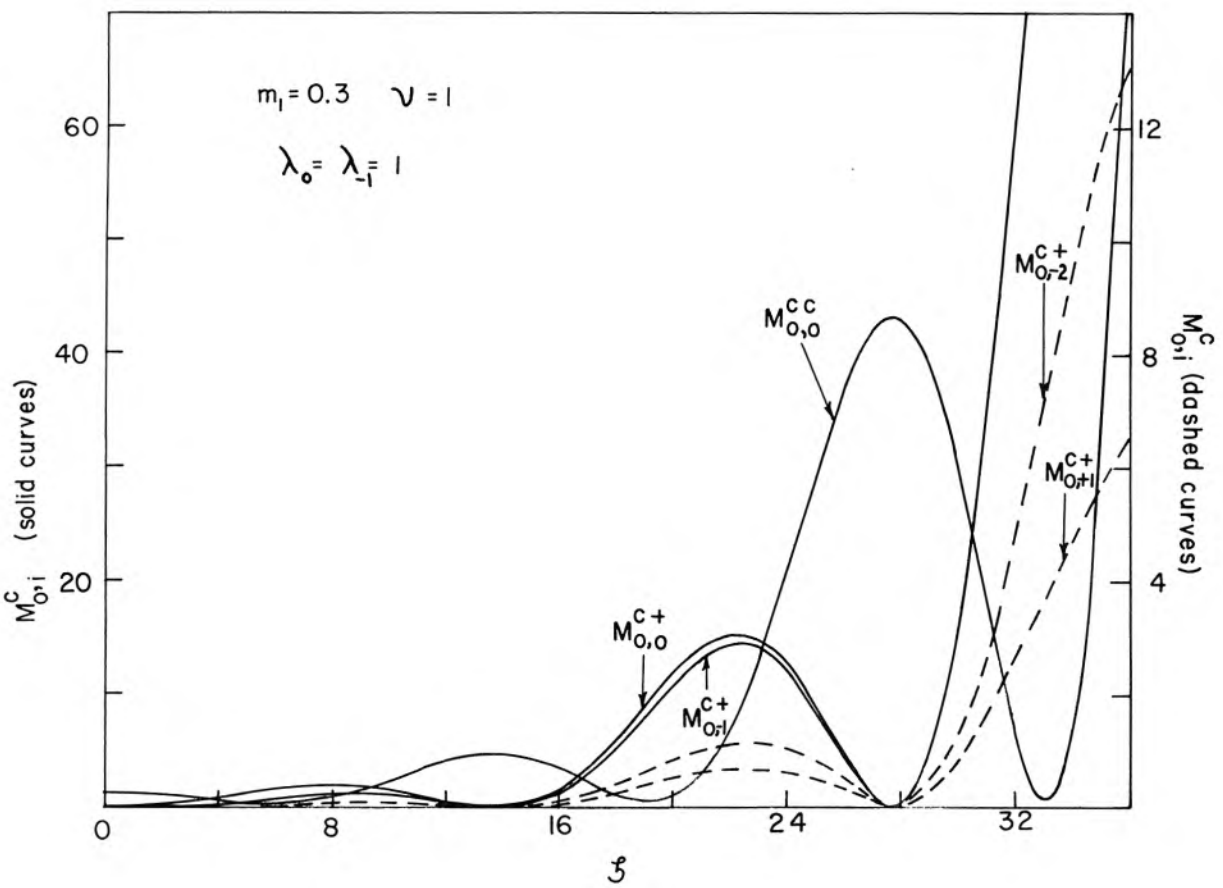

Fig. 5.15 Circuit-mode behavior due to unit excitation of each individual mode. Note that the null in the amplitudes due to excitation of the various beam space-charge modes occurs exactly at a point of peak gain.

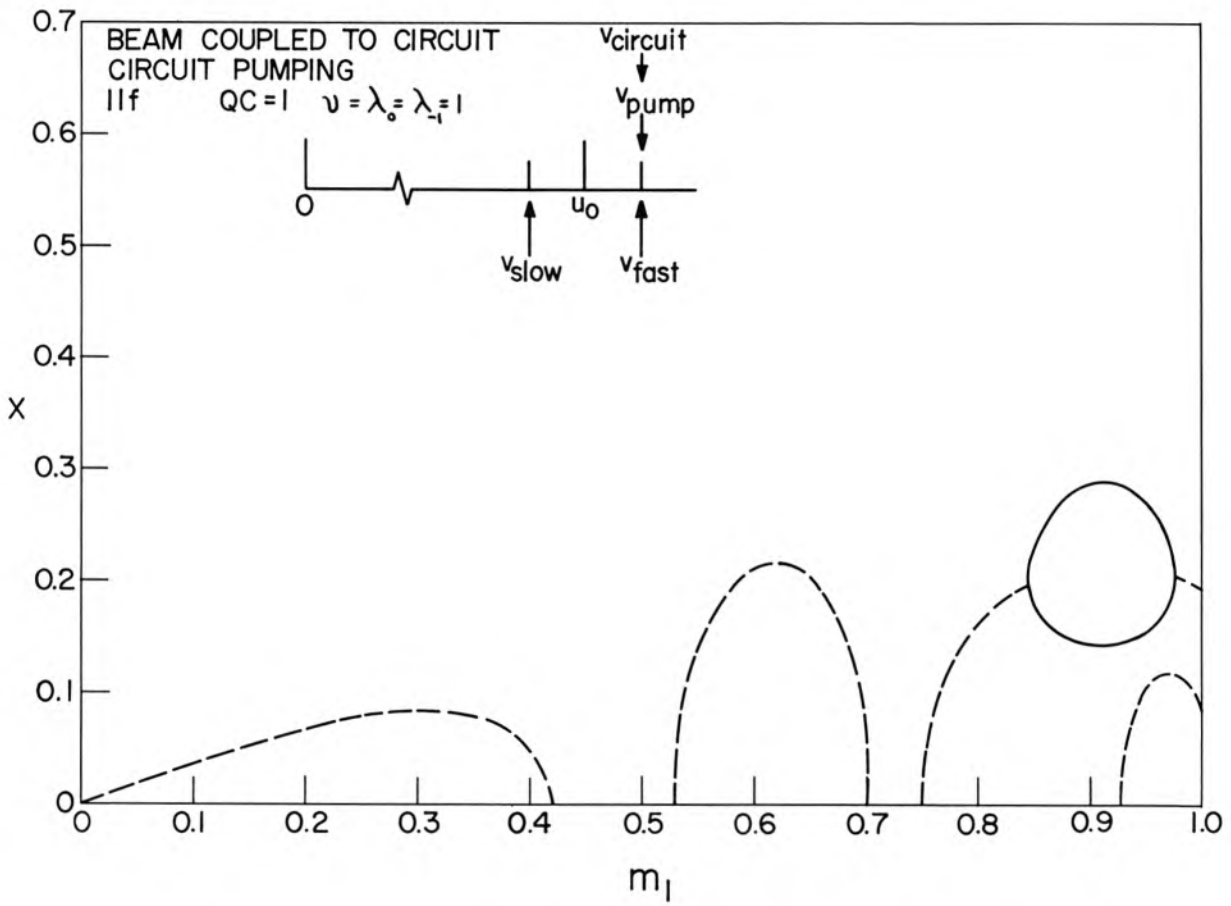

Fig. 5.16 The real parts of the propagation constants for the case in which a circuit is coupled to the beam at the signal and principal idler frequencies. Note that double roots occur at small m_1 .

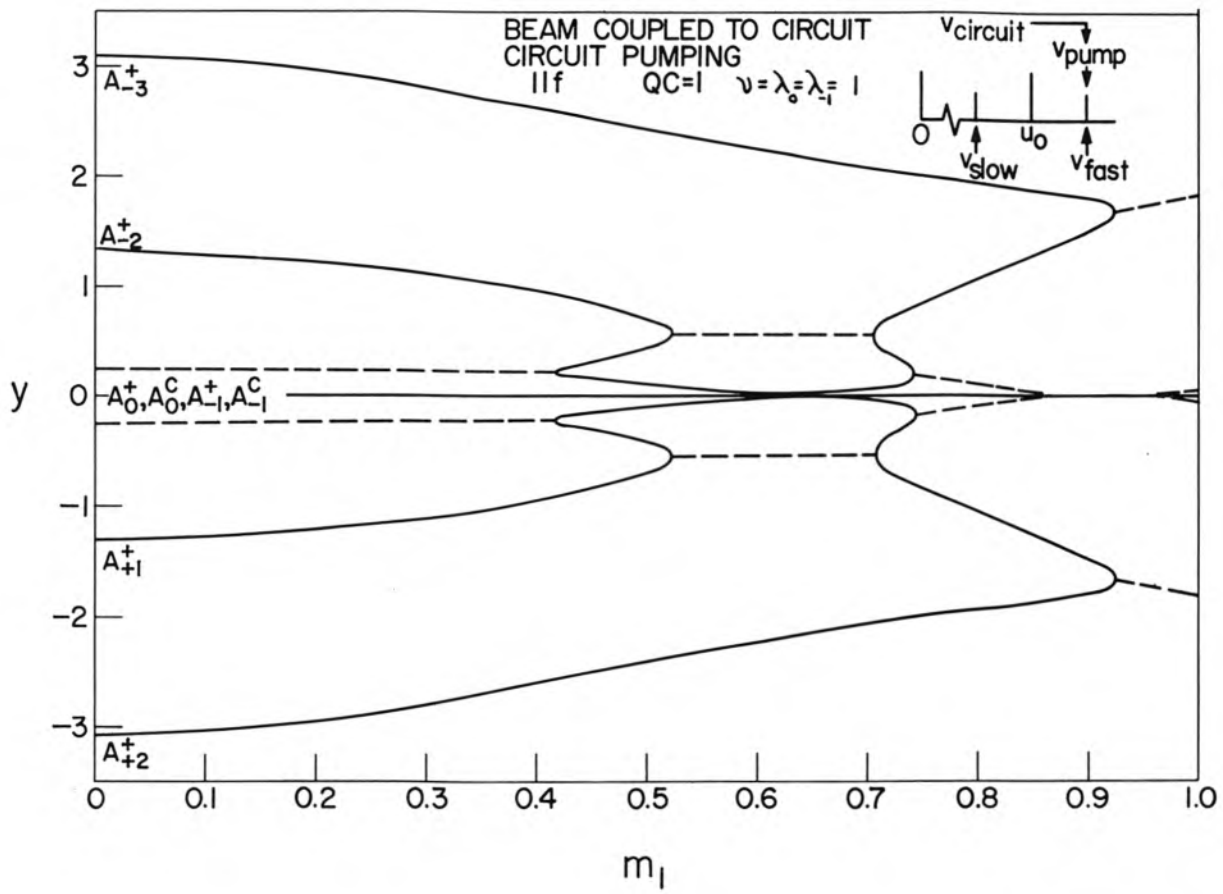

Fig. 5.17 The imaginary parts of the incremental propagation constants for the circuit-coupling case. The residual traveling-wave-tube coupling ($k_s \neq 0$) accounts for splitting of the modes at $m_1 = 0$.

elements with the exception of $M^{c\,c}_{0,-1}$ are 180^{o} out of phase with the $M^{c\,c}_{0,0}$ element. This means that any noise excited on the circuit by the space charge waves at signal and idler frequencies will beat back onto the beam at the point where $M^{c\,c}_{0,0}$ is maximum. Unfortunately, for the optimum case as shown, the power gain is very low except for lengths of $\lambda_q \gtrsim 4.5$.

From Fig. 5.17 it is seen that the higher growth region around $m_1 = 0.6$ in Fig. 5.16 again involves coupling to higher idlers, and that the circuit modes do not couple strongly. As a consequence the curves are seen to closely resemble Fig. 5.7 and 5.8 for the drifting beam in this area of operation.

In general the inclusion of a circuit coupled to the signal and idler waves does not markedly change the behavior from that of the drifting beam amplifier as long as the imaginary part of the propagation constants of the previously coupled $(m_1 = 0)$ system are appreciably different from the imaginary parts of the normal propagation constants of the parametrically coupled $(m_1 \neq 0)$ system in the gain regions. When this is not the case, the general effect is a lowered gain with attendant oscillatory effects. The significant difference in the passive coupling of the signal and idler waves to pairs of circuit waves, as contrasted to passive coupling to pairs of idler waves, is that the periodic energy transfer is completely reciprocal in the former case but not in the latter case. As a consequence, zero-value nulls are not encountered in the drifting-beam amplifier for any case of interest. These effects will become more evident in the general discussion of the matrix elements which is to follow.

In none of the cases studied were any of the four gain possibilities $M_{0,0}^{c\,c}$, $M_{0,0}^{c\,+}$, $M_{0,0}^{+\,c}$, or $M_{0,0}^{+\,+}$ as large as the corresponding drifting-beam ($k_s \to 0$) gain $M_{0,0}^{+\,+}$, nor was any improvement in the noise behavior evident except in the previously illustrated case. In view of these results, it is felt that little is to be accomplished by including circuit coupling of this type.

5.8 Properties of the Matrix Elements

The elements of the matrix defined by equation 5.2 have certain symmetry properties for the degenerate case which are useful in deducing some general physical properties of the amplifiers. These properties in turn provide the basis for a qualitative design philosophy. The properties of the matrix are all determined empirically from extensive data taken on the analog computer. No attempt was made to include circuit coupling, so that all of the properties hold only for the fast-wave drifting-beam amplifier.

If an adequate solution is obtained from n pairs of waves, and the column matrices of equation 5.2 are written as in equation 5.3, the $2n \times 2n$ square matrix M then has general position symmetry given by

$$M_{ij} = M_{2n+1-i,\,2n+1-j} \tag{5.17}$$

The physical significance of the symmetry expressed by this relationship can be seen by considering Fig. 5.18. The figure represents an example in which four pairs of fast waves (9 frequencies) are adequate for solution. M is therefore an 8×8 matrix. In this matrix, $M_{-2,+2}$ occupies the position M_{37} while $M_{+1,-3}$ occupies the position M_{62}, and the pair satisfies the condition 5.15. They represent, respectively,

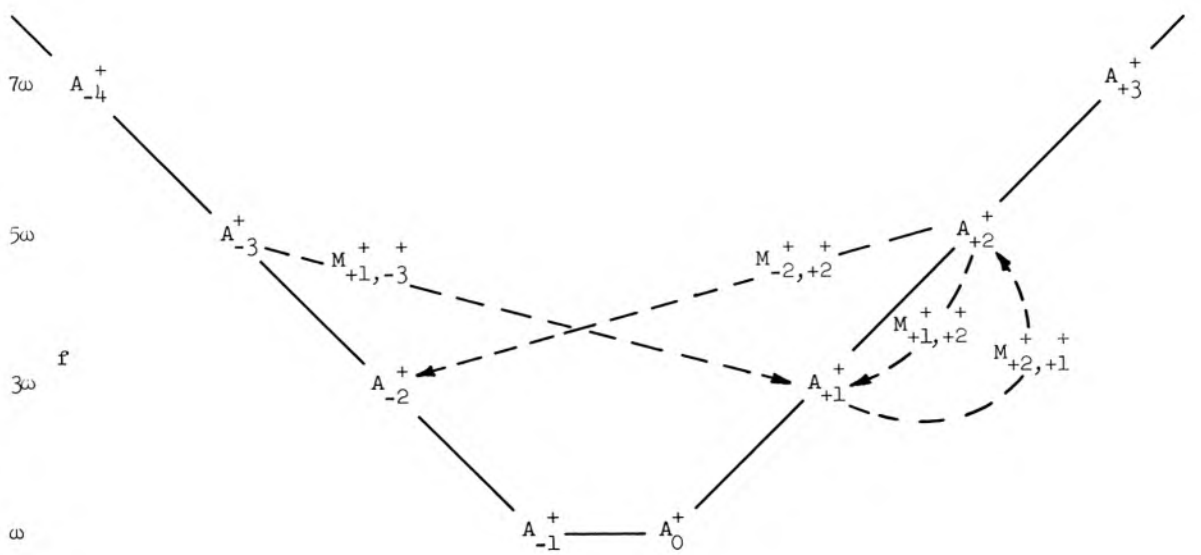

EXAMPLES OF MATRIX PROPERTIES

a) $M^{+\,+}_{-2,+2} = M^{+\,+}_{+1,-3}$

$M^{+\,+}_{0,-4} = M^{+\,+}_{-1,+3}$

$M^{+\,+}_{+2,+1} = M^{+\,+}_{-3,-2}$

b) $\dfrac{M^{+\,+}_{+2,+1}}{M^{+\,+}_{+1,+2}} = \left(\dfrac{5}{3}\right)^2$

$\dfrac{M^{+\,+}_{-2,-1}}{M^{+\,+}_{-1,-2}} = (3)^2$

Fig. 5.18 Typical illustrations of the symmetry properties of the matrix which describes the fast-wave parametric amplifier in the near-degenerate case.

the output on the -3ω mode due to initial excitation of the $+5\omega$ mode, and the output on the $+3\omega$ mode due to initial excitation of the -5ω mode. This behavior holds for all analogous situations and is anticipated because of the symmetry of the physical problem.

Another interesting property is illustrated in the lower right hand corner of Fig. 5.18. Here the elements expressing the reciprocal excitation of a pair of modes as shown obey the general relation

$$\frac{M^{+\,+}_{r,s}}{M^{+\,+}_{s,r}} = \left(\frac{f^{+}_{r}}{f^{+}_{s}}\right)^{2} \tag{5.18}$$

i.e., the ratio of the magnitudes of the elements is determined by the ratio of the frequencies of the modes involved. A typical set of data curves of the type from which these relations are inferred is shown in Fig. 5.19. It is seen that $M_{+2,+1} = M_{-3,-2}$ (positions M_{34} and M_{87} in the 10 x 10 matrix) and that $M_{+2,+1}$ differs from $M_{+1,+2}$ by a multiplicative constant which turns out to be given by

$$\frac{M_{+2,+1}}{M_{+1,+2}} = \left(\frac{f^{+}_{+2}}{f^{+}_{+1}}\right)^{2} = \left(\frac{5}{3}\right)^{2} \tag{5.19}$$

The fact that frequency plays an important role in this reciprocal behavior might well be the consequence of the form of the Manley-Rowe relation (equation 3.94). No attempt has been made to prove these relationships analytically.

5.9 General Discussion

Except for the space-charge-pumping case of Fig. 5.4, the first region of exponential growth encountered in every case, as m_1 increases from zero, arises from the coupling of the signal and principal idler

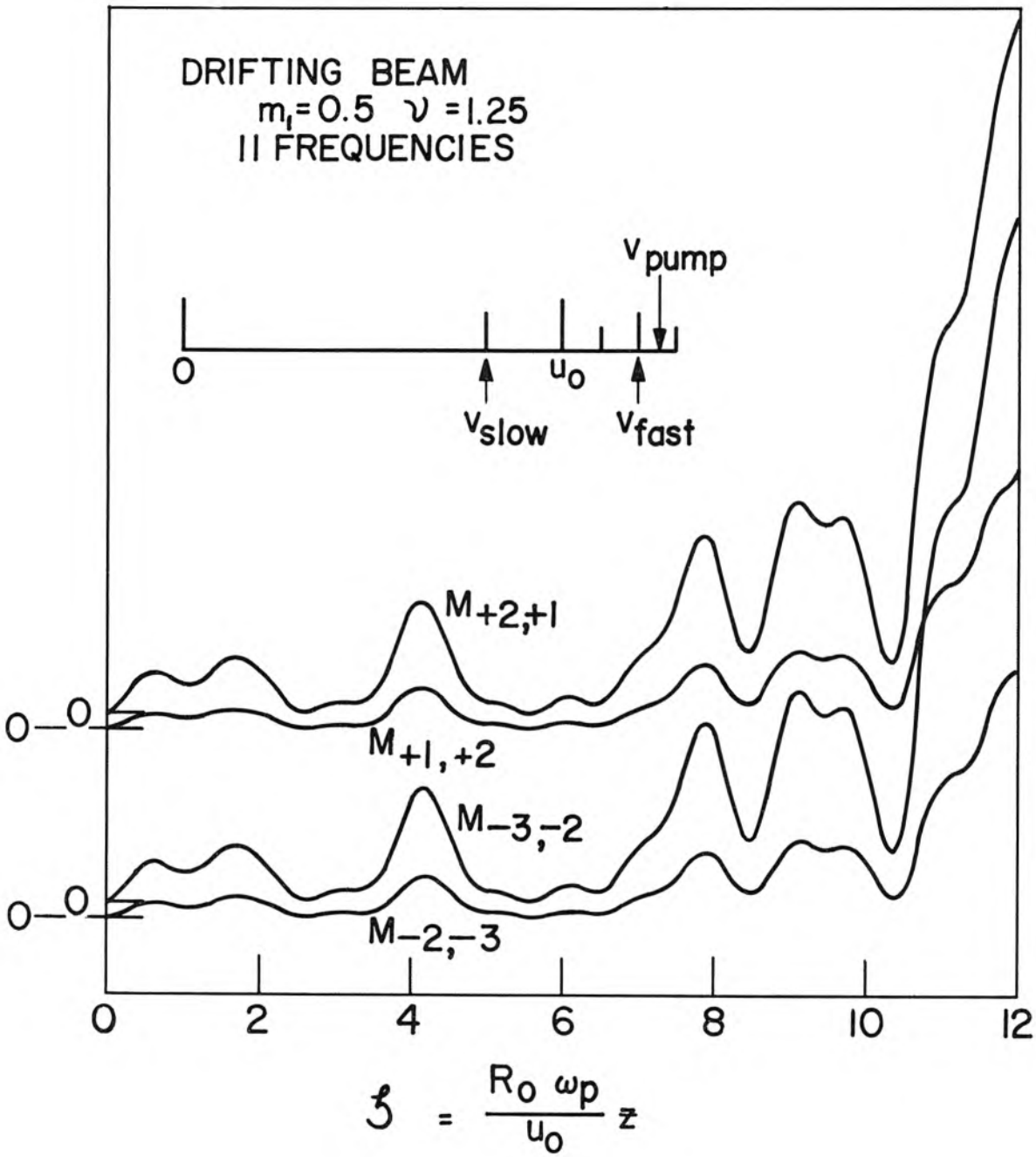

Fig. 5.19 Analog computer plots of several related matrix elements. The symmetry properties of the matrices are inferred from data of this type.

wave. The gain increases monotonically in these regions until the adjacent $M^{+}_{i,o}$ matrix elements, which increase with m_1, become as large as $M^{+\,+}_{0,0}$. The gain then decreases until the growth constant disappears. In this latter region of operation, the energy is being transferred rapidly to the higher idler waves. From equation 5.16 it is seen that the transfer of energy to the idler waves, represented by $M^{+}_{i,o}$ is always greater than the coupling of noise to the signal wave, represented by $M^{+}_{o,i}$. However, when the $M^{+}_{i,o}$ are of the same order of magnitude as $M^{+\,+}_{0,0}$ the sum of the noise contributions from all the waves becomes large. Thus it becomes obvious that the one way to insure low noise operation is to operate on the positively sloped portion of the growth factor curve where $M^{+}_{i,o} < M^{+\,+}_{0,0}$ as in Fig. 5.12 and thus be assured that the $M^{+}_{o,i}$ elements are small because of equation 5.18 and as shown in Fig. 5.13. Thus a slight sacrifice in gain per unit length pays dividends in terms of lowered noise temperature.

The gain regions resulting from the coupling to higher order idlers are to be avoided since the noise excitation on the growing wave in the coupled system will be large. Operation at higher values of m_1 ($m_1 > 0.5$) is not recommended because all of the idlers are tightly coupled in these regions and trouble from pump harmonics is also anticipated.

The achievement of higher gain and lower noise temperatures with increased pump-wave phase velocity is effected by reduced effective coupling to the higher idler waves. It is noted that by increasing ν the β's of the uncoupled modes (equations 3.1 and 3.2) are spread apart more rapidly than the coupling coefficients increase, and thus

the k_e of equation 3.6 is reduced. As a consequence, operation at higher values of m_1 is possible before these waves become troublesome.

CHAPTER VI

FURTHER APPLICATIONS OF THE GENERAL EQUATIONS

6.1 Introduction

In this chapter, the flexibility of the general theory is demonstrated by briefly discussing its application to several interesting multiple-frequency beam problems. No attempt is made to go into great detail in any of these areas. Again the single-pump-wave theory of Chapter III is used in each case.

6.2 Cooling the Slow Space-Charge Wave

The passive nature of the coupling of slow and fast space-charge waves by parametric pumping was noted in the discussion of the general form of the matrix H in equation 3.96. This is of vital interest since heretofore the interaction of slow space-charge waves through mutual-field coupling to positive a.c. energy carriers led to active coupling and, as a consequence, prevented removal of the slow-wave noise. As first realized by Sturrock (34) this new possibility of passive coupling to a fast space-charge wave provides a new mechanism of noise removal from the slow space-charge wave and, in principle, opens a new avenue of approach to the attainment of better noise performance in conventional beam-type amplifiers. One straightforward application of the mechanism is illustrated in Fig. 6.1. In the first section the noise is removed from the fast space-charge wave with the same type of coupler that is used in the parametric amplifier. In the "noise exchanger" the passive coupling of the space-charge waves is used to transfer the noise from the slow to the fast wave. Since the

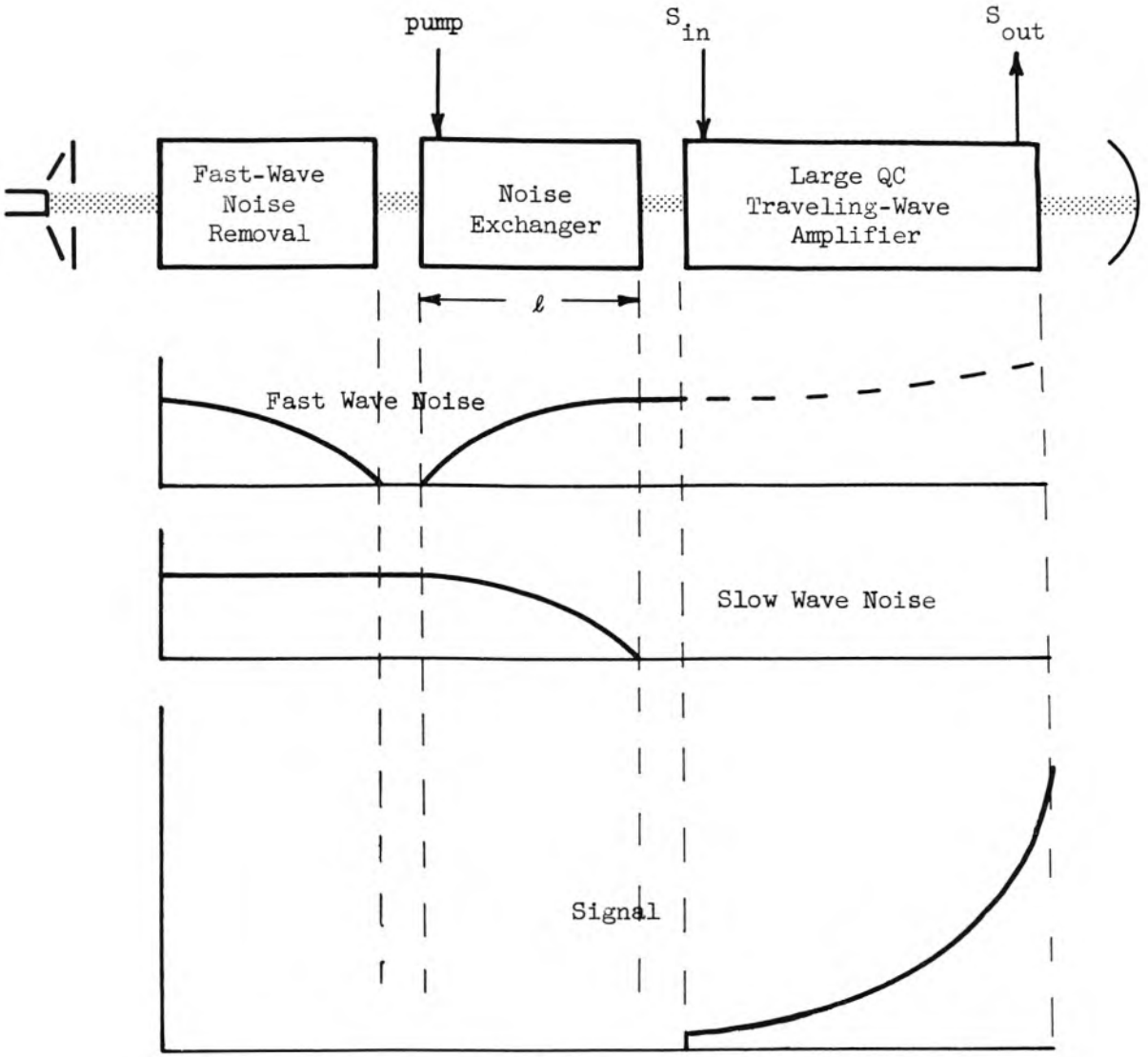

Fig. 6.1 Functional diagram of a typical application of the slow-space-charge-wave cooling principle. The reason for designing the traveling-wave amplifier for large QC will be discussed in the text.

initial noise excitation on each wave is periodically transferred to the other and since the fast wave is now initially noise free, the length ℓ of this section is adjusted so that all of the noise appears on the fast wave at the output end. It is well known that the coupling to the fast wave is weak in large QC traveling-wave tubes, so that very low-noise behavior can be expected in the device as indicated. Still better performance might be achieved by inserting another fast-wave noise coupler between the noise exchanger and the traveling-wave tube.

The performance of the traveling-wave tube will be somewhat complicated by the existence of fairly strong pump modulation induced on the beam in the noise exchanger. In the next two sections the performance of both the noise exchanger and that of the traveling-wave tube with pump modulation initially present on the beam will be investigated by application of the single-pump-wave theory. Other possible areas of application are also introduced.

6.3 Passive Coupling of Space-Charge Waves

If the velocity of the pumping wave is set equal to the average beam velocity u_o^* (i.e., $\nu = 0$), it is found that the effective coupling between mode pairs as expressed by the parameter k_e (equation 3.6) for the thick beam of Chapter V ($\beta_e b = 0.7$, $a/b = 3$) is as follows:

Coupled Pair	k_e	Coupled Pair	k_e
A^-_{-2} to A^-_{-1}	$.865m_1^2$	A^+_{-1} to A^-_{o}	$\to +\infty$
A^-_{-2} to A^+_{-1}	$-.057m_1^2$	A^+_{-1} to A^+_{o}	$-.062m_1^2$
A^+_{-2} to A^-_{-1}	$-.057m_1^2$	A^-_{o} to A^-_{+1}	$.865m_1^2$
A^+_{-2} to A^+_{-1}	$.865m_1^2$	A^-_{o} to A^+_{+1}	$-.057m_1^2$
A^-_{-1} to A^-_{o}	$-.062m_1^2$	A^+_{o} to A^-_{+1}	$-.057m_1^2$
A^-_{-1} to A^+_{o}	$\to +\infty$	A^+_{o} to A^+_{+1}	$.865m_1^2$

*Again the δ_2 mode of Pierce has this property for $QC = 1$, $b = 0.3$. See page 126, Reference 28.

The strong coupling between the fast signal and slow idler waves, and fast idler and slow signal waves respectively, is due to the fact that these waves are synchronous and the denominator in the expression for k_e becomes zero. Only the equations from $s = -2$ to $+1$ for the drifting beam are included (5 frequencies) and near-degeneracy is assumed.

Recalling that the condition for growing waves is $k_e < -1$, it is seen that all of the coupling is passive. The fast signal and slow idler waves are very tightly coupled, as are the fast idler and slow signal waves. The only other effectual coupling is between the four pairs for which $k_e = .865m^2$, and each pair is seen to consist of a signal or idler wave coupled to the adjacent higher order idler of the same type, i.e., fast to fast, etc.

The matrix elements $M^{--}_{o,o}$ and $M^{--}_{-1,-1}$, which are the same, are plotted in Fig. 6.2 for three frequencies. They are almost perfectly sinusoidal and absolute nulls are evident. The elements $M^{--}_{o,-1}$ and $M^{--}_{-1,o}$ are not plotted since their amplitude is always negligible. The form of the elements $M^{+-}_{o,-1}$ and $M^{+-}_{-1,o}$ is again sinusoidal, as are $M^{-+}_{-1,o}$ and $M^{-+}_{o,-1}$. The amplitudes of the two remaining elements $M^{-+}_{-1,-1}$ and $M^{-+}_{o,o}$ are negligible.

It is evident from Fig. 6.2 that noise introduced on the signal and idler slow waves is transferred to the idler and signal fast waves respectively, if the length of the section is terminated at the first null. It is fortunate that the noise is simultaneously removed from the slow idler wave since this wave will enter prominently into the gain process if the beam is used in a traveling-wave tube as discussed previously. The disadvantage evidenced by the curves is the need for exchangers whose lengths are on the order of a few plasma-wavelengths, even though relatively strong pumping is used as indicated by the $m_1 = 0.6$ curves.

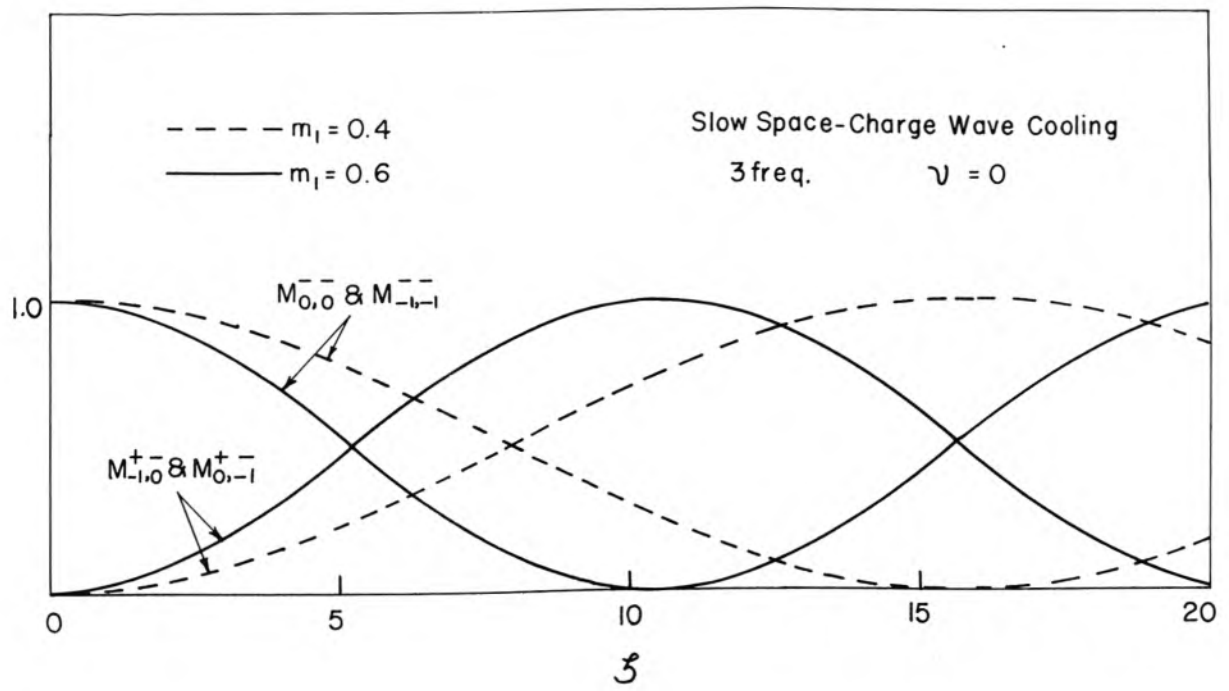

Fig. 6.2 The behavior of the dominant matrix elements in the slow-space-charge-wave cooling process. Note that the length needed for the noise exchange decreases as m_1 increases.

The effects of the inclusion of the A^{+}_{-2}, A^{-}_{-2}, A^{+}_{+1}, and A^{-}_{+1} waves are illustrated in Fig. 6.3. Minor perturbations of the sinusoidal behavior of the matrix elements occur, but the absolute null is still present. Minor contributions to noise from the higher order idlers were determined by evaluating the $M^{-}_{-1,i}$ and $M^{-}_{o,i}$ elements at the null. For m = 0.6, they are:

$$M^{-}_{-1,-2} = M^{-}_{0,+1} \approx .015$$

$$M^{-}_{-1,+1} = M^{-}_{0,-2} \approx .019$$

The remaining elements are negligible. Careful examination of the coupling presented in the table leads to anticipation that the aforementioned matrix elements will be the largest. Fortunately, their magnitude is sufficiently small so that the anticipated noise performance is still quite attractive. It is suspected that further contributions from still higher order idlers will be much smaller than these.

6.4 Traveling-Wave Tube with Pump-Space-Charge Waves Present

Two conflicting requirements become evident immediately when one considers the design of the traveling-wave-tube section of Fig. 6.1. One must now consider the relative magnitudes of the mutual-field coupling (k_s) and the parametric coupling $[D_i(s)]$ for typical ranges of the parameters. For small QC one finds that $k_s \gg D_i$, so that the mutual-field coupling predominates and the parametric pumping by space-charge waves is negligible. However, for small QC, appreciable coupling to the noisy fast signal-space-charge wave is present, and the noise temperature will suffer considerably. The gain per plasma wavelength is very high in this case so that in the short length required the noise

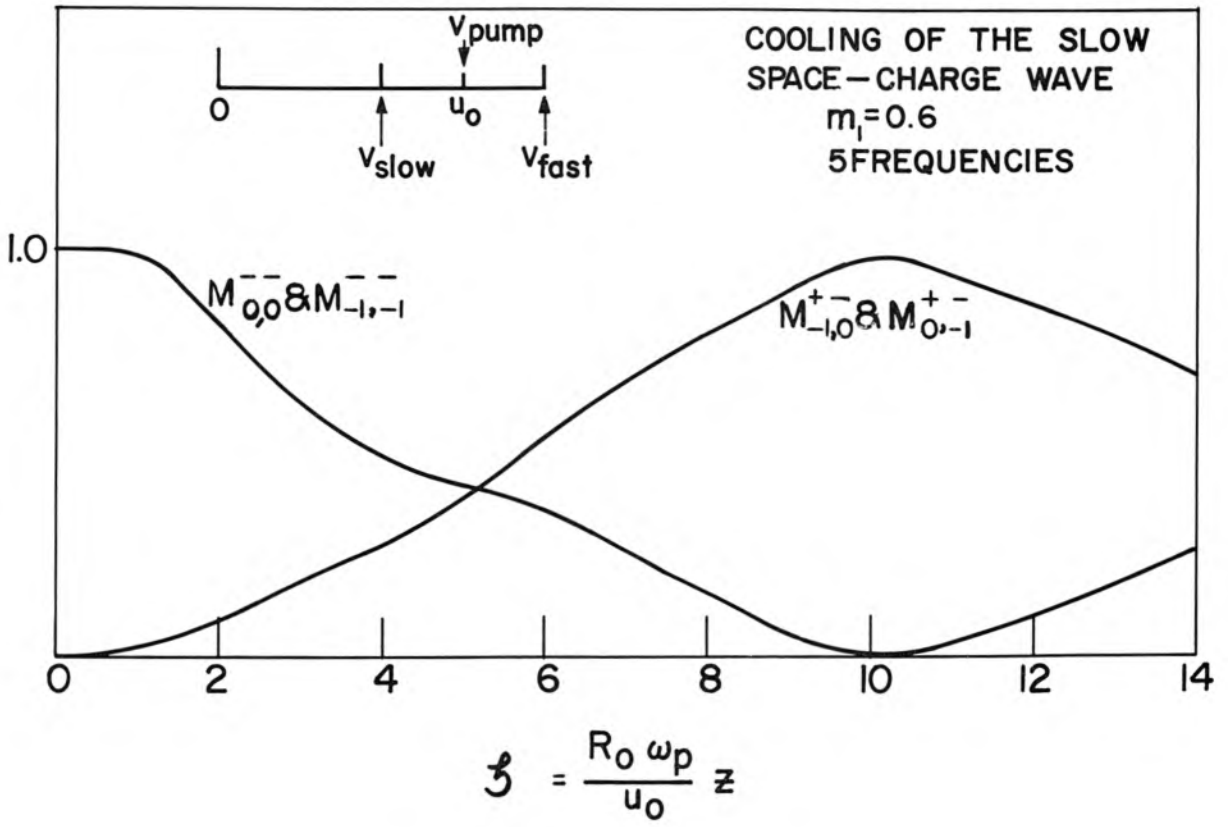

Fig. 6.3 The effect of the addition of higher idlers on the slow space-charge-wave cooling process. Note that the null is still absolute and occurs at the same ζ as in Fig. 6.2

contributions due to parametric coupling to higher idlers is probably negligible, even for strong pumping.

Conversely, for large QC the coupling to the fast-signal space-charge wave is weak, but the gain is low and the coupling due to parametric pumping which is now of the same order as the field coupling may introduce appreciable amounts of noise in the lengths required. Thus some compromise is sought in which it is hoped that neither source of noise presents a serious problem.

In the practical case both pump space-charge waves will be excited. For a complete solution the equations of Chapter IV would be used. However, it is found that the fast pump wave couples the fast signal and idler space-charge waves and that the slow pump wave couples the slow signal and idler space-charge waves, just as in a parametric amplifier. In either case the coupling from slow to fast space-charge waves is negligible. Only when the pump wave velocity is near u_o, as in the previous section, does this type of coupling become important. Since noise is carried at the entrance plane by the fast signal and idler waves and the traveling wave tube interaction is principally with the slow waves, it is expected that the major noise contribution at the signal frequency will be due to strong parametric coupling of the slow waves to the higher idler slow waves through the slow pump wave, rather than that caused by the relatively weak coupling of slow and fast waves through both fast and slow pump waves. Therefore, it would seem best to approximate the situation for single wave treatment by assuming a single slow pump wave. The validity of the arguments leading to this approximation can then be checked by noting the relative magnitude of

the effects on conventional traveling-wave tube performance when a fast pump wave is assumed.

A preliminary study of the traveling wave tube with a slow pump-space-charge wave has been completed. The model consists of a conventional traveling-wave tube except that a slow pump wave of modulation index m_1 is present on the beam. The noise excitation of the slow signal and idler waves (A_o^-, A_{-1}^-) are assumed zero. The fast signal wave and the higher order idlers are assumed to be excited to the cathode temperature T_K (^oK). Coupling to the circuit only at the signal and idler frequency is considered. The noise coupled in from the idler circuit wave A_{-1}^c is assumed to come from a termination at $\frac{1}{3} T_K$.

The equations for five frequencies were solved on an analog computer in the near-degenerate case for several values of QC. A typical plot of the various matrix elements is shown in Fig. 6.4. The power gain is represented by the matrix element $M_{0,0}^{c\,c}$ and the noise temperature is given by

$$T_e = \frac{T_K}{3M_{0,0}^{c\,c}} M_{0,-1}^{c\,c} + \frac{T_K}{M_{0,0}^{c\,c}} \sum_{i \neq 0,-1,-1}^{- \; -} M_{0,i}^{c\,c} \qquad (6.1)$$

The gain and noise performance is summarized in Figures 6.5 and 6.6. The matrix elements used in determining the noise temperature are evaluated for the length at which $M_{0,0}^{c\,c} = 100$, i.e., where the power gain is 20 db. In the absence of the pump wave ($m_1 = 0$), the noise temperature decreases as QC increases; also, the noise contributions due to parametric pumping are more consequential for large QC. This behavior is in accordance with expectations. In Fig. 6.6 the suppression of gain due to the presence of the pump wave is indicated. It also is more serious at

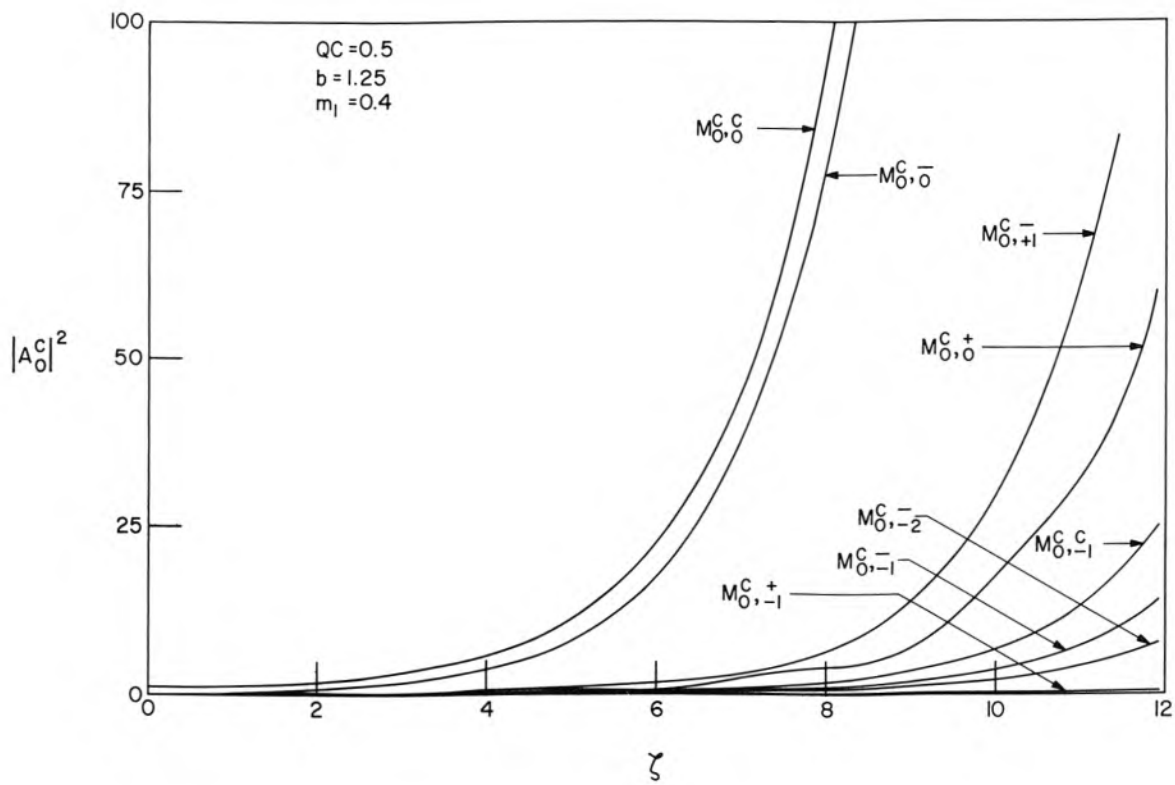

Fig. 6.4 A typical plot of the contributions to the circuit mode for a traveling-wave amplifier with a slow pump space-charge wave excited on the beam. The noise temperature of the amplifier is predicted from this type of plot.

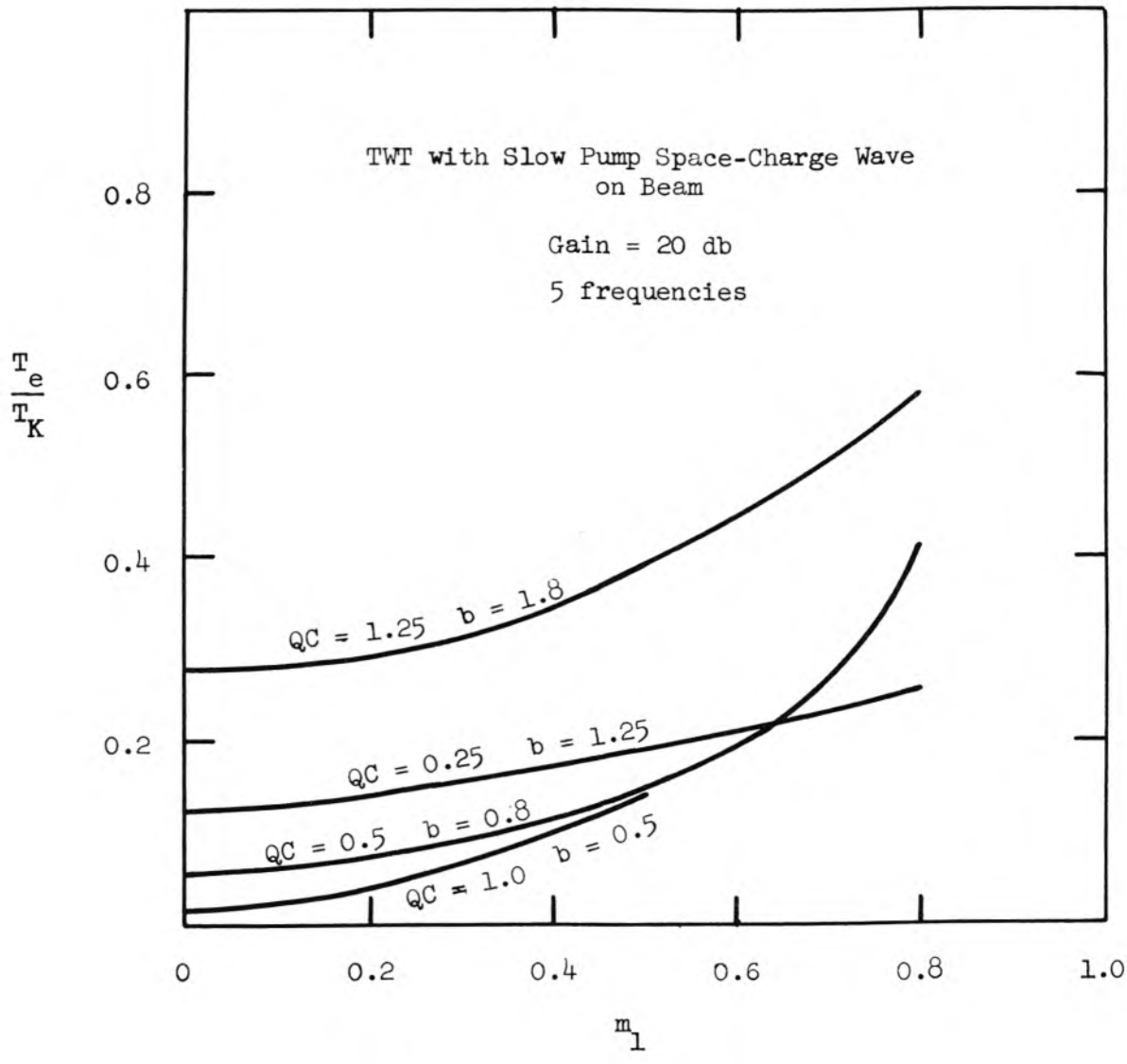

Fig. 6.5 The noise temperature of a traveling-wave amplifier with a slow pump space-charge wave excited on the beam. The noise is assumed to be removed from the slow signal and idler wave.

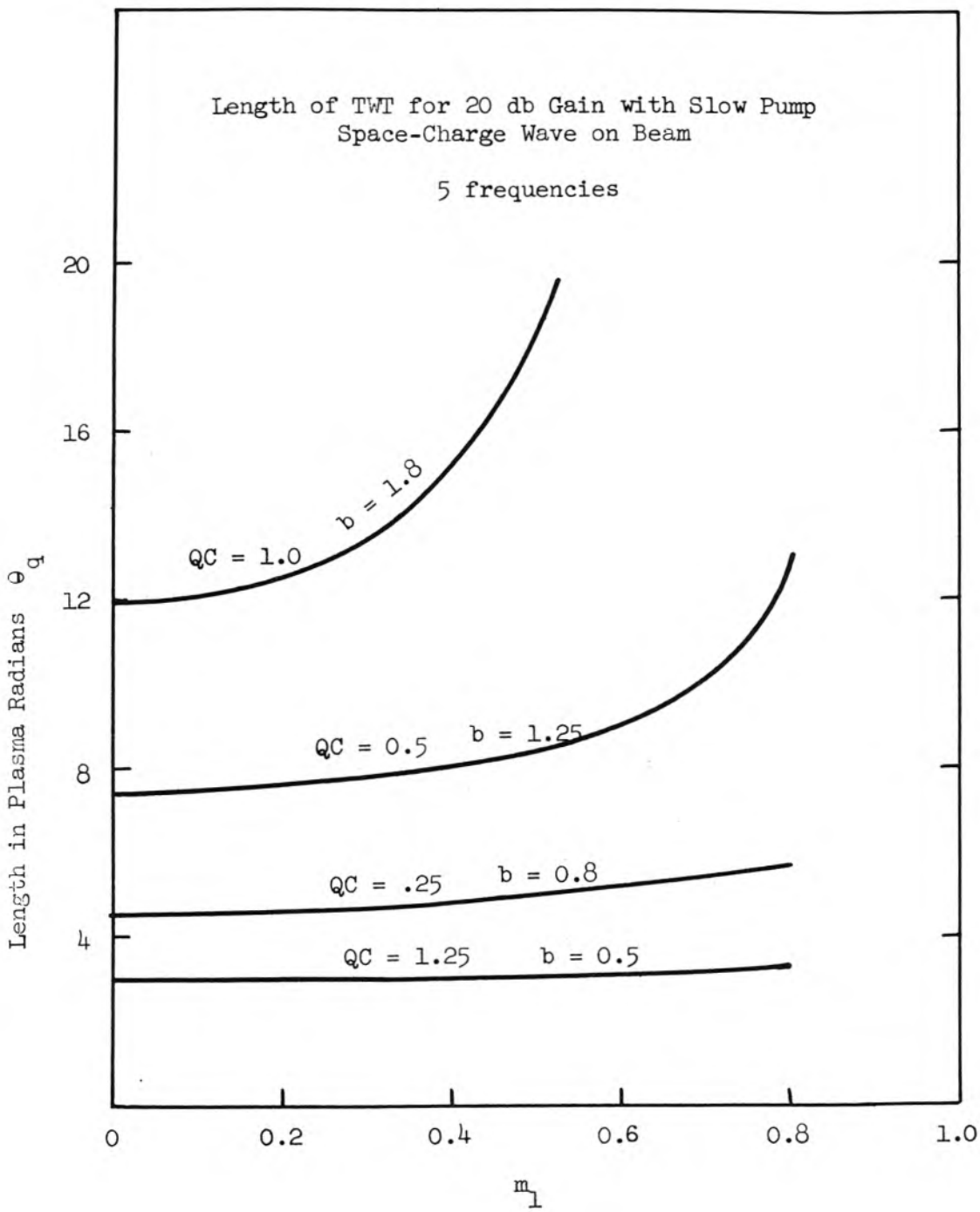

Fig. 6.6 The effect of a slow pump space-charge wave on the gain of a traveling-wave amplifier. Note the large effect at large QC where the parametric coupling tends to be of the same order of magnitude as the mutual-field coupling.

large QC.

Examination of the curves again reveals the necessity for compromise. Operation at large QC and small m_1 yields the lowest noise temperature, but again requires considerably more length for both traveling-wave tube and noise exchanger. As might be anticipated from the results of the parametric amplifier study, a cursory examination of a few cases for which the circuit phase velocity is faster than that for optimum traveling-wave tube performance shows that some improvement over the results in Figures 6.5 and 6.6 can be obtained. A more detailed study which includes ranges of the b parameter is needed to optimize the results. In all cases the contribution to the noise temperature due to the presence of higher order fast space-charge waves was negligible.

6.5 Other Applications of the Theory

The next obvious application of the theory is to traveling-wave mixers. In this case the pump would be the local oscillator signal and the mixer output signal would be at the idler frequency. Conversion gain and noise performance can be obtained from straightforward solution of the equations. The most thorough mixer analysis to date (35) does not take into account the effects of higher order mixing products or the reciprocal effects of the mixing products on the signal wave.

Another related application might be to the theory of up-conversion by use of electron beams. In this case the signal frequency would be much less than the local oscillator frequency, and the output signal would be at the $s = +1$ idler frequency.

These and all related problems involving the generation of mixing products through the presence of two or more signals of different frequencies on the nonlinear beam should lend themselves readily to solution by these equations and techniques.

CHAPTER VII

COMPARISON OF EXPERIMENTAL RESULTS WITH PREDICTIONS OF THE THEORY

7.1 Introduction

Several experimental space-charge-pumped amplifiers were built in the initial stages of the study in an attempt to verify some of the theoretical predictions of Louisell and Quate and, in addition, to attempt to obtain an experimental confirmation of the expected low-noise feature of these amplifiers. Typical gain and pump saturation characteristics of these amplifiers are discussed and are felt to be fairly well understood in light of the theories presented in the previous chapters. The employment of a helix as the pump coupler leads to some interesting speculations about the gain and noise performance. Discussion of the difficulties encountered in using a helix for the pump coupler leads to some observations on requirements for this important element.

7.2 Design of the Experiments

Two successful amplifiers were built in the course of the investigation. Since the principles of operation of both amplifiers were the same and the performance was very similar, only typical results obtained from what was felt to be the best of the two will be presented. A schematic representation of the tube is presented in Fig. 7.1 and a photograph in Fig. 7.2. The input coupler performs a dual function by injecting the signal onto the fast space-charge wave and simultaneously removing the noise from it. The second coupler is designed to transfer the pump energy to the fast pump space-charge wave. The exponential

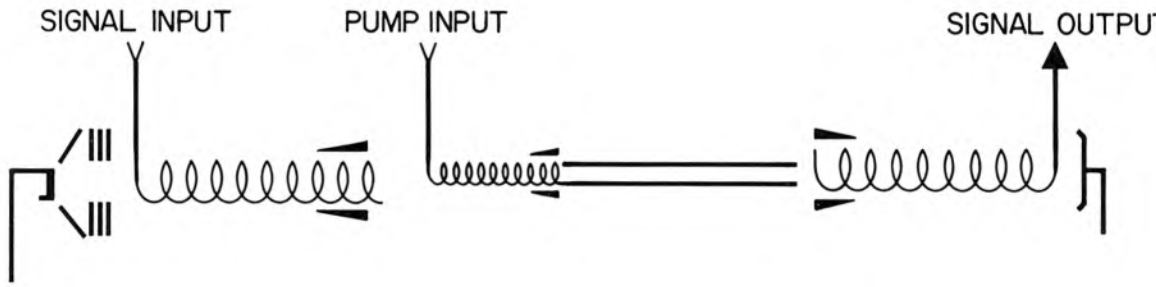

Fig. 7.1 Schematic representation of a parametric amplifier of the drifting-beam space-charge-pumped type. All helix sections are fast-wave couplers designed to operate at large QC and Kompfner dip.

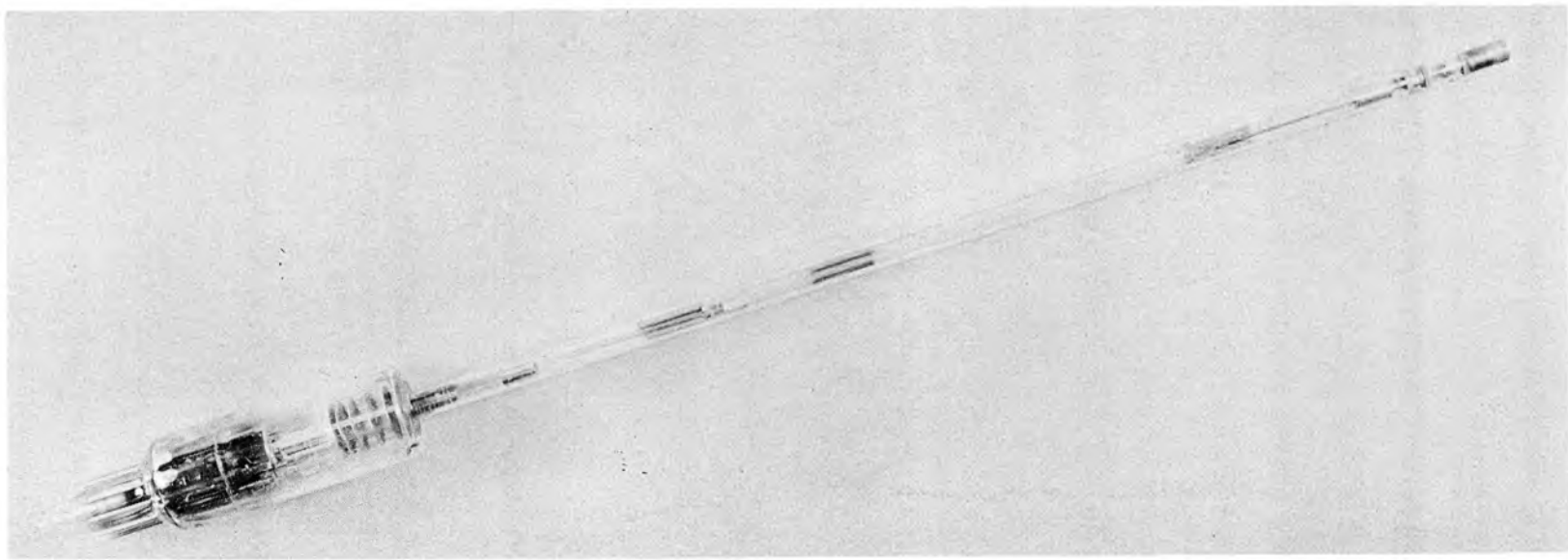

Fig. 7.2 The experimental drifting-beam type of parametric amplifier. The drift tube is about one and one-half plasma wavelengths long and is operated at the pump coupler potential.

waves are allowed to grow in the drift region and the amplified signal is removed in the output coupler.

Design of the Couplers. The S-band signal helix couplers were designed to be essentially fast space-charge-wave couplers at 3 kMc by operating at large QC and at Kompfner dip (29,30). The pump helix coupler was designed in the same manner at 6 kMc. Under these conditions, as shown by Gould (21) and Ashkin et al (22), the coupling to the slow space-charge wave is small, and the power on the circuit can be transferred almost entirely onto the fast space-charge wave.

A matrix relating the output mode amplitudes of the circuit wave, the slow space-charge wave, and the fast space-charge wave to the corresponding input amplitudes can be defined as follows (17)

$$a_{i_{out}} = L_{ij} a_{j_{in}} \tag{7.1}$$

where the subscripts, i,j = 1,2, or 3, are used to denote the modes in the order mentioned above. Gould (21) has shown that under conditions of large QC and Kompfner dip, the magnitudes of the matrix elements are very nearly given by

$$L = \begin{vmatrix} 0 & 0 & 1 \\ 0 & 1 & 0 \\ 1 & 0 & 0 \end{vmatrix} \tag{7.2}$$

Thus the couplers transfer the circuit input power to the fast space-charge wave, and the fast space-charge wave excitation (noise in the input coupler and signal modulation in the output coupler) to the circuit output load. The magnitude of matrix elements can be made exactly

as shown in 7.2 by using more complex arrangements. However, it was felt that such complexity would not be necessary in the preliminary experiments to demonstrate first-order effects.

The S-band signal coupler was placed before the C-band pump coupler so that no parametric amplification would take place before the noise had been removed from the fast signal-space-charge wave. The pump helix was designed to be dispersive in order that the circuit-wave velocity at the signal frequency might be much faster than the velocities of the interacting space-charge waves and the pump circuit wave. As will be explained, this design objective was defeated by the effects of dielectric loading; this difficulty was the prime cause of confusion in interpreting some of the measured results. The drift-tube length was about one and one-half plasma wavelengths. The pertinent parameters are listed below.

	QC	C	γb	b/a	L
S-band Couplers	1.24	0.021	0.94	0.33	2.8"
C-band Couplers	1.8	0.017	1.88	0.43	1.63"
Drift Region	-	-	-	0.46	4.5"

7.3 Gain Performance

The gain characteristics of the amplifier are shown in Fig. 7.3. The maximum electronic gain (defined as the difference in output level with the pump on and off, respectively) was about 34 db. The insertion gain of the amplifier was much less, however. The curves were taken at a fixed setting of the voltage on the pump helix.

Examination of Fig. 7.4 reveals the reason for the high insertion

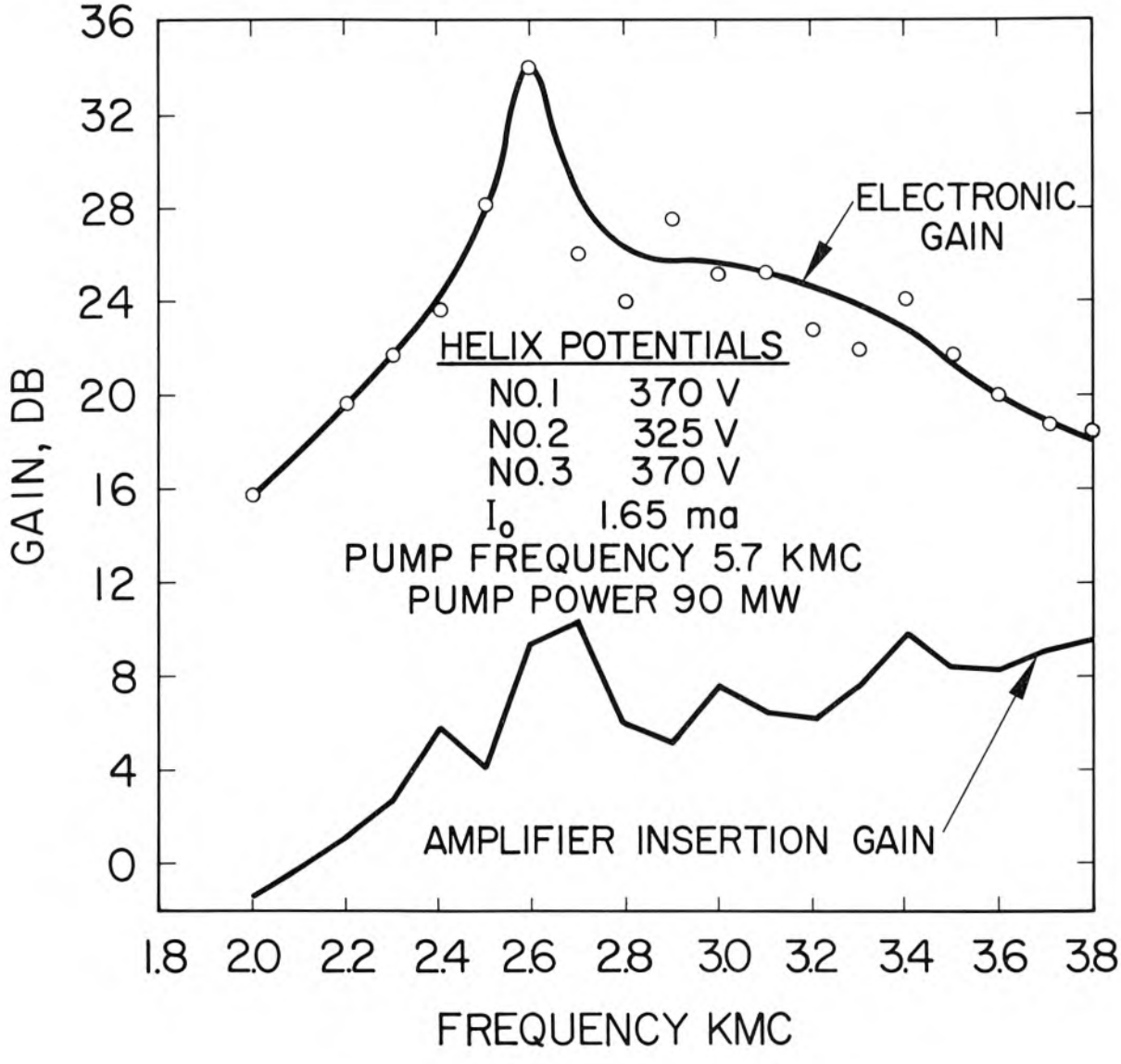

Fig. 7.3 Gain characteristics of the experimental amplifier. The electronic gain is the difference in output levels with the pump on and off, respectively. The estimated power necessary to saturate the beam was 50 mω.

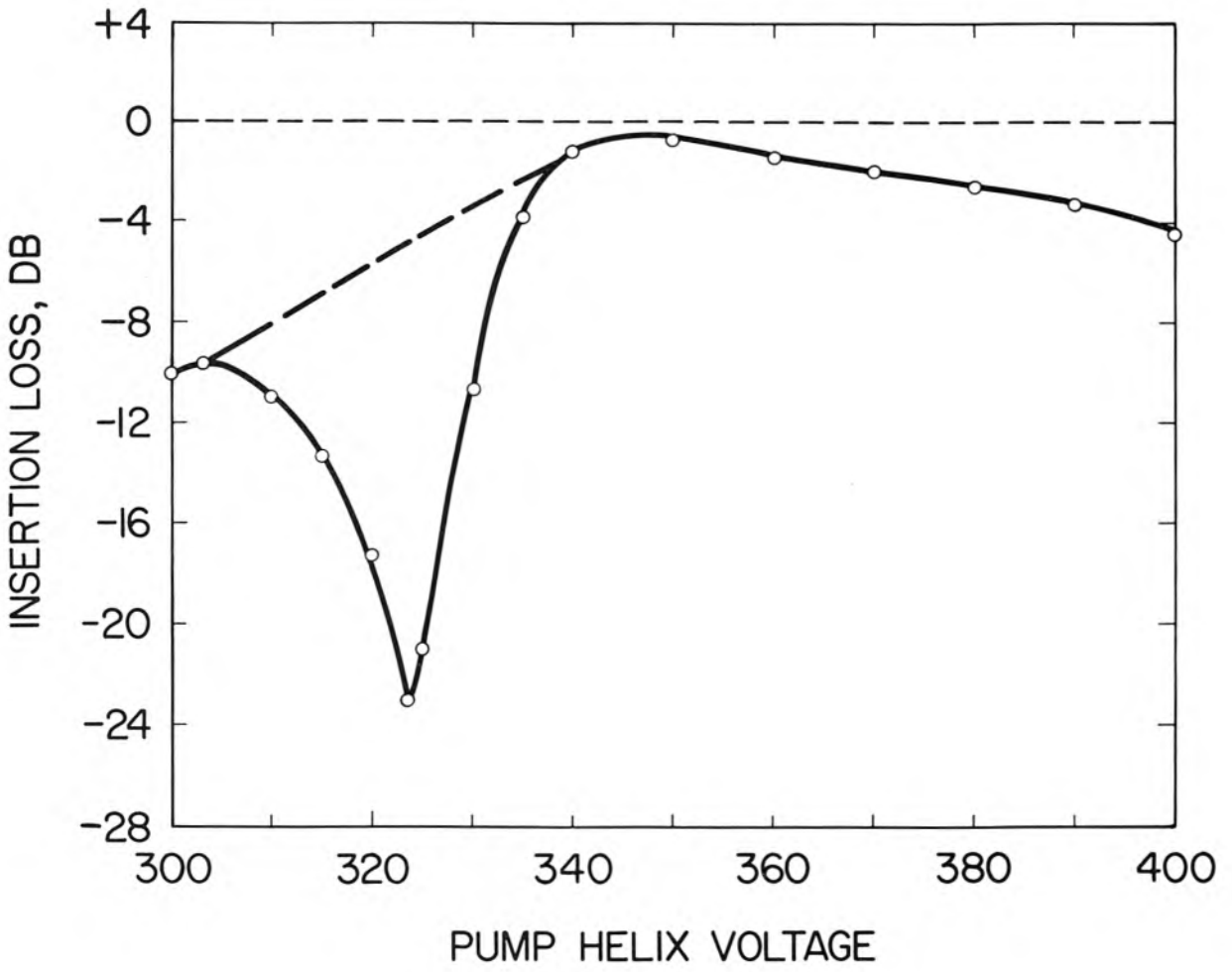

Fig. 7.4 The insertion loss of the experimental amplifier with the pump off. The sharp dip is due to coupling of the fast signal space-charge wave to the circuit wave in the pump helix coupler. The dashed line is an estimate of the performance which might be obtained with an ideal pump coupler.

loss with the pump off. Because of dielectric loading, the dispersion characteristics of the pump helix were so altered that strong coupling to the fast signal-space-charge wave took place. Small C measurements showed a difference of only a few volts in synchronous phase velocities for the signal and pump frequencies. Also, calculations show that at the signal frequency the length of this helix is almost that necessary for Kompfner dip. Unfortunately, the dip shown in Fig. 7.4 occurs at almost the same voltage as was necessary for optimum gain. Further study reveals that because of dielectric loading effects it is impossible to make a large QC helix at C-band which will not be somewhere near synchronism at S-band; hence, special circuits are thought to be necessary for the pump coupler. This problem will be discussed later in more detail.

The curves presented here were taken at an optimum gain setting. Since the design current was 1 ma. and the current setting for optimum gain was 1.65 ma., the reduced plasma wavelength at the signal frequency is shortened somewhat. Under these conditions the length of the pump coupler is about three-quarters of a plasma wavelength, and that of the drift region very nearly two plasma wavelengths.

Several striking arguments can be made which seem to indicate that some circuit-wave pumping occurred in the pump coupler. First, the electronic gain achieved in this amplifier is considerably higher than that achieved in amplifiers (3) with pump couplers of the type described in Appendix I. Second, the optimum gain occurred at a pump helix potential of 325 volts. Experimental measurements indicated that the helix was synchronous with the fast pump-space-charge wave at 335 volts. Considering Fig. 7.5, one sees that as u_o is lowered, the beam waves and

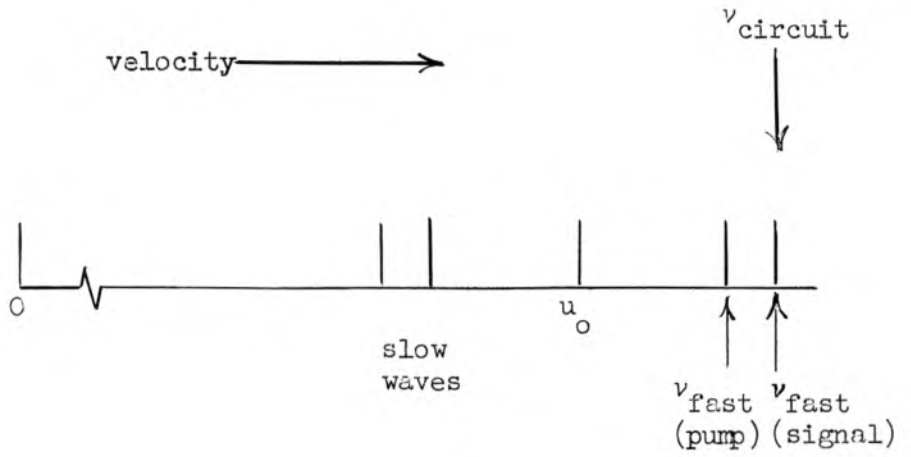

Fig. 7.5 The behavior of the space-charge wave velocities relative to a fixed circuit-wave velocity as the beam voltage is varied.

u_o move left on the diagram past the fixed circuit-wave velocity. At 325 volts the circuit wave velocity expressed in terms of voltage is 10 volts faster than the pump-space-charge wave. The fast signal-wave phase velocity is not known, but from theoretical considerations it should lie on the order of 10 volts higher than the fast pump wave, as estimated in the diagram. A third argument is proposed on the basis of Fig. 7.6 which shows how gain varies with pump power. Note the qualitative agreement between this curve and the growth constant plotted in Fig. 5.10, in particular the threshold and the steep leading edge. The failure of the experimental curve to drop back down as does the theoretical curve may be explained by the fact that the analysis is good only for small m_1. There are definitely no minor humps as predicted by Fig. 5.4 for the space-charge-wave pumped amplifier.

Unfortunately, more conclusive measurements are unavailable since

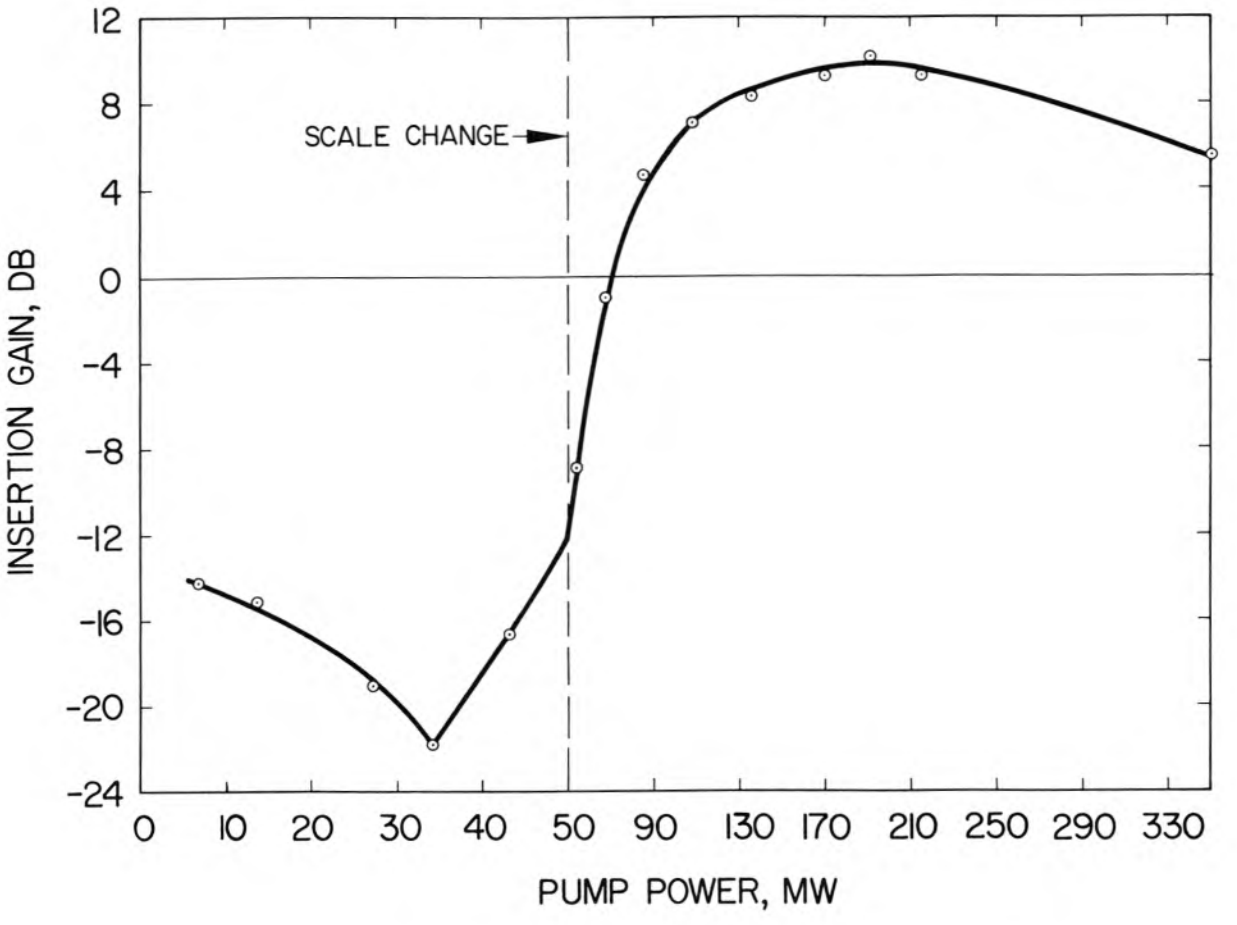

Fig. 7.6 Gain characteristics of the experimental amplifier. Note the threshold value of pump power that was needed before gain could be obtained. The scale has been expanded below 50 mω on the abscissa to emphasize the region where the threshold occurs.

the tube was accidentally broken, and at that time it was felt that it should not be rebuilt because of the difficulties encountered with the pump helix. It is felt, however, that a sufficient amount of reliable data was taken to substantiate these arguments.

7.4 Noise Performance

The measured noise figure was about 23 db. However, this high value can be partially explained by noting that the signal-to-noise ratio is greatly reduced in the pump coupler when it removes signal modulation from the beam. In addition, a minimum intercepted current to the helices of 65 μa certainly contributed appreciable amounts of noise. An estimate of the deleterious effect of signal removal in the pump coupler can be obtained if one now neglects the possibility of circuit pumping in this region, and keeps in mind the reciprocal properties of the matrix elements describing the helix.

Let the signal input power be S_{in} and assume that the signal input coupler is ideal so that $L_{13} = L_{31} = 1$ in equation 7.1. Let the corresponding elements for the pump coupler be α. Then the signal power at the beginning of the drift region becomes

$$S_{out} = (1-\alpha)S_{in} \tag{7.3}$$

and the noise power is given by

$$N_{out} = 2(1-\alpha)kTB + 2\alpha kTB = 2kTB \tag{7.4}$$

The noise contribution from thermal noise at the idler frequency is included in this expression. From Fig. 7.4 (using the dashed curve as an estimate of optimum performance), one can estimate that the signal reduction is about 15 db in the pump region. This corresponds to an α of

0.968 . Using the standard definition of noise figure

$$F = \frac{N_{out}/S_{out}}{N_{in}/S_{in}} \tag{7.5}$$

and substituting, it is found that the noise figure for the section of the tube comprising the input signal and pump couplers becomes

$$F = \frac{2}{1-\alpha} = 63.3 \text{ , or } 18 \text{ db.} \tag{7.6}$$

If this section and the drifting-beam section are regarded as two amplifiers in cascade and if the formula for the noise figure of cascaded amplifiers

$$F_{12} = F_1 + \frac{F_2 - 1}{G_1} \tag{7.7}$$

(where F_{12} is the over-all noise figure and F_1 and F_2 are the noise figures of the first and second stages, respectively) is applied, it is found that an F_2 of 5 db is necessary to account for the over-all 23 db noise figure. It must be emphasized that no definite conclusions can be drawn from these calculations since they are based on only crude estimates and are carried out only to illustrate the influence of the pump coupler on the noise performance.

7.5 Conclusions and Discussion of Ideas for Future Modifications

In view of the fact that the prime objective in the design of a parametric amplifier is the achievement of a low noise figure, much more experimental work is necessary to demonstrate whether or not the longitudinal beam type of amplifier is able to compete with existing low noise amplifiers. It is felt that, although the results obtained in these experiments do not shed much light on the noise problem, they do

seem to substantiate to first order some of the theory that has been proposed. They have also pointed up some important pitfalls to be avoided in future work.

In the experiments where the signal frequency was not exactly half of the pump frequency, commonly referred to as nondegenerate operation, the idler frequency component present at the output was usually about one db below the signal frequency level. All the measurements were made with a narrow-band receiver for a detector so that the quantities plotted in the figures represent only the signal frequency components.

In future experimental amplifiers several modifications are indicated. The theoretical conclusions reached in Chapter V show that the drift region should be eliminated and that circuit pumping should be used exclusively. The pump circuit should be very dispersive and have a large γa . The dispersion characteristics of one promising possibility are shown in Fig. 7.7. These characteristics are for a helix surrounded by a dielectric with conducting rings outside the dielectric and were calculated by Birdsall (36). The experimental measurements were made on some scale models of a circuit proposed for an amplifier. The sheet model was used for some impedance calculations at large γa .

Another modification might be the inclusion of a large QC lossy helix between the gun and signal coupler. An examination of the properties of such helices, which are discussed by Brewer and Birdsall (37), reveals that continuous extraction of noise from the fast-space-charge wave may be possible without appreciably affecting the slow wave. Such a circuit could relieve some of the stringent requirements on the input coupler and allow more broadband operation at low noise figure.

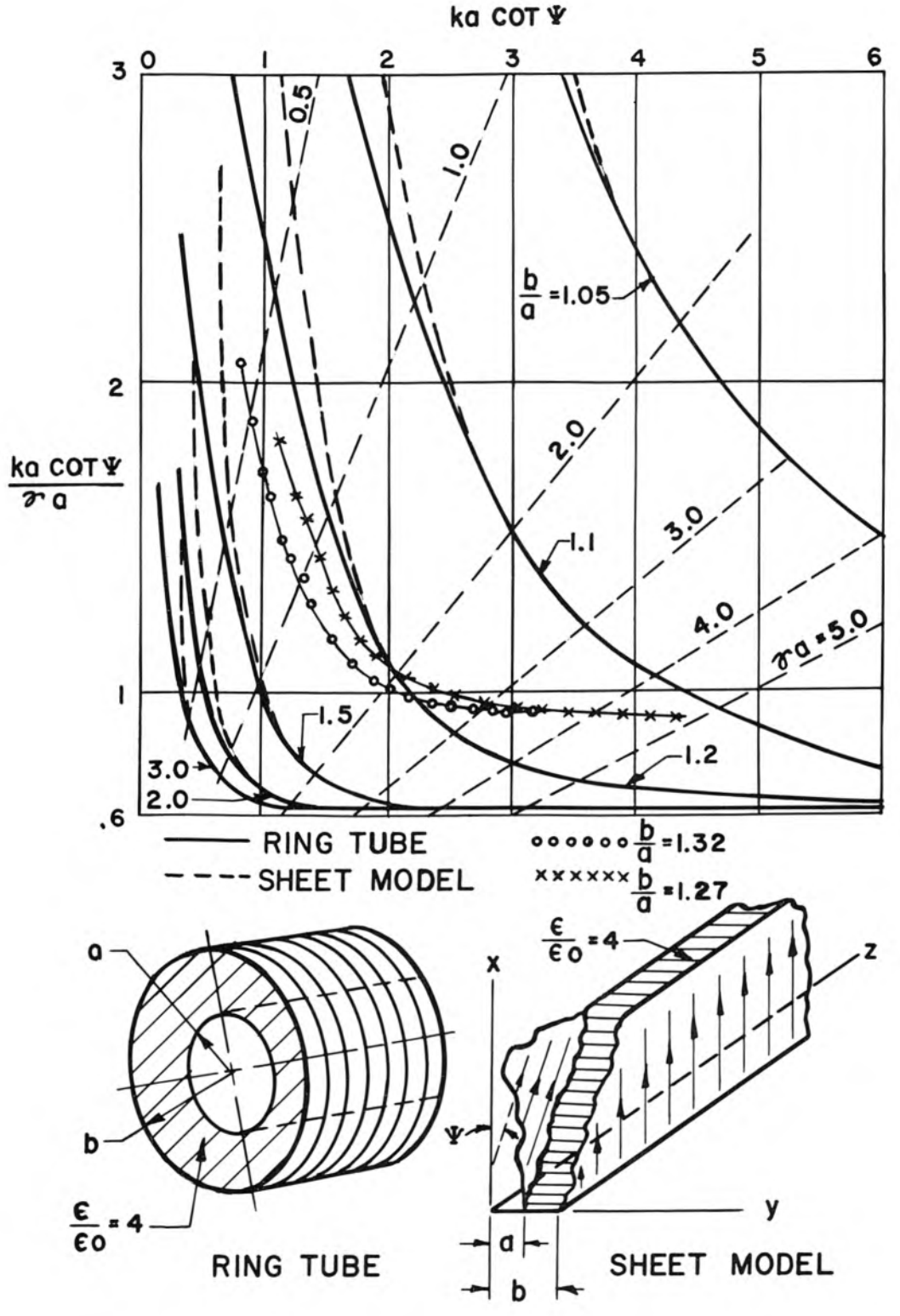

Fig. 7.7 The dispersion characteristics of a ring loaded helix section. The sheet model is valid for the region $\gamma a > 1.5$. The experimental curves were obtained on large scale models of proposed circuits.

CHAPTER VIII

SUMMARY, CONCLUSIONS, AND SUGGESTIONS FOR FUTURE INVESTIGATIONS

8.1 Summary

Three separate analyses have been presented which predict the behavior of an electron beam under the stimulus of a weak signal source and a strong pumping source. All are linearized, one-dimensional analyses in which the pump quantities are much smaller than d.c. quantities, but much larger than the signal quantities.

The analysis presented in Chapter II extends the work of Wade and Adler (24) in that it allows for arbitrary velocity and frequency of the pump wave relative to the signal wave. It is approximate in that it includes only one constant-amplitude pump wave and neglects the effects of the higher order mixing products.

In Chapter III the general equations are put into coupled-mode form in order to allow simplified solutions which account for the effects of the higher order mixing products. Provision is made for coupling to a circuit at each frequency. Again, the single-pump-wave approximation is used. A kinetic power theorem is derived which turns out to be a generalization of the Manley-Rowe relation. Consideration of the form of the equations from the generalized coupled-mode point of view leads to some interesting observations on the behavior of positive and negative a.c. energy carriers when parametrically coupled.

In Chapter IV a more general set of coupled-mode equations are derived which do not rely on the single-pump-wave approximation, and are valid for the general case of arbitrary circuit pumping. The

coefficients in the differential equations are functions of the pump mode amplitudes of the uncoupled system, and thus become variable coefficients. No solutions were sought for this set of equations.

The equations of Chapter III were applied to the space-charge-wave parametric amplifier in Chapter V. The reasons for the failure of the space-charge-pumped experimental amplifiers were established. Successful operation of the circuit-pumped amplifier is predicted if the phase velocity of the pump wave is adjusted to be slightly higher than that of the fast signal wave.

In Chapter VI further application of the theory shows that it should be possible to cool the slow space-charge wave of an electron beam by parametric pumping. This concept leads to new approaches in the achievement of low noise in conventional amplifiers. Encouraging results are obtained from a study of the practical application of such a beam in a traveling-wave tube.

The experimental results presented in Chapter VII tend to substantiate the circuit-pumping concept but shed little light on the noise performance because of shortcomings in the experimental tubes.

8.2 Conclusions

Two possibilities for microwave amplifiers with improved noise performance have been discussed. Both the space-charge-wave parametric amplifier and the application of the cooled slow space-charge wave to conventional amplifiers have been shown to be theoretically capable of noise temperatures under $100^{\circ}K$. The failure of the experimental parametric amplifiers cannot be attributed to unavoidable coupling to higher idlers since it has been shown that the attendant degradation

in performance is not as serious as had been anticipated. It is felt that successful amplifiers can be built if the concepts which have been developed here are kept in mind and some attention is directed toward optimum transformation of the space-charge waves between the cathode and the interaction region.

Of more fundamental interest is the demonstration that it is possible to obtain active coupling of two positive a.c. energy carriers and passive coupling of one positive and one negative a.c. energy carrier. In each case this is achieved through the application of the parametric pumping principle.

8.3 Suggestions for Future Investigations

In order to use the coupled-mode theory effectively for noise problems, more knowledge of the noise carried into the interaction region by the space-charge waves is needed. Excitation of the modes in the cathode region and their subsequent transformation must be studied in order to obtain optimum performance. Very little justification exists for the assumption that the thermal excitation is determined by the cathode temperature.

Further application of the single-wave theory in the study of beam cooling, traveling-wave tubes, mixers, and upconverters is necessary for more complete understanding of these devices. The preliminary studies presented in Chapter VI are for five frequencies only, and more should be included. A more thorough study should also include closer inspection of the various combinations of the parameters. All of the solutions of the coupled-mode equations are restricted to the near-degenerate case; they should be extended to obtain operational bandwidth

information.

The consequences of the single-pump-wave approximation should be determined for all of these devices by application of the general equations of Chapter IV. It is possible that the results may be altered considerably. If this should be the case, methods and conditions for exciting single pump waves should be sought.

The need for further experimental work is obvious. Fundamental experiments on some of the "building blocks" of the various devices, as well as application of the various principles in the devices themselves, are needed.

APPENDIX I

The velocity and current modulation on an electron beam can be described by

$$V(z) = V_f e^{j\beta_f z} + V_s e^{-j\beta_s z} \tag{A1.1}$$

$$I(z) = \frac{I}{W_o} \left(V_f e^{-j\beta_f z} - V_s e^{-j\beta_s z} \right) \tag{A1.2}$$

where V is the kinetic voltage $\left(-\frac{\eta}{u_o} v\right)$, I is the total a-c beam current, and W_o the equivalent beam impedance. The subscript f is used for fast-wave quantities and s for slow-wave quantities. The propagation constants are

$$\beta_f = \frac{\omega - \omega_q}{u_o} , \qquad \beta_s = \frac{\omega + \omega_q}{u_o} \tag{A1.3}$$

where ω_q is the reduced plasma frequency.

For only the fast wave to be excited, the following condition must be fulfilled.

$$\frac{V(z)}{I(z)} = W_o \tag{A1.4}$$

This can be seen from equations A1.1 and A1.2. The model to be considered is shown in Figure A1.1. The gaps are considered to be ideal, i.e., the transit time through the gap is assumed to be negligible.

By applying the boundary conditions at $z = 0$ that $I(0) = 0$, $V(0) = V_1$, Equations A1.1 and A1.2 for the region between the gaps becomes

$$V(z) = V_1 \cos \beta_q z \; e^{-j\beta_e z} \tag{A1.5}$$

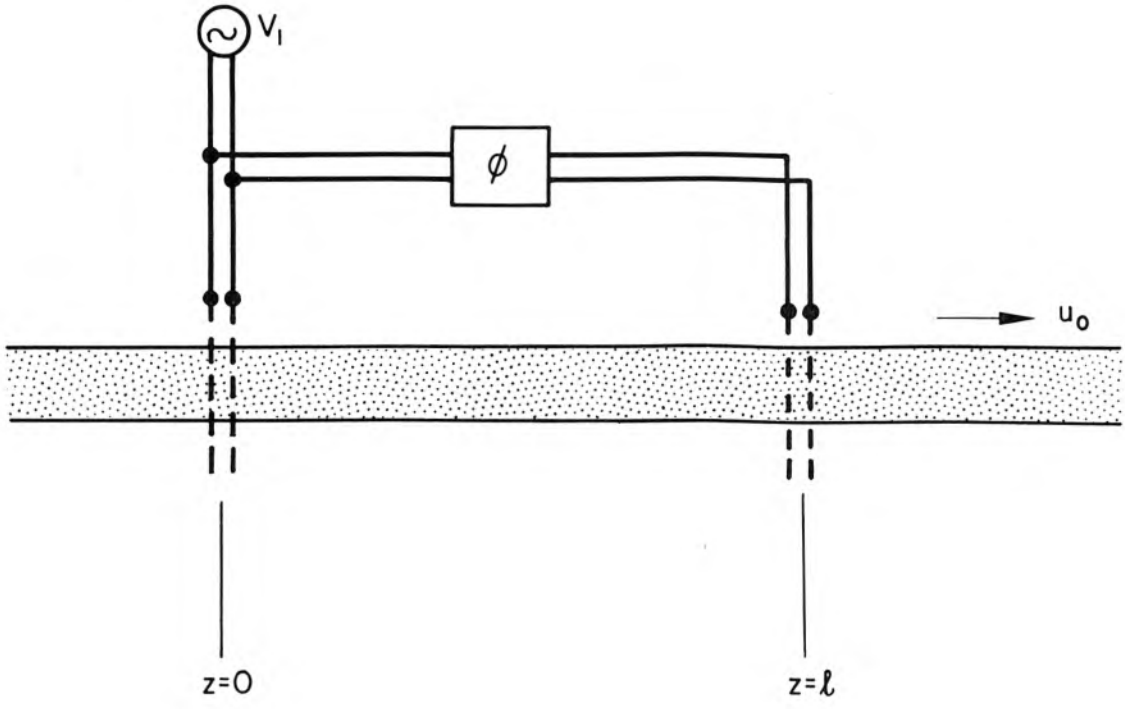

Fig. A1.1 The model for two cavity gaps with arbitrary driving phase which is used in determining the conditions for optimum excitation of the fast space-charge wave.

$$I(z) = j \frac{V_1}{W_o} \sin \beta_q z \, e^{-j\beta_e z} \tag{A1.6}$$

where

$$\beta_q \equiv \frac{\omega_q}{u_o} \quad , \qquad \beta_e \equiv \frac{\omega}{u_o} \tag{A1.7}$$

At $z = \ell$, these become

$$V(\ell) = V_1 \cos \beta_q \ell \, e^{-j\beta_e \ell} + V_1 e^{j\phi} \tag{A1.8}$$

$$I(\ell) = j \frac{V_1}{W_o} \sin \beta_q \ell \, e^{-j\beta_e \ell} \tag{A1.9}$$

When condition A1.4 is applied to these equations, the condition for fast space-charge wave excitation becomes

$$\theta_e + \theta_q = \phi + (2n+1)\pi \tag{A1.10}$$

where

$$\theta_q \equiv \beta_q \ell \, , \qquad \theta_e \equiv \beta_e \ell \tag{A1.11}$$

For slow-wave excitation, the condition is

$$\frac{V(z)}{I(z)} = - W_o \tag{A1.12}$$

and the resulting requirement on the phase angles becomes

$$\theta_e - \theta_q = \phi + (2n+1)\pi \tag{A1.13}$$

Expressions A1.10 and A1.13 are the conditions to be fulfilled for cancellation of the undesired wave in the output gap. Another condition should be put on the couplers to ensure optimum coupling to the desired wave. Substituting relation A1.10 into A1.8 and solving for the condition for

maximum $V(\ell)$ one gets

$$\theta_e - \theta_q = \phi + 2n\pi \tag{A1.14}$$

Similarly by using equation A1.13 in A1.8 the condition for maximum excitation of the slow space-charge wave becomes

$$\theta_e + \theta_q = \phi + 2n\pi \tag{A1.15}$$

The two important conditions for the fast-wave coupler are therefore given by A1.10 and A1.14. As implied by the analysis, the shunt conductance of the cavities must also be equal to the beam admittance or, equivalently,

$$G_{shunt} + G_{load} = \frac{1}{W_o} \tag{A1.16}$$

The common double gap or "drift-tube" cavity which can also be used in this manner is represented by the special case where $\phi = 0$.

REFERENCES

1. W. H. Louisell and C. F. Quate, "Parametric Amplification of Space-Charge Waves", Proc. IRE 46, 707-716 (April 1958).
2. W. H. Louisell, "A Three-Frequency Electron Beam Parametric Amplifier and Frequency Converter", Jour. Electronics and Control, VI, 1-25, (Jan. 1959).
3. A. Ashkin, private communication.
4. D. C. Forster and M. R. Currie, Research Report 111, Hughes Aircraft Company (June 1959).
5. M. E. Hines, "Amplification in Nonlinear Reactance Modulators", presented at 15th Annual Conf. on Electron Tube Research, Berkeley, Calif., June 1957.
6. M. R. Currie and D. C. Forster, "New Mechanism of Noise Reduction in Electron Beams", J. Appl. Phys., 30, 94-103 (Jan. 1959).
7. J. M. Manley and H. F. Rowe, "Some General Properties of Nonlinear Elements--Part I", Proc. IRE, 44, 904-913 (July 1956).
8. E. D. Reed, "The Variable Capacitance Parametric Amplifier", IRE Trans. Vol. ED-6, 216-224 (April 1959).
9. H. Suhl, "A Proposal for a Ferromagnetic Amplifier in the Microwave Range", Phys. Rev. 106, 384-385 (April 1957).
10. M. T. Weiss, "Microwave Ferromagnetic Amplifier and Oscillator", Phys. Rev. Vol.107, p.317 (July 1957).
11. T. J. Bridges, "An Electron Beam Parametric Amplifier", Proc. IRE, 46, 494 (Feb. 1958).
12. P. K. Tien and H. Suhl, "A Traveling-Wave Ferromagnetic Amplifier", Proc. IRE, 46, 700-706 (April 1958).
13. M. R. Currie and R. W. Gould, to be published.
14. L. J. Chu, "A Kinetic Power Theorem", 1951 IRE Conf. on Electron Devices, Durham, N.C., June 1951.
15. W. C. Hahn, "Small Signal Theory of Velocity-Modulated Electron Beams", Gen. Elec. Review, 42, 258-270 (June 1939).
16. S. Ramo, "The Electronic Wave Theory of Velocity Modulation Tubes", Proc. IRE, 27, 757-763 (Dec. 1939).
17. H. A. Haus and F.N.H. Robinson, "The Minimum Noise Figure of Microwave Beam Amplifiers", Proc. IRE, 43, 981-991 (August 1955).
18. Siegman, Watkins and Hsieh, "Density-Function Calculations of Noise Propagation on an Accelerated Multivelocity Electron Stream", JAP 28, 1138-1148 (October 1957).

19. R. Adler, "Parametric Amplification of the Fast Electron Wave", Proc. IRE 46, 1300-1301 (June 1958).

20. R. Adler, G. Hrbek, G. Wade, "Some Possible Causes of Noise in Adler Tubes", Proc. IRE 48, 256 (Feb. 1960).

21. R. W. Gould, "Traveling-Wave Couplers for Longitudinal Beam-Type Amplifiers", Proc. IRE, 47, 419-426 (March 1959).

22. A. Ashkin, W. H. Louisell, and C. F. Quate, "Fast Wave Couplers for Longitudinal Beam Parametric Amplifiers", Jour. Electronics and Control, VII, 1-33 (July 1959).

23. R. Adler, G. Hrbek, and G. Wade, "The Quadrupole Amplifier, a Low-Noise Parametric Device", Proc. IRE, 47, 1713-1724 (Oct. 1959)

24. G. Wade and R. Adler, "A New Method for Pumping a Fast Space-Charge Wave", Proc. IRE 47, 79-80 (Jan. 1959).

25. C. C. Johnson, "Theory of Fast-Wave Parametric Amplification", Tech. Memo. No. 540, Hughes Aircraft Company (Feb. 1959).

26. F. Paschke, "On the Nonlinear Behavior of Electron-Beam Devices", RCA Review XVIII, 221-242 (June 1957).

27. G. M. Branch and T. G. Mihran, "Plasma Frequency Reduction Factors in Electron Beams", IRE Trans, Vol. ED-2, 3-12, April 1955.

28. J. R. Pierce, Traveling Wave Tubes, D. Van Nostrand Co., Inc., New York, 1950.

29. R. Kompfner, "On the Operation of the Traveling-Wave Tube at Low Level", Brit. J. IRE 10, 283-289 (Aug.-Sept. 1955).

30. H. R. Johnson, "Kompfner Dip Conditions", Proc. IRE 43, 874 (July 1955).

31. R. W. Gould, "A Coupled Mode Description of the Backward-Wave Oscillator and the Kompfner Dip Condition", IRE Trans. Vol. ED-2, 37-42, Oct. 1955.

32. G. M. Roe and M. R. Boyd, "Parametric Energy Conversion in Distributed Systems", Proc. IRE 47, 1213-1219 (July 1959).

33. S. Bloom and R. W. Peter, "A Minimum Noise Figure for the Traveling-Wave Tube", RCA Review, Vol.15, 252-267 (June 1954).

34. P. A. Sturrock, "Parametric Refrigeration--A Mechanism for Removal of Noise from the Slow Wave of an Electron Stream", Microwave Laboratory Report No. 656, Microwave Laboratory, Stanford University; October, 1959.

35. R. W. DeGrasse, PhD Thesis, Stanford University, 1958.

36. C. K. Birdsall, Memo for File ETL-12, July 1, 1953, Hughes Aircraft Company

37. G. R. Brewer and C. K. Birdsall, "Traveling-Wave Tube Propagation Constants", IRE Trans. Vol. ED-4, 140-144 (April 1957).

38. J. S. Cook and W. H. Louisell, "Traveling-Wave Tube Equations Including the Effects of Parametric Pumping", Proc. IRE 47, 2016, (November 1959).

39. J. S. Cook, W. H. Louisell and C. F. Quate, private communication.

DISTRIBUTION LIST

Chief of Naval Research 2
Navy Department - CODE 427
Washington 25, D. C.

Director, Naval Research Lab.
Washington 25, D. C.
Attn: CODE 5240 1
CODE 7130 1
CODE 2000 6
CODE 5430 1

Commanding Officer 1
ONR Branch Office
1000 Geary Street
San Francisco, California

Scientific Liaison Officer 25
ONR, London
c/o Navy 100, Box 39, FPO
New York, New York

Commanding Officer 1
ONR Branch Office
1030 E. Green Street
Pasadena, California

Commanding Officer 1
ONR Branch Office
The John Crerar Library Bldg.
86 E. Randolph Street
Chicago 1, Illinois

Commanding Officer 1
ONR Branch Office
346 Broadway
New York 13, New York

Officer-in-Charge 3
Office of Naval Research
Navy 100, FPO
New York, New York

Chief, Bureau Aeronautics EL4 1
Navy Department EL43 1
Washington 25, D. C. EL45 1

Chief, Bureau of Ordnance
Navy Department Re 4 1
Washington 25, D. C. Re 9 1

Chief of Naval Operations Op20X 1
Navy Department Op421 1
Washington 25, D. C. Op 55 1

Director, Naval Ordnance Lab. 1
White Oak, Maryland

Director, Naval Electronics Lab 1
San Diego 52, California

Dept. of Electronics-Physics 1
U.S. Naval Post Grad. School
Monterey, California

Commander CODE 366 1
Naval Air Missile Test Center
Point Mugu, California

U.S. Naval Proving Ground 1
Attn: W. H. Benson
Dahlgren, Virginia

Commander 1
U.S.Naval Air Development Center
Johnsville, Pennsylvania

Thermionics Branch 5
Signal Corps Eng. Labs.
Evans Signal Lab, Bldg.42
Belmar, New Jersey

Commander 5
Armed Services Tech. Inform.
ATTN: TIPDR
Arlington Hall Station
Arlington 12, Virginia

Ballistics Research Labs 2
Aberdeen Proving Ground
Maryland
Attn: D.W.H. Delsasso

Chief, Ordnance Develop. Div. 2
Natl.Bureau of Standards
Connecticut Av, Van Ness St.NW
Washington 25, D. C.

Naval Research Laboratory 6
Washington 25, D. C.

Committee on Electronics 1
Research and Development Board
Department of Defense
Washington 25, D. C.

Director, Natl.Bureau of Stds. 1
Washington 25, D. C.
Attn: Div.14.0 CRPL, Librarian

Commanding Officer 1
Engineering Res. and Dev. Lab
Fort Belvoir, Virginia

Commanding Officer 1
Frankford Arsenal
Bridesburg, Philadelphia, Pa.

Air Research and Dev. Command 1
ATTN: RDSBTL(Hq.Tech.Library)
Andrews Air Force Base
Washington 25, D. C.

Commanding General WCLC 1
Wright Air Devel.Center WCLRC 1
Wright-Patterson AF Base, Ohio

Commanding General, CRRE 1
A.F. Cambridge Research Center
230 Albany Street
Cambridge 39, Massachusetts

Commanding General RCRW 1
Rome Air Development Center
Griffiss Air Force Base
Rome, New York

Chief, West Coast Office 1
Signal Corps Eng. Labs
75 So. Grand Avenue
Pasadena 2, California

Signal Corps Resident Engineer 1
Electronic Defense Laboratory
P.O. Box 205
Mountain View, California

Chief, Bureau of Ships 816 1
Department of the Navy 820 1
Washington, D. C. 840 1

Material Lab. Library 912B 1
New York Naval Shipyard
Brooklyn 1, New York

Office of Technical Services 1
Department of Commerce
Washington 25, D. C.

Director CR4582 1
Air University Library
Maxwell A.F. Base, Alabama

Chief, Western Division 1
Air Research and Devel.Command
Office of Scientific Research
P.O.Box 2035, Pasadena, Calif.

Technical Library 1
Research and Development Board
Pentagon Building
Washington 25, D. C.

Advisory Group on Electron Tubes 1
346 Broadway (8th Floor)
New York 13, New York

Dr. G. E. Barlow 1
Australian Joint Service Staff
Box 4837
Washington 8, D. C.

Microwave Library 1
W. W. Hansen Labs. of Physics
Stanford University
Stanford, California

Engineering Library 1
Stanford University
Stanford, California

Electronics Lab. Library 1
Stanford University
Stanford, California

Technical Library 1
General Electric Microwave Lab.
601 California Avenue
Palo Alto, California

General Electric Company 1
Electronic Components Div.
Power Tube Department
Microwave Lab at Stanford
Palo Alto, California

Dr. E. D. McArthur 1
Electron Tube Laboratory
General Electric Company
Schenectady, New York

University of Michigan 1
Electron Tube Laboratory
Ann Arbor, Michigan
Attn: J. Rowe

Johns Hopkins University 1
Radiation Laboratory
1315 St. Paul Street
Baltimore 2, Maryland
Attn: M.Poole, Librarian

Research Lab. of Electronics 1
Massachusetts Inst. of Tech.
Cambridge 39, Massachusetts

Sloane Physics Laboratory 1
Yale University
New Haven, Connecticut
Attn: R. Beringer

Mr. H. J. Reich 1
Department of Electrical Eng.
Yale University
New Haven, Connecticut

Laboratory for Insulation Res. 1
Massachusetts Inst. of Tech.
Cambridge 39, Massachusetts
Attn: A. von Hippel

Lincoln Laboratory 1
Massachusetts Inst. of Tech.
Cambridge 39, Massachusetts

Dr. J. M. Lafferty, Manager 1
Physical Studies
General Electric Company
P.O. Box 1088
Schenectady, New York

General Electric Company 1
One River Road
Schenectady 5, New York
Attn: Miss W. Crain, Librarian

Technical Report Collection 1
303A Pierce Hall
Harvard University
Cambridge 38, Massachusetts

Electron Tube Section 1
Electrical Engineering Dept.
University of Illinois
Champaign, Illinois

Chairman, Div.of Elec. Eng. 1
University of California
Berkeley 4, California

Radiation Laboratory 1
Tech. Information Division
University of California
Berkeley 4, California

Dr. A. W. Trivelpiece 1
Department of Elec. Eng.
University of California
Berkeley 4, California

Periodicals Librarian 1
General Library
California Inst. of Technology
Pasadena, California

Dr. Z. Kaprielian 1
Electrical Engineering Dept.
University of Southern Calif.
Los Angeles 7, California

Supervisor of Research Lab. 1
Electrical Engineering Bldg.
Purdue University
Lafayette, Indiana

Georgia Institute of Techn. 1
Atlanta, Georgia
ATTN: Librarian

W. E. Lear 1
University of Florida
Department of Electrical Eng.
Gainesville, Florida

Director Electronics Defense 1
Engineering Research Inst.
University of Michigan
Ann Arbor, Michigan

Cornell Aeronautical Lab 1
Cornell Research Foundation
Buffalo 21, New York

Director, Microwave Res.Inst. 1
Polytechnic Inst.of Brooklyn
55 Johnson Street
Brooklyn 1, New York

University of Washington
Department of Elec. Eng.
Seattle, Washington
ATTN: E. A. Harrison 1
A. V. Eastman 1

University of Colorado 1
Department of Elec. Eng.
Boulder, Colorado

University of Colorado 1
Engineering Experiment Sta.
Boulder, Colorado
ATTN: W. G. Worcester

Electrical Engineering Dept. 1
Princeton University
Princeton, New Jersey

Professor W. P. Dyke 1
Linfield College
McMinnville, Oregon

Research Lab.of Electronics 1
Chalmers Institute of Tech.
Gothenburg, Sweden
ATTN: Librarian

Columbia Radiation Lab. 1
538 W. 120th Street
New York 27, New York

Mr. John S. McCullough 1
Eitel-McCullough, Inc.
San Bruno, California

Cascade Research 1
5245 San Fernando Road
Los Angeles 39, California

Fred D. Wilimek 1
Varian Associates
611 Hansen Way
Palo Alto, California

John Dyer 1
Airborne Instrument Lab
Mineola, New York

Bell Telephone Laboratories 1
Murray Hill, New Jersey
ATTN: J. R. Pierce

Hughes Aircraft Company 1
Culver City, California
ATTN: Mr. Milek, Librarian

Hughes Aircraft Company 1
Microwave Laboratory
Culver City, California
ATTN: Dr. A. D. Berk

Bell Telephone Laboratories 1
Technical Information Library
463 W. Street
New York 14, New York

RCA Laboratories 1
Princeton, New Jersey
ATTN: Dr. W. M. Webster

Federal Telecommunic. Labs 1
500 Washington Avenue
Nutley, New Jersey
ATTN: W. Derrick
K. Wing 1

Countermeasures Laboratory 1
Gilfillan Brothers, Inc.
1815 Venice Boulevard
Los Angeles, California

The Rand Corporation 1
1700 Main Street
Santa Monica, California
ATTN: Librarian

Motorola Riverside Res. Lab. 1
8330 Indiana Avenue
Riverside, California
ATTN: Mr. John Byrne

Ramo-Wooldridge Corporation 1
Control Systems Division
P.O. Box 900B
Hawthorne, California
ATTN: Librarian

Microwave Physics Laboratory 1
Sylvania Electric Products
P. O. Box 1296
Mountain View, California

Dr. J. E. Shepherd 1
Sperry Gyroscope Company
Great Neck, New York

W. L. Maxson Corporation 1
460 West 34th Street
New York 1, New York
ATTN: M. Simpson

Bertram G. Ryland, Manager 1
Spencer Laboratory
Raytheon Manufacturing Co.
Burlington, Massachusetts

Westinghouse Electric Corp. 1
Electronic Tube Division
Elmira, New York
ATTN: Mr. S.S.King, Librarian

Mr. Gilbert Kelton 1
Security Officer
Philips Laboratories
Irvington-on-Hudson, New York

R. E. McGuire, Librarian 1
Boeing Airplane Company
P.O. Box 3707
Seattle 24, Washington

Dr. Donald W. Kerst 1
General Atomic
P. O. Box 608
San Diego, California

Image Instruments, Inc. 1
2300 Washington Street
Newton Lower Falls 62, Mass.

Sylvania Electric Prod. Inc. 1
Waltham, Massachusetts
ATTN: Charles A. Thornhill

Research Division Library 1
Raytheon Company
28 Seyon Street
Waltham 54, Massachusetts

ITT Laboratories 1
15151 Bledsoe Street
San Fernando, California

Technical Research Group Inc. 1
2 Aerial Way
Syosset, New York